DETERMINATION OF FLOOD RISK AREAS AND DEVELOPMENT OF MITIGATION STRATEGIES IN KABUL RIVER BASIN, AFGHANISTAN

A Thesis Submitted to
the Graduate School of Engineering and Sciences of
Izmir Institute of Technology
in Partial Fulfillment of the Requirements for the Degree of

MASTER OF SCIENCE

In International Water Resources

by
Esmayel BAREZ

June 2023
IZMIR

We approve the thesis of **Esmayel BAREZ**

Examining Committee Members:

_____
Prof. Dr. Gökmen TAYFUR
Civil Engineering Department, Izmir Institute of Technology

_____
Prof. Dr. Ali GÜL
Civil Engineering Department, Dokuz Eylül University

_____
Assist. Prof. Dr. Doğan KISACIK
Civil Engineering Department, Izmir Institute of Technology

13 June 2023

_____
Prof. Dr Gökmen TAYFUR
Supervisor, Civil Engineering Department,
Izmir Institute of Technology

_____
Prof. Dr. Alper BABA
Co-Supervisor, International Water Resources Department Izmir Institute of Technology

_____
Prof. Dr. Alper BABA
Head of the Department of International Water Resources, Izmir Institute of Technology

_____
Prof. Dr. Mehtap EANES
Dean of the Graduate School

ACKNOWLEDGMENT

Greatness be to Allah, who inspires me everywhere and has given me the energy and potential to complete my Master's degree in the International Water Resources Program at Izmir Institute of Technology.

I want to convey my heartfelt gratitude to my outstanding supervisor, Prof. Dr. Gökmen TAYFUR, for his positive attitude, time, insightful guidelines, and suggestions. This thesis would not have been achievable without his supervision and ongoing help.

In addition, I would like to thank my co-supervisor, Prof. Dr. Alper BABA, for his advice, guidance, and assistance in carrying out this study. In addition, I am grateful to him for providing me with an opportunity to do this research in the Department of International Water Resources, where I learned a lot about water politics, water diplomacy, water right, and management of water resources.

I want to express my gratitude to my family for their guidance, encouragement, and tremendous and unconditional support during the thesis process. I believe myself to be the luckiest person on the planet to have such a family.

ABSTRACT

DETERMINATION OF FLOOD RISK AREAS AND DEVELOPMENT OF MITIGATION STRATEGIES IN KABUL RIVER BASIN, AFGHANISTAN

Flooding is a devastating and natural catastrophe to population, environment, and socioeconomic development globally. Floods occur frequently in Afghanistan, especially in Kabul River Basin. Many geographical techniques have been established in recent years to map, predict and model flood risks. This research investigates identification of flood-prone zones and development of mitigation measures in Kabul River Basin.

First, in this research, GIS and MCDA methodology was applied to generate flood risk map. Also, AHP method was applied to determine the best weights to be assigned to the factors that influence risk of flooding. A flood risk map of KRB was produced using 10 conditioning criteria; soil, rainfall, lithology, LULC, TWI, NDVI, distance to stream channels, curvature, elevation, and slope. Based on the weighted overlay integration of GIS-AHP technique, KRB was grouped into four flood vulnerability zones; very low, low, high, and very high. Generated flood risk map indicates a good match with the flood risk areas and location of past floods in the basin over recent years.

Second, 2D HEC-RAS model and flood frequency analysis were developed for different scenarios to simulate the flow of river and to develope mitigation measures with a 500-year return period in the main river of Kunar and the lower Kabul sub-basin. Manning's n values were used to calibrate HEC-RAS model, and past flood events applied for validation. Flood mitigation strategies, including river restoration, construction of dam, and reservoir improvement were proposed on the Kunar and lower Kabul sub-basin.

Keywords: Flood Inundation Map, Hydraulic Modelling, ArcGIS-MCDA

ÖZET

TAŞKIN RİSKİ ALTINDAKİ ALANLARIN BELİRLENMESİ VE ÖNLEM STRATEJİLERİNİN GELİŞTİRİLMESİ: KABİL NEHİR HAVZASI, AFGANİSTAN

Seller, çevre, nüfus ve sosyo-ekonomik açıdan yıkıcı etkileri olan doğal afetlerdir. Afganistan'da özellikle Kabil Nehir Havzasında sıklıkla seller meydana gelmektedir. Son zamanlarda taşkın risklerini haritalamak, tahmin etmek ve modellemek için birçok coğrafi teknik geliştirilmiştir. Bu tez kapsamında ilgili havzada sele eğilimli alanların tespiti ve sellerin yarattığı yıkıcı etkilerin azaltımasıyla amaçlı çalışmalar gerçekleştirilmiştir.

Bu amaçla öncelikle tezin ilk bölümünde, taşkın duyarlılık haritasının oluşturulması için GIS ve MCDA kullanılmıştır. Daha sonra sel riskini etkileyen değişkenlerin ağırlıklarının belirlenmesi amacıyla AHP yöntemi kullanılmıştır. 10 farklı değişken toprak, yağış, litoloji, LULC, TWI, NDVI, akışa olan mesafe.

kanallar, eğrilik, yükseklik ve eğim kullanılarak çalışma alanı taşkın risk haritası üretilmiştir. GIS-AHP tekniğinin ağırlıklı entegrasyonuna dayalı olarak, Kabil Nehri Havzası dört sel zarar görebilirlik bölgesine (Çok Yüksek, Yüksek, Düşük, Çok Düşük) kategorize edilmiştir. Oluşturulan taşkın risk haritasıyla, geçişte meydana gelmiş taşkınlar arasında makul korelasyonlar olduğu gözlemlenmiştir.

Tezin ikinci bölümündeyse Kunar ana nehri ve aşağı Kabil alt havzasında nehrin akışını simüle etmek ve 500 senelik periyotta etki azaltma önlemlerini geliştirmek için 2 boyutlu HEC-RAS hidrolik modeli geliştirilmiş ve taşkın frekans analizleri yapılmıştır. HEC-RAS modeli, nehir yataklarındaki Manning pürüzlülük katsayıları kullanılarak kalibre edilmiştir ve tarihsel yüksek debili sel akımları kullanılarak doğrulanmıştır. Yapılan analizler sonucunda sel risklerini azaltmak amacıyla bölgeye yönelik nehir ıslahı, baraj inşaatı ve rezervuar iyileştirmeleri gibi yöntemler önerilmiştir.

Anahtar Kelimeler: Hidrolik Modelleme, Taşkın risk haritası, ArcGIS-MCDA

Dedicated to my Parents

TABLE OF CONTENTS

LIST OF FIGURES

Figure **Page**

Figure **Page**

LIST OF TABLES

LIST OF ABBREVIATIONS

AHP	Analytical Hierarchy Process
DEM	Digital Elevation Model
GIS	Geographic Information System
LULC	Land use/Land Cover
NDVI	Normalized Difference Vegetation Index
TWI	Topographic Wetness Index
DTR	Distance to River
FFA	Flood Frequency Analysis
KRB	Kabul River Basin
MCDA	Multi-Criteria Decision Analysis
DTM	Digital Terrain Model
HEC-RAS	Hydrologic Engineering Center River Analysis System
HEC-SSP	Hydrologic Engineering Center's Statistical Software Package
OCHA	Office for the Coordination of Humanitarian Affairs
UTM	Universal Transverse Mercator
2D	2 Dimensional
CR	Consistency Ratio
CI	Consistency Index
WLC	Weighted Liner Combination
DWE	Diffusion Wave Equations
USGS-NLCD	US geological survey of National Land Cover Database
GEVD	Generalized Extreme Value Distribution
DSM	Digital Surface Model
ALOS	Advanced Land Observation Satellite
ASDC	Afghanistan Spatial Data Center
DHI	Danish Hydraulic Institute
SCS	Soil Conservation Service
DUH	Dimensionless Unit Hydrograph
IDW	Inverse Distance Weighting
UNOCHA	United Nations Office for the Coordination of Humanitarian Affairs
ASDC	Afghanistan Spatial Data Center
IPCC	Intergovernmental Panel on the Climate Change

CHAPTER 1

INTRODUCTION

This chapter highlights research background, problem statement, importance of the study, scope, and objective.

1.1. Research Study Background

Flood is considering to be one of the very devastating and commonplace mother earth catastrophes. It has become to be of most frequent calamities caused by nature worldwide, including heavy rainfall, rapid snow melting, land use change, unplanned urbanization, inadequate infrastructure design, dam break, effects of climate change, etc. Based on these factors, flooding hazards have increased along with frequency of intense rainfall.

Flood damage has been extraordinarily severe across the globe. No other natural hazard has frequently occurred, resulting in many casualties, economic losses, destruction of productive land, and loss of properties and residential areas. Based on (WHO), more than 2 billion people were affected by floods from 1998 to 2017. The most defenseless individuals to floods are those who live on floodplains, in weak structures, or who do not have warning systems and awareness of the hazard of flooding in countries with low GDPs and incomes.

Depending on the origins, causes, depth, speed, and effects of the floods, several types of flooding occur, such as pluvial floods, coastal floods, fluvial floods and floods due to failure of hydraulic structures (reservoir, dike).

Afghanistan is severely inclined to severe and frequent natural disasters such as floods, earthquakes, landslides, and droughts. Afghanistan experiences numerous large- and medium-sized floods each year. According to the Climate Risk Index (CRI) for 2019, Afghanistan was placed fifth in terms of its susceptibility to extreme weather (Eckstein et al., 2021). Throughout the year, Afghanistan experienced numerous landslides and floods due to intensive rainfall, and snow-melting. In the region, floods are considered to be the country's most commonly occurring and dangerous natural hazard. Baes on

(ASDC), around one million buildings and over 7.5 million people (22% of population the country) are at risk of flooding. Floods (small or large) can severely impact Afghanistan's economy since agriculture and livestock production are its main economic drivers.

Kabul River Basin (KRB) is the most vulnerable and susceptible to flooding catastrophes in Afghanistan. Rainfall, glaciers, and melting snow are main water source in the KRB. In addition, in Afghanistan land use change, unplanned urbanization, lack of water resource management directive, insufficient water infrastructure, and conflict can lead to variations in discharge, flood peaks, and flood frequency.

To use mitigation approaches and to reduce the impact of floods, it is imperative to assess and identify flood risk zones and research area features. Analysis of hydrologic, hydraulic, topographic, and other components is necessary for studies on flood catastrophes and floodplains. Computer-based mathematical models (e.g., GIS, HEC-RAS, MIKE 21, FLO-2D, etc.) have increasingly become essential for coordinating, mapping, and designing flood control strategies.

1.2. Problem Statement of the Study

Floods are Afghanistan's common and hazardous natural catastrophes, resulting in enormous losses to human life, the economy, societal assets, and property yearly. Kabul River Basin is vulnerable to floods due to severe rainfall, rapid melting of snow and glaciers, and anthropogenic activities. Identification of flood risk assessment, mapping, and mitigation strategies in the KRB is a need to reduce runoff, intensive rainfall management, and unplanned urbanization.

Inter-governmental Panel on the Climate-Change (IPCC, 2014) concludes that South Asian countries like Afghanistan and Pakistan will have frequent and extreme events like heavy rainfall, flooding, and droughts. Flood hazard mapping, assessment, vulnerability, and flood management techniques are new in Afghanistan. There are no empirical and systematic studies related to flood hazard mapping, planning, and evaluation of flood-prone zones in KRB.

Floodplain management in the KRB through flood risk mapping and mitigation strategies (structural and non-structural measures) can lessen the possible effect that flooding could have on persons, the economy, the environment, and the region's ecology.

1.3. Importance of Research

Floods are considered to be very typical types of natural disasters causing considerable damage worldwide. Flood catastrophes often occur in Afghanistan, especially in Kabul River Basin (KRB), due to severe and frequent precipitation and melting of snow and glaciers. It is crucial to develop appropriate flood mitigation systems and flood hazard mapping to prevent flooding in the basin.

This research will assist in establishing how successful flood mitigation techniques and flood hazard mapping work to prevent the study area from flooding.

This study's findings would also benefit academics and scholars and might serve as an essential roadmap for additional related research on the nation and the region. Furthermore, flood hazard maps are designed to be informative to various parties, including local and regional governments, insurance companies, and individuals, as a tool for emergency management, spatial planning, technical protection, awareness, and communication.

1.4. Study Objective

The general objective of the research is to assess the areas of the Kabul River Basin that are on brink of flooding and to suggest secured and cost-effective flood prevention techniques. These components can be summarized as follows:

The main objective of the research is to identify and map the potential zone for flooding based on MCDA integrated with GIS using the AHP technique by examining the influence of flood requirements on the flooding procedure, such as precipitation, slope, stream channels, LU-LC, soil, geology, and elevation in a watershed scale.

In addition, a 2-D HEC-RAS hydraulic model and flood frequency analysis will be developed to simulate river flow and propose mitigation strategies in the Kunar main river and lower Kabul sub-basin with a 500-year return period. The goal of the HEC-RAS model is to identify river flood problems and provide appropriate remedial actions in the Kunar and lower Kabul sub-basin.

The following are the primary objectives of this research within the scope:

- Creation of a catchment-scale methodology to locate and map the flood-prone areas in rapidly growing catchment area of the Kabul River Basin.

- River flow and flood map generation using the HEC-RAS model in KRB.
- To propose several structural mitigation measures to protect Kunar and the lower Kabul sub-basin from flood hazards depending on the generated flood inundation maps.
- To investigate examination of flood incidence for different scenarios for flood occurrence.
- To assess GIS-MCDA methodology for flood mapping and identification using AHP method.
- Developing flood-related parameters such as altitude, distance to stream channels, precipitation, LULC, soil, TWI, slope, etc.
- Identifying factors affecting the flood risk zones.

1.5. Research Questions

To fulfill the overall purpose and goals of the research, the following research concerns are addressed:

- Which strategy, data, and software are appropriate for finding detailed flood-hit areas?
- What are the environmental and geographical parameters that contribute greatly to floods?
- What methods and tools are currently available for mapping floods, and how applicable are they?
- How can the flood control structures like detention basins or dams be improved by using HEC-RAS to assess their efficiency?
- How can flood be simulated using the HEC RAS model?

1.6. Thesis Structure

This thesis is organized into seven chapters. First chapter provides an overview that briefly covers floods, their negative consequences, and their types and modeling. This chapter also discusses the reason for this research, the problem description, the goals, and the scope.

The second chapter highlights relevant scientific studies, approaches, applied methods, determination of flood-prone areas, flood type, flood inundation, and mitigation measures worldwide. The third chapter discusses methodology and literature review on geospatial and statistical flood methodologies, flood modeling based on hydraulics and GIS-AHP modeling, flood consequence, risk and hazard techniques, and conditioning criteria. The forth chapter gives background information about the study area, geography, climate, geology, land use and cover, and soil characteristics. Also, it gives a summary of the Kabul River Basin, and it covers all required information and data.

The fifth chapter describes the result and discussion of flood risk mapping for the KRB using GIS-AHP technique. The sixth chapter investigates different scenarios to simulate flow, design mitigation measures with a 500-year return period in Kunar's main river and the lower Kabul sub-basin, and describes the result and discussion of the HEC-RAS model. The seventh chapter summarizes this investigation by reviewing the findings and suggestions for additional research and study.

CHAPTER 2

LITERATURE REVIEW

This chapter highlights relevant scientific studies, approaches, and applied methods, the determination of flood-prone areas, flood inundation mapping, and mitigation measures worldwide.

2.1. Overview of Floods

One of the most severe and common natural disasters is flooding, resulting in economic losses, environmental catastrophes, public and private infrastructure damage, agricultural damage, and human lives. Floods are among the most catastrophic and frequent natural hazards (Douben, 2006; Ouma & Tateishi, 2014), resulting in a financial loss of US$ 50-60 billion worldwide annually (Douben, 2006). The total economic damage from natural disasters was around US$ 630 billion between 1986 and 1995.

With increasing population density, extreme hydro-meteorological events, improper land use, urbanization changes in flood-prone areas, inadequate response to disasters, and flood damage have been extremely severe and have risen in recent decades throughout the world (D Dutta, 2003; W.-H. Teng et al., 2006; Wu et al., 2012; Zoleta-Nantes, 2002). By 2050, an estimated 450 million people will be affected by floods, along with 430,000 square kilometers of cultivated land, according to climatic trends and projected mitigation measures (Haltas et al., 2021). From 1985 to 2003, the world experienced between 1700-2500 flood events. At the continental level, Asia, approximately 45%, and most of these floods, >50%, happened in developing countries (D Dutta, 2003).

Flooding is caused by a variety of events, including intense and prolonged rainfall, torrential rain, monsoon precipitation, melting of snow and glaciers, and the failure of hydraulic systems like levees and reservoirs. (Douben, 2006; Fendler, 2008; Hunter et al., 2005; Khan, 2011; Ramos & Reis, 2002; Zhang et al., 2008).

Floods can only be mitigated and cannot be stopped or prevented (Sahni et al., 2001). Flood mitigation measurements have been used globally to raise risk tolerance and

identify flood-prone areas for better land use and urbanization management (O'Brien et al., 2006). Mitigation of flood and hazard study will identify the most critical areas of flooding and determine the best alternative for flood damage control and reduction by structural and non-structural methods (Heidari, 2009). Structure-based mitigation strategies include the construction of levees, dams, spillways, storm surge protection, and dike (Tang & Yen, 1993; Tung, 2005; Vrijling, 1993), while non-structural techniques include preparation of flood hazard maps, risk assessment, identification of flood-prone areas, flood plain regulations and laws, setting development policy, land use regulation, raising public awareness, and flood-related database, (Abbas et al., 2015; Andjelkovic, 2001; Faisal et al., 1999; Kundzewicz, 2002).

It is essential for the design of water resource management systems to be aware of the characteristics of excessive discharge or precipitation. Hydraulic structures and management of flood-prone areas (Chebana et al., 2014; Khattak et al., 2016), which are typically determined by frequency analysis approaches for flood events such as Gumbel, Log-Pearson type III, Lognormal, Normal, Generalized Extreme Value distribution (Katz, 1999; Khattak et al., 2016; Renard & Lang, 2007; Rumsby, 1991).

Modeling and mapping flood areas is a crucial component of disaster management functions to enhance flood planning mitigations (Giustarini et al., 2015; Manavalan, 2017). Flood risk maps indicate information related to depth, velocity, and extent of inundation associated with various scenarios (e.g., livestock, financial damage, number of people affected) (Kjellgren, 2013; Mysiak et al., 2013). The maps of flood risk are designed to be informative to various parties, including local and regional governments, insurance companies, and individuals, as a tool for emergency management, spatial planning, technical protection, awareness, and communication purposes (European-Directive, 2007; Kjellgren, 2013).

Due to decades of conflict and prone to natural disasters, lack of water directives, regulations, and awareness of natural disasters, floods in 2005, 2006, 2013, 2019, and 2022 destroyed infrastructure, agricultural areas, livestock, and thousands of people lost their homes in Afghanistan which is likely to experience more flooding as a result of higher winter snowfall, intense rainfall, and warmer summers, that can cause heavy floods in the plains. Floods in Afghanistan can happen in many different forms, including riverine floods, mudflows, debris flows, flash floods, and floods on alluvial fans (Hagen & Lu, 2011). Afghanistan experiences numerous large- and medium-sized floods each

year. According to (ASDC), one million buildings and 7.5 million persons (22% of the population of the country) are in danger of flooding.

The KRB is the most vulnerable and susceptible to flooding catastrophes in Afghanistan. Snow and glaciers are the main sources of surface water in the KRB (Mayar et al., 2020; Vick, 2014).

Flood hazard map assessment and creation in developing countries, such as Afghanistan, is crucial to comprehend the potential impact of flood risk, disaster reduction, flood inundation mapping, and to assess the usage of flood hazards. According to J. Teng et al. (2017), flood simulations have been carried out all over the world since the 1970s for different purposes, such as flood risk and damage assessment (Budiyono et al., 2015; Merz et al., 2010), identification of flood-prone areas (Bhandari et al., 2017), water resource management (Welsh et al., 2013), and sediment transport modeling (Marriott, 1992; Merritt et al., 2003) using hydraulic and hydrological modeling program.

2.2. Definition of Flood and Its Types

Flood is a natural process that refers to the temporary situation of surface water (river, lake, stream, or sea) when the water level and/or discharge exceed a particular value, causing it to overflow from its usual boundaries through a floodplain as a result of rainfall, snow, glacier melting (Munich-Re, 1997). There are various types of floods (e.g., flash floods, riverine floods, coastal floods, and pluvial floods), and each has a unique effect on how it happens and the damage it produces. Also, there are distinctive forms of flooding, such as tsunamis, groundwater increases, levee overtopping, and mud and debris flow events (Kron, 2005).

Floods in Afghanistan are generally happening by excessive rainfall, snow-melting, or a mix of the two. The main types of flooding in Afghanistan are flash floods, floods on alluvial fans, and river (fluvial) floods. The varieties of the flood are described briefly below.

2.2.1. Flash flood

Flash floods are unexpected, catastrophic floods that happen in an instant of time. Flash floods are one of the deadliest hazards in the world because they significantly disturb a wide range of infrastructure, human lives, society, and properties since there is very little time before a flash flood for preventative action and warning issues.

Flash floods frequently occur in Afghanistan, where they cause significant property damage and casualties as they are so powerful that they can remove homes and bridges, having a devastating and expensive effect. According to Hagen and Lu (2011), an analysis of previous flood incidents shows that flash floods are the main reason for fatalities associated with flooding in Afghanistan. Local and regional governments could use a flood map to develop a warning system for flood zone areas.

2.2.2. Coastal (Surge) Flood

A coastal flood happens in places that are near an ocean or sea. The large amount of water produced by the sea and storm surges usually results in coastal flooding, along with waves, which can exceed coastal barriers and low-lying flood regions, potentially causing damage to property and loss of life. Several variables, such as the storm's strength, size, speed, and direction, affect a coastal flood's severity. Afghanistan does not have coastal floods since it is a completely landlocked country.

2.2.3. River (Fluvial) Flood

Fluvial flooding happens when rivers, streams, and coastal storm surges overflow due to continuous periods of heavy rainfall and hurricanes onto natural or low-lying floodplains or areas. Future predictions indicate that due to increased excessive discharges and climate changes, fluvial floods will occur more frequently in many places, particularly in Africa and Asia (Hirabayashi et al., 2013). Afghanistan is highly subjected to destructive river floods due to intense heavy precipitation and snow melting, a regular occurrence in the country.

2.2.4. Pluvial (Rainfall) Flood

Pluvial flooding is a hazard to many communities globally, especially considering it has occurred more frequently in recent years due to intense precipitation and climate changes. Its impact can be more destructive when rainfall exceeds the capacity of urban drainage systems (Martina et al., 2006). Therefore, a significant concern in urban water management is planning and managing urban pluvial floods for authorities through flood hazard mapping and predicting rainfall characteristics (e.g., Duration, timing, and peak intensity).

Management and planning of pluvial floods is a big challenge in Afghanistan due to a lack of meteorological data, inflow data, water infrastructure, academic studies, statistical information, past flood data, flood risk map, and spatial analysis of where and when Afghan floods can happen. Flood hazard mapping and modeling can be helpful techniques for decision-makers and authorities in Afghanistan for better urban flood management, planning, and prediction.

2.3. Flood Management

Flood management, including flood mapping, evacuation, forecasting, and relief operations, can be improved using hydraulic and hydrological tools and modern technology. These techniques can be used to mitigate floods and reduce economic and environmental damage. According to Tranfield et al. (2003), flood risk management systems are mainly concerned with flood forecasting and mapping techniques to identify disaster-prone zones.

It is vital to increase the understanding of the hydraulics of river networks and how flood modeling is widely used for different objectives, such as water resource planning (Gallegos et al., 2009; Welsh et al., 2013), flood hazards mapping and risk assessment (Afshari et al., 2018; Apel et al., 2006; Merz et al., 2010), engineering related to flooding (Gallegos et al., 2009), catchment and hydrology of river system (Abbott et al., 1986; Dushmanta Dutta et al., 2013).

The use of flood modeling has been expanded effectively to include modeling that aims to develop strategies for risk reduction, sustainable flood management systems, flow depth, velocities, flood extent, and adaptation to climate change, along with climate

models, hydrological models, and hydraulic models. Mathematical hydraulic models based on momentum and mass conservation by resolving the continuity and Navier Stokes equations and fluid motion simulations are carried out.

Numerous hydrodynamic models are currently available to simulate flood situations in 1D, 2D, and integrated hydraulic modeling 1D/2D (Quirogaa et al., 2016). One-dimensional (1D) hydraulic modeling is the conventional method for simulating flow in river systems by using cross-sections describing the river and floodplain's topography. Flow in the channel and pipe can be represented by 1D modeling (J. Teng et al., 2017). The most extensively used programs for 1D river modeling are HEC-RAS (G. W. Brunner, 2002; Dyhouse et al., 2003) and MIKE 11, which was created by the DHI.

Although modeling techniques may be effective in some situations, particularly for channels, a 2D model is more appropriate for overflow analysis since it transforms into a 2D dynamic and provides better results (Mignot et al., 2006; Srinivas et al., 2008; Tayefi et al., 2007). Therefore, by integrating topographic factors into account, 2D modeling becomes more suitable for determining the inundation area. However, the main disadvantages of 2D modeling are higher computation times and data availability (Cook & Merwade, 2009; El Kadi Abderrezzak et al., 2009; Pathirana et al., 2011; Quiroga et al., 2013).

To simulate 2D flow modeling, there are numerous programs available, including HEC-RAS (Rangari et al., 2019), SOBEK software (Pinho et al., 2015), FLO-2D (Erena et al., 2018), MIKE 21.

In order to estimate the effects of flooding events and determine the amount of flood inundation, 2D hydraulic models are widely used. Quirogaa et al. (2016) employed HEC-RAS 2D for flood hazard assessment of Mamore River to simulate flood duration, flow velocity, flood depth, and extent. Mihu-Pintilie et al. (2019) have successfully applied HEC-RAS 2D modeling to create flood hazard maps. According to G. Brunner (2018), HEC-RAS 2D performs better compared to similar models (e.g., SOBEK, MIKE FLOOD, and TUFLOW) in terms of performance.

Furthermore, the development of practical techniques for floods mapping, vulnerability, risk analysis, and assessment has been facilitated through GIS and RS technologies with different approaches and techniques over a large area to delineate flood risk maps such as Analytical Hierarchy Process (AHP) (Fernández & Lutz, 2010; Hu et al., 2017; Nasiri et al., 2013; Ouma & Tateishi, 2014; Papaioannou et al., 2015), Multiple Criteria Analysis (MCA) (Hajkowicz & Collins, 2007; Hazarika et al., 2018; Papaioannou

et al., 2015), and various modeling techniques used in a GIS environment (Khosravi et al., 2016; Sanyal & Lu, 2006), and remote sensing methods to extract characteristics of flood areas by using satellite images (Lin et al., 2016; Sharma et al., 2019; Webster, 2010).

Analytical Hierarchy Process (AHP) techniques are being used frequently and effectively for flood risk mapping, assessment, and susceptibility of inundation due to solid applications in practice and a realistic perspective. Many publications characterize AHP as a user-friendly, economic, practical tool for assessing disaster (Bathrellos et al., 2016; Chakraborty & Joshi, 2016; Chandio et al., 2013; Fernández & Lutz, 2010; Ghosh & Kar, 2018; Golden et al., 1989; Hu et al., 2017; Kazakis et al., 2015; Levy, 2005; Pourghasemi et al., 2012; Rahmati, Pourghasemi, & Melesse, 2016; Rozos et al., 2011; Saaty, 1988; Siddayao et al., 2014; Stefanidis & Stathis, 2013).

Hydraulic and hydrological models will enable the creation of a long-lasting flood management system by extending the scope of flood events in terms of determining flow depths, velocities, flood extents, etc. Flood control is essential to decrease the risk of damage.

2.3.1. Flood mitigation measures

Flood mitigation strategies aim to minimize and control the hazards that flooding causes to people's health, properties, environment, and cultural heritage. Flood mitigation measures can be used to locate flood-prone zones, map the extent of the flooding, identify the properties and people at risk, and take the necessary precautions to lower the danger of flooding (e.g., designing flood directives, and legislation, engineering hard and soft structures, investments, flood preparation (European-Directive, 2007). Flood mitigation strategies are divided into structural and non-structural.

Structural measure plans are well-known flood measure techniques used for flood management strategies. Structural measures include reservoirs, detention structures that store flood water, channel improvement, floodwalls, diversion schemes, levees, and dams. Structural mitigation strategies depend on engineering designs with various design requirements or return periods with the maximum flood occurrence.

The non-structural measure used to mitigate and reduce flood risk and impact of flood by flood directives, legislation, warning, evacuation system, training, and education rather than actual physical building (UNISDR, 2009).

The flood management strategy that mainly relies on structural measures may appear to provide a short-term solution. Still, it has been demonstrated in multiple cases that such actions do not always provide adequate protection against large floodwaters (Cigler, 1996). The philosophy of hazard and the risk management approach offer this more comprehensive picture, which covers the coordinated and planned application of structural and non-structural actions.

Floods may increase and occur more frequently due to climate change and global warming. Flood hazard mapping and management are vital for flood disaster management and protecting properties and life. Investing in prevention strategies that attempt to take responsibility before the natural event occurs is the only way to reduce post-disaster efforts and expenses. As flooding seems to be a random and unpredictable phenomenon, historical data on a given basin can be statistically assessed to forecast the frequency of floods for the most severely affected part of the watershed, and mitigation strategies can mitigate it.

CHAPTER 3

METHODOLOGY

This chapter explains GIS-MCDA multi-criteria decision analysis techniques and HEC-RAS 2D software for hydraulic modeling, steps in developing a research area's model, mitigation measures for flood protection, and flood mapping of Kabul River Basin.

3.1. Assessment of Flood-Prone Zones Using GIS-MCDA

In this research, the AHP techniques were selected over several MCDA methods to find weights of the criteria (e.g., rainfall, slope, LULC, elevation, soil, geology, distance to the channels, etc.) for flood potential zone identification. Flowchart of the methodology to locate flood-prone locations in KRB illustrated in Figure 3.1.

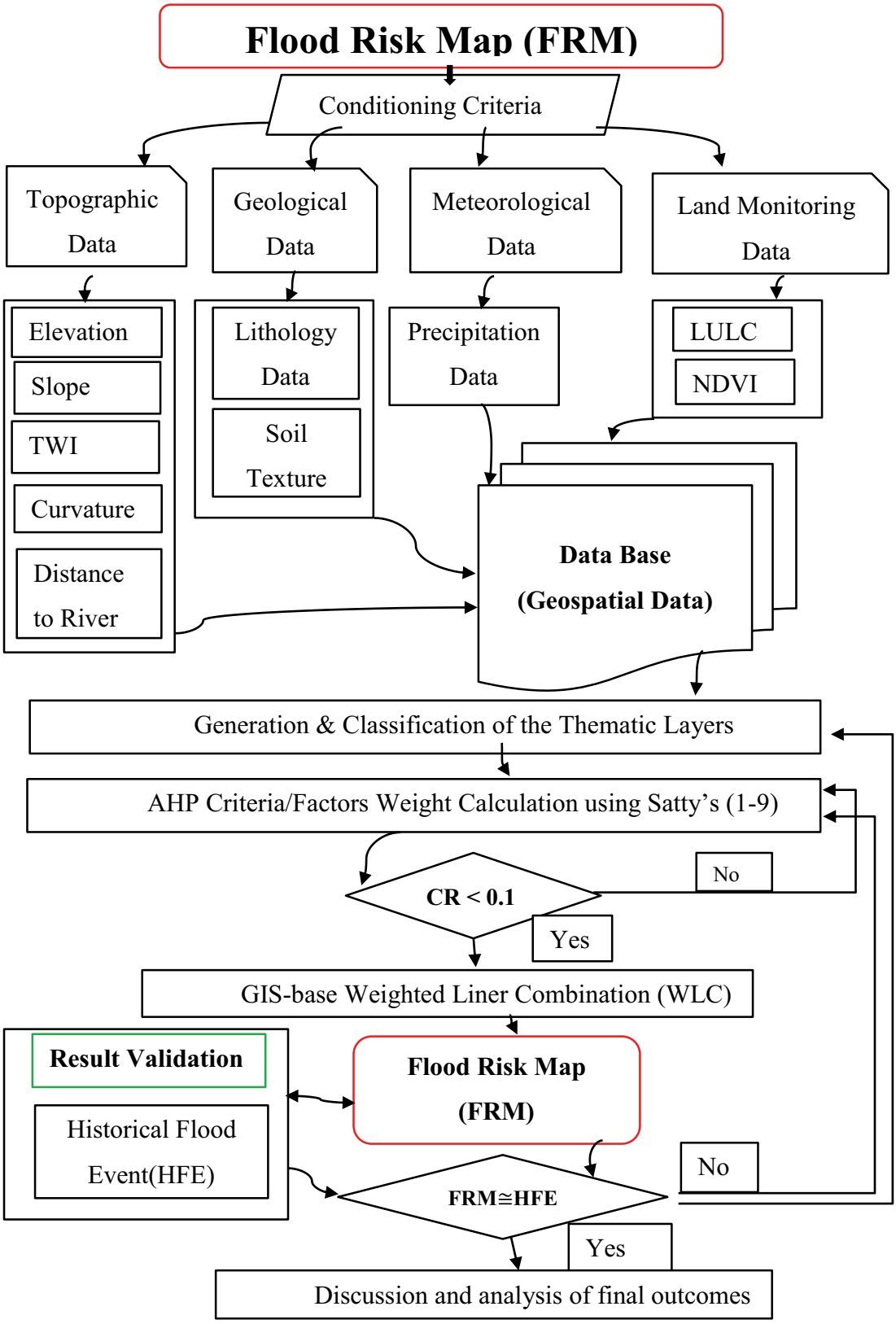

Figure 3.1. Flow diagram for identifying flood hazard areas

3.1.1. Available Data

The available data for the objective of flood susceptibility mapping come from two sources; (1) open-source spatial data (satellite images) and (2) secondary data from various sources, including the local government, land development, and disaster management departments. Afghanistan's Ministry of Energy and Water provided annual precipitation data for 18 locations from 2009 to 2018. Table 3.1 summarizes the data type, its description, and its related source.

Table 3.1. Sources of spatial layer data used to determine flood hazard map

No.	Data	Details	Source
1	DEM	Aster DEM 30 m	ALOS World 3D - 30m
2	LULC	ESA Sentinel-2 imagery at 10m resolution	Esri Land Cover 2021
3	Soil Data	Soil Texture map	FAO Soil Map of the World
4	Rainfall Data	Excel File (2008-2019)	Afghanistan Ministry of Energy and Water
5	Lithology Data	Lithology Map	U.S Department of Interior Lithology of Afghanistan
6	Slope	Topographical Factor	Obtained from DEM
7	Curvature	Topographical Factor	Obtained from DEM
8	TWI	Topographical Factor	Obtained from DEM
9	NDVI	Environment Factor	USGS Earth Explorer
10	DTR	Anthropological Factor	Local Knowledge

3.1.2. Flood Hazard assessment

To properly prepare for any natural hazard susceptibility mapping, regulating the risk's contributing factors is essential. Various research studies recommend the selection of primary parameters and effectiveness for flood monitoring (Li et al., 2019; Saaty,

1988). These fundamental criteria were divided into five major groupings according to their shared characteristics and effectiveness, including (1): morphologic factors (e.g., elevation, landforms, slope, curvature, distance from the river, topographic ruggedness index (TRI)); (2): hydrological criteria (e.g., rainfall, SPI, river network density); (3): permeability factors (e.g., soil type, geology, TWI, soil moisture, soil erodibility factor); (4): LULC factors (e.g., NDVI, LULC, soil-adjusted vegetation index (SAVI)); (5): anthropogenic criterion (e.g., settlement areas, population density, distance from roads) (Swain et al., 2020).

Based on the literature review assessment, research, study area, and expert recommendations, ten fundamentals and primary criteria were selected and developed using a raster dataset with 28x28 m cells for mapping flood hazards using the AHP technique. The effective criteria on the flood potential are determined to be elevation, precipitation, slope, LU/LC, soil type, lithology, distance to stream channels, NDVI, curvature, and TWI.

The AHP method is used to evaluate the weights of each criterion after ranking them according to the literature review, hydrologists, and the expert's recommendations, water resources, and soil management. ArcGIS 10.8 software was applied to investigate the primary criteria and effects of floods. Every indicator or criterion was split into five categories of the propensity for flooding zones: 5: very high, 4: high, 3: moderate, 2: low, and 1: extremely low.

3.1.3. AHP Modeling Approach

By using the AHP technique, planners can use their scientific experience and knowledge to break down a problem into a hierarchical structure and solve it using the AHP methodology. The AHP was selected as an application for natural hazard estimation over several MCDA techniques to calculate the weights of the criteria/factors (Saaty, 1988).

According to Hosseinali and Alesheikh (2008), the AHP methodology generally involves six phases: 1) State the goals and unstructured problem; 2) Perform pairwise comparisons to construct comparison matrices; 3) Identify specific factors and alternatives; 4) evaluate the relative weights of the decision criteria using eigenvalue

method; 5) Obtain a general assessment of the alternatives (by integrating the weighted judgment criteria); and 6) Calculate the consistency index of the matrices.

A comparison rating questionnaire based on a ranking scale of 1-9 in Table 3.2 (Saaty, 1980) was developed to assess the importance and weight of each factor. According to this scale, the AHP calculator was used to construct a pairwise comparison matrix to evaluate the normalized weights of influencing factors/criteria by the eigenvector method. The pairwise comparisons of each parameter were used as inputs, and the AHP approach outputs were the factors' relative weights. Table 3.2 represent Saaty's scale for pairwise comparison of the AHP technique.

Table 3.2. Saaty's scale (Saaty, 1980) for pairwise comparison of the AHP technique.

Ranking	Importance Level
1	Equal Importance
2	Equally to moderately
3	Moderately important
4	Moderately to strongly
5	Strongly preferred
6	Strongly to very strongly
7	Very much strongly
8	Very strongly to extremely
9	Extremely important

The consistency-based comparison analysis during the AHP technique must be verified consistently using Consistency Index (CI) in Equation 3.2. and the Consistency Ratio (CR) in Equation 3.1. The CR must be less than 0.1 (Saaty, 1980) for the comparisons to be valid and thus accepted. A numerical index called CR is utilized to evaluate the pairwise comparison matrix's consistency 3.1.

$$\mathrm{CR} = \frac{\mathrm{CI}}{\mathrm{RI}} \tag{3.1}$$

Where the matrix order determines the value of the random index RI, and CI is the consistency index. The Saaty scale (Saaty, 1980) is used to calculate RI.

$$CI = \frac{\lambda - n}{n - 1} \quad (3.2)$$

Where n represents the number of criteria, λ is the eigenvalue of the matrix. Consequently, all criteria are compared to one another using a pairwise comparison matrix.

3.1.4. Flood Hazard Potential Zone (FHPZ)

In this study, ten criteria were used to determine the FHPZ. Using the Weighted Liner Combination (WLC) technique in ArcGIS 10.8 environment, all factor layers and their weights were combined to delineate potential flood zones. Equation 3.3 is used to calculate the flood hazard potential zone (FHPZ).

$$FS = \left(\sum_{i=0}^{i=n} X_i \times W_i \right) \quad (3.3)$$

Where FS is the flood susceptibility, n refers to the number of factors, X_i is the specific normalized criterion, and W_i It is the criterion's weight.

All layers were aggregated in the ArcGIS using the WLC technique, using Equation 3.3, to prepare flood potential zones in the Kabul river Basin (KRB).

3.2. HEC-RAS Approach

In hydrodynamic modeling, the fluid motion can be simulated using the continuity and momentum equations, generally known as the Navier-Stokes equations. The Navier-Stokes equations are greatly simplified by the Saint-Venant equations when combined with numerical models under various assumptions.

Hydraulic models (e.g., HEC-RAS, FLO-2D) have been used for many years to evaluate the effects of fluvial and pluvial flood scenarios using different governing equations, numerical solutions, and models (e.g., 1D, 2D). This research uses software developed by the US Army Corps of Engineers, HEC-RAS Hydrologic Engineering Center's River Analysis System, to execute the hydraulic modeling.

In 1D models, the river and floodplain's topography is defined by several cross-sections. In contrast, in 2D hydrodynamic models, topography of the basin is described by cells on a two-dimensional computer grid. 1D or 2D computer and mathematical models can be used to analyze problems (e.g., flood hazard assessment, flood mapping, etc.) and develop solutions as engineering applications.

In this study, the simulation of fluid motion and flood risk mapping is carried out using the HEC-RAS 2-D model with different return periods. The following section covers a general overview of 1-D, 2-D models. Flow diagram illustrating the overall structure of the HEC-RAS model (Figure 3.2).

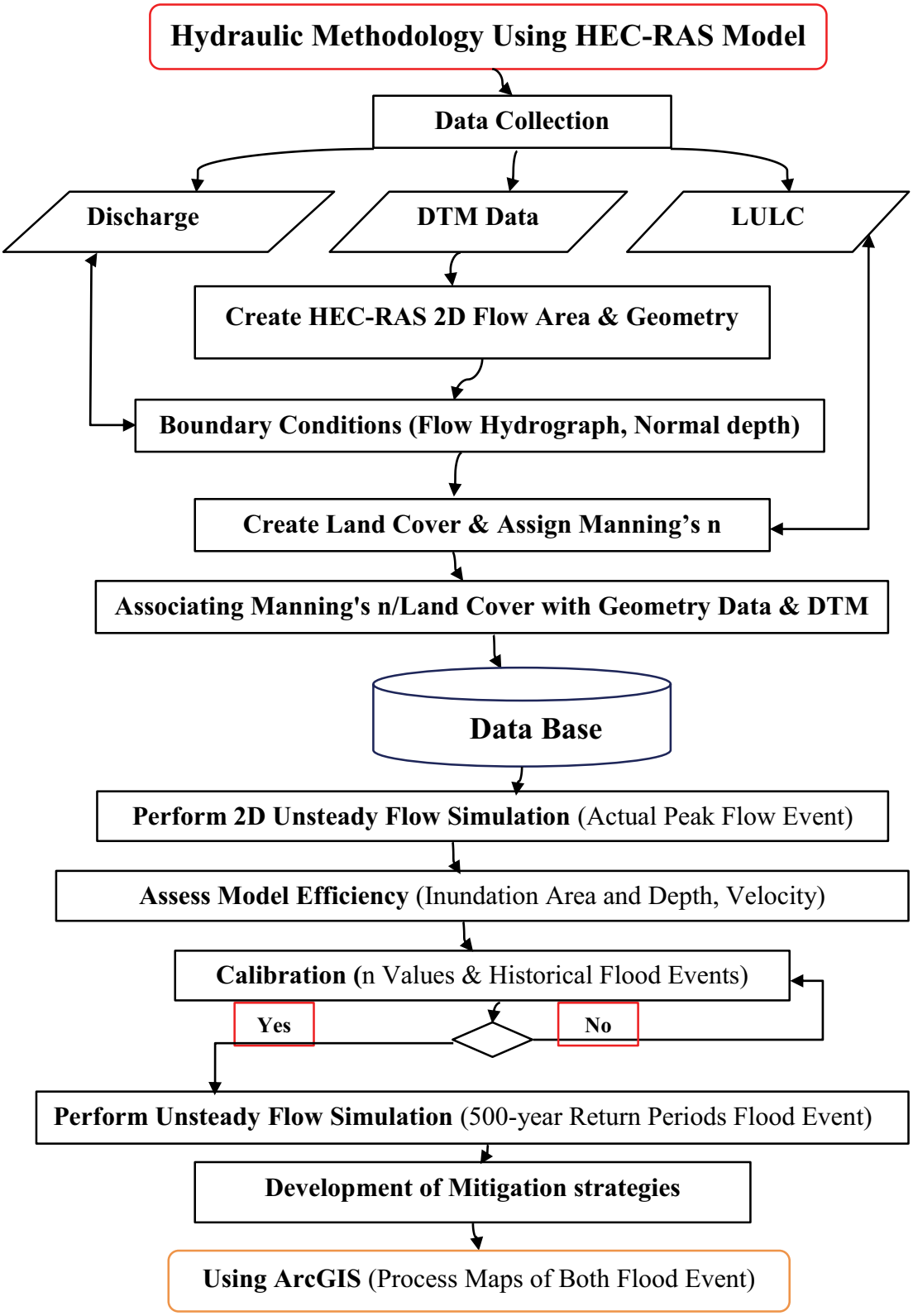

Figure 3.2. Flow diagram illustrating the overall structure of the HEC-RAS

3.2.1. 1-D Model

The Saint-Venant formulas can be used to calculate river water levels and flows or floodplains under suitable downstream and upstream boundary conditions (Chanson, 2004). The Saint-Venant formulas are written as follows equations 3.4 and 3.5.

$$\frac{\partial \mathrm{A_{CS}}}{\partial \mathrm{t}} + \frac{\partial \mathrm{Q}}{\partial \mathrm{x}} = 0 \tag{3.4}$$

$$\frac{\partial \mathrm{Q}}{\partial \mathrm{t}} + \frac{\partial}{\partial \mathrm{x}}(\mathrm{uQ}) + \mathrm{gA_{CS}}\left(\frac{\partial \mathrm{h}}{\partial \mathrm{x}} - \mathrm{S_0}\right) + \mathrm{gAS_f} = 0 \tag{3.5}$$

where A_{CS} indicates the area of the cross-section, Q denotes the flow rate, S_0 reflects the channel bottom slope, h is the water depth, x is the Cartesian coordinates, u is the velocity, g is the gravitational acceleration, and S_f is the friction slope.

3.2.2. 2-D Model

Two-dimensional hydraulic models are most frequently used to evaluate flood risk and map flood extent. Two-dimensional (2-D) simulations are effective and preferable to one-dimensional (1-D) due to the interaction of floodplain and river channels. The capabilities of a 2D flood model allow it to simulate river flow both parallel and perpendicular to the stream. Flood velocity, depth, and extent are the direct outputs of the two-dimensional hydraulic (2-D) models.

The 2-D depth-averaged Saint-Venant equations can be expressed in equation 3.6:

$$\frac{\partial \mathrm{h}}{\partial \mathrm{t}} + \frac{\partial(\mathrm{hu})}{\partial \mathrm{x}} + \frac{\partial(\mathrm{hv})}{\partial \mathrm{y}} = 0 \tag{3.6}$$

Where h is the flow depth, q is the lateral flow, u, and v are velocities in the x-y direction, .and t is time.

The equations for depth-averaged momentum that are used to explain fluid flow in open channels are described in equations 3.7 and 3.8. By averaging the velocity and pressure over the depth of the flow, these equations give a simplification of the dynamics of fluid flow.

$$\frac{\partial \mathrm{u}}{\partial \mathrm{t}} + \mathrm{u}\frac{\partial \mathrm{u}}{\partial \mathrm{x}} + \mathrm{v}\frac{\partial \mathrm{u}}{\partial \mathrm{y}} + \mathrm{g}\frac{\partial \mathrm{h}}{\partial \mathrm{x}} = \mathrm{g}(\mathrm{S_{0x}} - \mathrm{S_{fx}}) \tag{3.7}$$

$$\frac{\partial \mathrm{v}}{\partial \mathrm{t}} + \mathrm{u}\frac{\partial \mathrm{v}}{\partial \mathrm{x}} + \mathrm{v}\frac{\partial \mathrm{v}}{\partial \mathrm{y}} + \mathrm{g}\frac{\partial \mathrm{h}}{\partial \mathrm{y}} = \mathrm{g}\left(\mathrm{S_{0y}} - \mathrm{S_{fy}}\right) \tag{3.8}$$

Where, S_{0x} is the bottom slope in the x-direction, S_{0y} is the bottom slope in y-direction, S_{fx} is friction slope in x-direction, and S_{fy} is friction slope in y-direction.

The friction coefficient is shown in equations 3.9 and 3.10, using Manning's formula or Chezy's equation:

$$\mathrm{S_{fx}} = \frac{n^2 u\sqrt{u^2 + v^2}}{R^{\frac{4}{3}}} \tag{3.9}$$

Where R is the hydraulic radius, u is velocity, and n is Manning's roughness.

$$\mathrm{S_{fy}} = \frac{n^2 v\sqrt{u^2 + v^2}}{R^{\frac{4}{3}}} \tag{3.10}$$

If the problem is one-dimensional, the x or y direction and the flow velocity in both directions is negligible or zero, the friction coefficient produces a simplified form that is represented by equations 3.11 and 3.12.

$$S_{fx} = \frac{n^2 u^2}{R^{\frac{4}{3}}} \tag{3.11}$$

$$S_{fy} = \frac{n^2 v^2}{R^{\frac{4}{3}}} \tag{3.12}$$

Roughness is crucial for simulation, which depends on factors (e.g., vegetation, surface roughness, LULC, etc.). Manning's roughness values were used according to LULC of the region.

HEC-RAS can also use Diffusion Wave Approximation (DWA). This research uses the Diffusion Wave Approximation, which is more stable, fast, and more tolerant numerically than Full Momentum Formula. Additionally, it has the benefit of allowing for the use of more significant time steps while generating numerically correct and stable solutions. The DWA neglects the acceleration terms. The HEC-RAS model uses the normal depth, rating curve, flow, and/or stage hydrographs as boundary conditions.

The computation time intervals were chosen based on the flow velocity and cell size to ensure that the Courant number was (HEC-RAS, 2016). The stability of unstable numerical approaches is referred to as Courant number. The model provides acceptable stability as high as 5.0 when using DWE (HEC-RAS, 2016). Typically, for simulation of the model, the computation interval or time step should be small to let fluid movement into 2D flow cell area. In the present research, the model simulation is initially run with a time step of 30 seconds. Also, the courant condition (see equation 3.13) for diffusion wave equations (DWE) is applied for a more stable and accurate result.

$$C = \frac{V\Delta T}{\Delta x} \leq 2.0 (\text{ with a max } C = 5.0) \tag{3.13}$$

Where ΔT is the computing time step, C is the courant number, V is the wave celerity (m/s), and Δx cell size.

3.2.3. Boundary Requirements

Boundary conditions are applied to define upstream and downstream flow conditions in 2-D flow areas. These criteria are vital parameters that determine the flow pattern at the 2-D domain's boundaries. To specify boundary conditions for 2-D flow areas, four types of external boundary conditions can be used, these are:

- Normal Depth
- Stage Hydrograph
- Rating Curve
- Flow Hydrograph

This study area has four inflows hydrograph and one outflow as boundary requirements for a 2-D flow area. This research uses the discharge hydrograph as inflow for the upstream boundary for model simulation.

3.2.4. Digital Terrain Model

DTM represents the ground surface which includes topographic characteristics like ridges and break-lines that can affect the flow movement across the floodplain (HEC-RAS, 2016). DTM can be generated from Digital Elevation Model by the HEC-RAS environment. HEC-RAS supports the representation of the ground surface using a DTM. The constructed DTM must be linked to model geometry to generate the inundation map.

3.2.5. Roughness Coefficient

Roughness Coefficient is one of the essential factors in hydraulic modeling and analysis of 2-D flow area, which can be used for model simulation, calibration, accuracy, and validation. Manning's roughness coefficient values can be established according to various rules and tables for natural channels and floodplains. Hydraulic flow simulation models (e.g., HEC-RAS, FLO-2D) typically use remote sensing imagery to generate floodplain roughness values for various land cover classifications, such as vegetation, land use, forest area earth surface, etc.

HEC-RAS software enables the allocation of roughness coefficient values and percentage imperviousness based on the land cover characteristics. ESRI 2020 land use land cover data with the 10-meter resolution is applied to create a roughness coefficient for the study area in the HEC-RAS environment. ESRI land uses land cover data was linked with the 2-D geometry data set of the study area for simulation. Manning's n (roughness coefficient) was assigned for each land cover type base on the HEC-RAS manual and the USGS of NLCD (Dewitz, 2016; HEC-RAS, 2016). Table 3.3 presents roughness coefficient for each land cover type.

Table 3.3. Manning's n values-based on NLCD and HEC-RAS

NLCD Land Cover Type	Range of n (HEC-RAS 2D Manual)
Open Water	0.025-0.05
Developed, Open Space	0.03-0.05
Developed, Low Intensity	0.06-0.12
Developed, Median Intensity	0.08-0.16
Developed, High Intensity	0.12-0.20
Woody Wetlands	0.045-0.085
Deciduous Forest	0.1-0.20
Evergreen Forest	0.08-0.16
Mixed Forest	0.08-0.20
Dwarf Scrub	0.025-0.05
Shrub/Scrub	0.07-0.016
Emergent Herbaceous Wetlands	0.05-0.085
Cultivated Crops	0.020-0.05
Pasture/Hay	0.025-0.05
Sedge/ Herbaceous	0.025-0.05
Grassland/ Herbaceous	0.025-0.05
Perennial Ice/Snow	N/A
Barren Land (Rock/sand/clay)	0.023-0.03

3.2.6. 2-D Flow Computation

The HEC RAS two-dimensional flow area defines size of the region in which 2-D flow assessments are carried out using HEC-RAS 2D. A 2D flow area can be connected to the storage area, river, or another 2-D flow region by a particular connection type defined by HEC-RAS software. The 2D flow area should be situated at either a reach's upstream end or downstream end (HEC-RAS, 2016). A two-dimensional computational mesh was generated as 100 x100 m cell size, with a total of 2480781 computational cells for the 2-D flow area. Also, the river's main channel is refined with a cell size of 10 x 10 m, and a break-line is generated in the river center for a better representation of the ground surface and water movement path. A flow hydrograph is used as inflow to conduct the simulations in a 2D flow environment. Figure 3.3 shows the properties of cell within the computational grid.

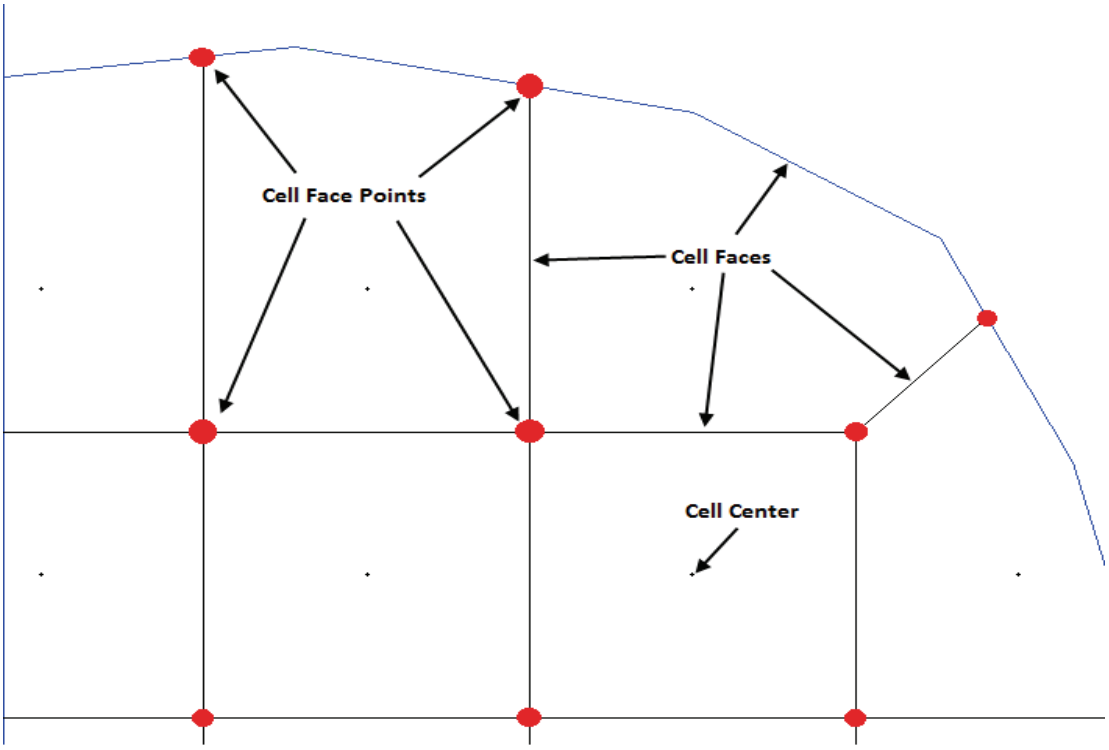

Figure 3.3. HEC-RAS 2-D modeling computational mesh (HEC-RAS, 2016)

3.2.7. Flood Frequency Analysis

Flooding is a destructive natural hazard and phenomenon that has a negative impact on human beings, properties, environment; which requires a range of responses, including mitigation measures (structural and non-structural mitigation strategies), land-use management, forecasting, flood directive, etc. Design floods event or theoretical peak discharge graphs has been used frequently to assess flood prevention systems (Tian & Wang, 2022). Hydraulic and hydrologic engineering design, planning, and management issues necessitate an in-depth understanding of flood occurrence characteristics, such as flood peak, duration, and volume. To overcome these challenges, an accurate assessment of flood flow frequency analysis and magnitude of floods is needed for risk or hazard assessment (Dunne & Leopold, 1978; Jery R Stedinger & Griffis, 2008). The economic and environmental construction of large engineering projects like reservoirs, dams, dikes, levees, storage ponds, bridges, and floodplain management is based on accurate flood frequency analysis for an event with a specific interval (e.g., 50-year flood, 100, 200, 500, or even 1000-year flood, or flood peak, and volume).

According to Kidson and Richards (2005), flood frequency analysis can be performed from annual peak flow data observed at a specific river gauge station. Frequency distribution graphs are created by the statistical calculations of the standard deviation, average, and skewness for the flood frequency evaluation. Distribution functions, such as Log Normal, Gumbel EV1, Normal, Generalized Extreme Value, Exponential, and the Log Pearson Type III, have been used for frequency analysis (Kidson & Richards, 2005). This study uses annual peak discharge data for assessment of flood frequency and generation of maximum flood design events.

The most specific category of these classical flood frequency analyses (FFA) models includes two-parameter functions (shape and location) that can be fitted statistically, such as the Extreme Value (EVI) and the Log-Normal model. The Generalized Extreme Value (GEV) and Log Pearson type III (LP3) models are types of 3-parameter models (location, scale, and shape) (Kidson & Richards, 2005). According to NERC (1999), the 3-parameter systems, with the additional scale parameters, can fit a more significant number of catchments' datasets. Still, the ease and simplicity of fitting the 2-parameter models is an advantage. Some flood frequency analysis models have been described in the following section.

3.2.7.1. Generalized Extreme Value Distribution (GEVD)

Gumbel Distribution or Extreme Value is an effective statistical technique applied in scientific research, including hydrology, geology, meteorology, economy, and other fields of environment for estimating extreme events (Beirlant et al., 2004; Chow et al., 1988a). In this distribution, peak recorded flow rate in a year will be selected as the maximum or minimum data value.

There are three forms of Extreme Value Distributions (EVD): Extreme Value type I, type II, and type III distributions were established by Gumbel (1941), Frechet (1927), and Weibull (1939) (Chow et al., 1988a). The Extreme Value Distribution (EVD), which is known as the Gumbel distribution, is mainly used in meteorological and hydrological assessments (e.g., estimation of flood peak or maximum rainfall for a specific duration) (Hosking & Wallis, 1997). Location and scale are the only two characteristics used by the EV1 distribution. The PDF and CDF of the Gumbel EV type-1, as defined in (Chow et al., 1988b; J R Stedinger, 1993), are stated as follows (3.14 and 3.15):

$$\mathrm{f(x)} = \frac{1}{\alpha}\left[-\frac{\mathrm{x}-\mathrm{u}}{\alpha} - \exp\left(-\frac{\mathrm{x}-\mathrm{u}}{\alpha}\right)\right] \mathrm{pdf} \tag{3.14}$$

$$F(x) = \exp\left(\left[-exp\left(-\frac{x-u}{\alpha}\right)\right]\right) cdf \tag{3.15}$$

$-\infty \leq x \leq \infty$ is

Where x is the recorded data, u is the mode of distribution (equation 3.16 and 3.15).

$$\alpha = \frac{\sqrt{6}}{\pi}\mathrm{S_x} \tag{3.16}$$

$$\mathrm{u} = \bar{\mathrm{x}} - (0.5772\alpha) \tag{3.17}$$

Jenkinson (1955) developed a particular case of a single distribution called GEVD (Chow et al., 1988a). General Extreme Value distribution is the combination of Gumbel, Weibull, and Frechet EVD.

The probability distribution function for the General Extreme Value Distribution is defined by Equation 3.18:

$$F(x) = \exp\left[-\left(1 - k\frac{x-u}{\alpha}\right)^{1/k}\right] \tag{3.18}$$

Where k, u, and α are scale, location, and shape parameters to be calculated.

Predicted discharge (Q_p) can be estimated for various return durations using the conventional normal distribution equation. (Samantaray & Sahoo, 2020) as follows:

$$Q_p = \mu + K_T\sigma \tag{3.19}$$

Frequency factor for GEVD can be evaluated by Equation 3.20:

$$K_T = -\frac{\sqrt{6}}{\pi}\left\{0.5772 + \ln\left[\ln\left(\frac{T}{T-1}\right)\right]\right\} \tag{3.20}$$

Return period T in terms of K_t:

$$T = \frac{1}{1 - \exp\left\{-\exp\left[-\left(y + \frac{\pi K_T}{\sqrt{6}}\right)\right]\right\}} \tag{3.21}$$

where Q_p is the predicted discharge value for a given return period in m^3/s, K_T is the frequency factor, T represents return period, μ is the mean of the data, and σ is standard deviation.

3.2.7.2. Log-Pearson Type III Distribution

For the investigation of flood frequency, the Log-Pearson Type III distribution has been extensively employed. The U.S. Water Resources Committee recommended using the Log-Pearson Type III distribution developed from Pearson Type III for frequency analysis in the USA (USWRC, 1975). According to Benson (1968), The typical distribution for frequency examination of the worst-case flood scenarios in the USA is the Log-Pearson Type III. The LP type III has been in the USA applied, where data from all watersheds are fitted to it for management, development, and policy considerations. This distribution was designed to generate a curve that would fit the data and has indicated reliable outcomes in several meteorological and hydrological applications.

The frequency analysis using Log-Pearson Type III can be evaluated as follows: First, logarithms of the hydrologic data should be determined, $y = \log(x)$. The mean $\bar{y}$, standard deviation S_y, and skewness coefficient C_s should be calculated (Chow et al., 1988b). The frequency element depends on the skewness coefficient C_s and Twhich represent return period . When $C_s = 0$, the frequency parameter is equal to the standardized normal variable z. When $C_s \neq 0$, the frequency factor K_T can be estimated by (Kite, 1977) as shown in equation 3.22:

$$K_T = Z + (Z^2 - 1)K + \frac{1}{3}(Z^3 - 6Z)K^2 - (Z^2 - 1)K^3 + ZK^4 + \frac{1}{3}K^5 \qquad (3.22)$$

where $k = \frac{C_s}{6}$ and coefficient of skewness C_s can be determined as:

$$C_s = \frac{n \sum_{i=1}^{n}(y_i - \bar{y})}{(n-1)(n-2){S_y}^3} \qquad (3.23)$$

As a result, the expected flood peak data for a particular return period or FFA would be computed as follows (equations 3.24, and 3.25):

$$Q_p = 10^{Y_T} \qquad (3.24)$$

$$Y_T = \bar{y} + K_T S_y \qquad (3.25)$$

In this study, GEV is used to calculate the maximum flood peak data for Flood Frequency Analysis (FFA), as this model is suggested for annual maximum precipitation and streamflow in many scientific research and studies.

3.2.8. HEC-SSP Program

HEC-SSP software allows users to perform statistical studies. HEC-SSP is capable of performing a variety of frequency analyses, including flood frequency analysis for low or high flows, duration analysis, etc. (HEC-SSP, 2019).

The flood frequency analysis was calculated using the HEC-SSP tool. The software was supplied with the maximum annual flow rate observed between 2008 and 2019. The software analyzes the predicted peak flood of a particular return period using various statistical distribution techniques. These statistical distributions include the Gumbel-Max, Log-Normal, Log-Pearson 3, Normal, and GEVD.

Each station's expected maximum flood discharge data were determined using HEC-SSP software with their exceedance probability. General Extreme Value distribution based on the HEC-SSP software result was selected as the estimated peak discharge with different time intervals (2, 5, 10, 20, 50, 100, 200, and 500) years. The predicted discharge values for HEC-RAS model were the peak flow value that corresponds to 500 years of return period for the General Extreme Value distribution (GEV).

3.2.9. Data Used for Flood Frequency Analysis

Maximum flow data is an essential component of flood frequency assessment, a statistical technique for calculating possibility of various flood occurrences. The peak flow is the highest flow rate ever observed in a stream or river at a specific location during a flooding.

Maximum annual discharge (m^3/s) data from the Asmar, Pul-Behsod, Pich, and Sultanpur gauging stations were taken from Afghanistan's MWE. They were utilized to analyze flood frequency. In this research, data from 2008 to 2019 were used to analyze flood frequency. The peak discharge of the data has been listed in Table 3.4.

The duration of the data record is a crucial factor to take into account while analyzing flood frequency. A relatively long data record is typically a better indicator of the flood regime and can offer a more accurate evaluation of the frequency of flooding. Since Afghanistan has been through political instability and civil war for so long, there is not enough recorded data on the discharge or rainfall, so data from 2009 to 2018 were used to analyze flood frequency. Table 3.4 shows the maximum Peak discharge data at gauge station for the study area.

Table 3.4. Illustrating Peak discharge data at gauge station for the study area

Gauge Station	Mean (m^3/s)	Historical Peak (m^3/s)
Asmar	351	2698 (The year 2019)
Pich	47.1	374 (The year 2019)
Sultanpur	4.65	180.9 (The year 2018)
Pul-Behsod	151	878.1 (The year 2018)

HEC-SSP software can provide the best-fitted distribution among various distribution types, including Log Pearson-3, GEV distribution, Gumbel, Log Normal, etc. GEV distribution was the best fit distribution based on the HEC-SSP distribution result. The peak discharge was estimated using the General Extreme Value distribution (GEV) with different return periods intervals of 2, 5, 10, 20, 50, 100, 200, and 500 for the study area (Table 3.5). The associated highest possible discharge value of 500 years of return time was used to construct the design hydrograph value in the HEC-RAS model for the specified location.

The design hydrograph for the research region is estimated using the SCS Dimensionless DUH approach using equations 3.26 and 3.27).

$$Q_p = \frac{2.08 * A}{T_p} \tag{3.26}$$

$$T_p = \frac{2.08 * A}{Q_p} \tag{3.27}$$

Where Q_p is the peak discharge derived from the study of frequency of flooding in the HEC-SSP environment, A is catchment Area, T_p is the time to peak, and it is calculated for each design hydrograph. Using equations 3.26 and 3.27, the design hydrograph is generated for the maximum flow and 500-year flood occurrence, as presented in Figure 6.2 and Figure 6.3.

The exceedance probability of maximum discharge to the probable peak flow of each river and tributary has been calculated and shown in Figure 3.4, Figure 3.5, Figure 3.6, and Figure 3.7 using HEC-SSP software.

Table 3.5. Maximum expected flood discharges (m^3/s) using (GEV) distribution

Return Period (Year)	2	5	10	20	50	100	200	500
Asmar	1312	1859	2218	2580.4	3112.4	3563.7	4051.7	4837
Pich	215.6	281	322.5	360.6	407.8	441.7	474.2	515.4
Pul-Behsod	551.8	746	850	928.2	1009	1068	1128.5	1206
Sultanpur	64	110	136.4	163.4	202.2	232.7	268.3	320.7

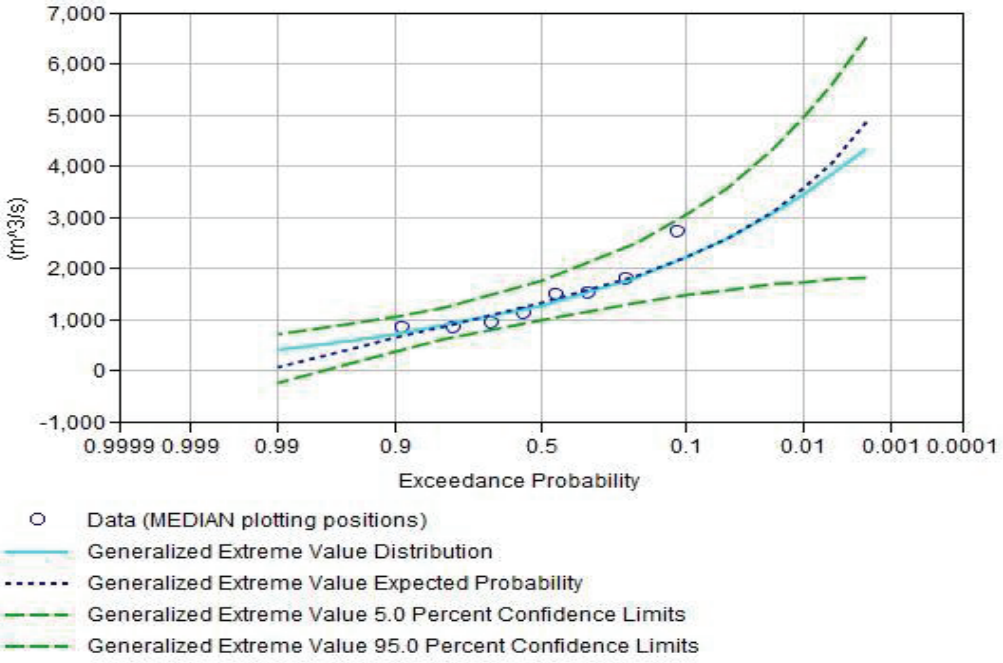

Figure 3.4. Exceedance probability for Asmar station using HEC-SSP Software

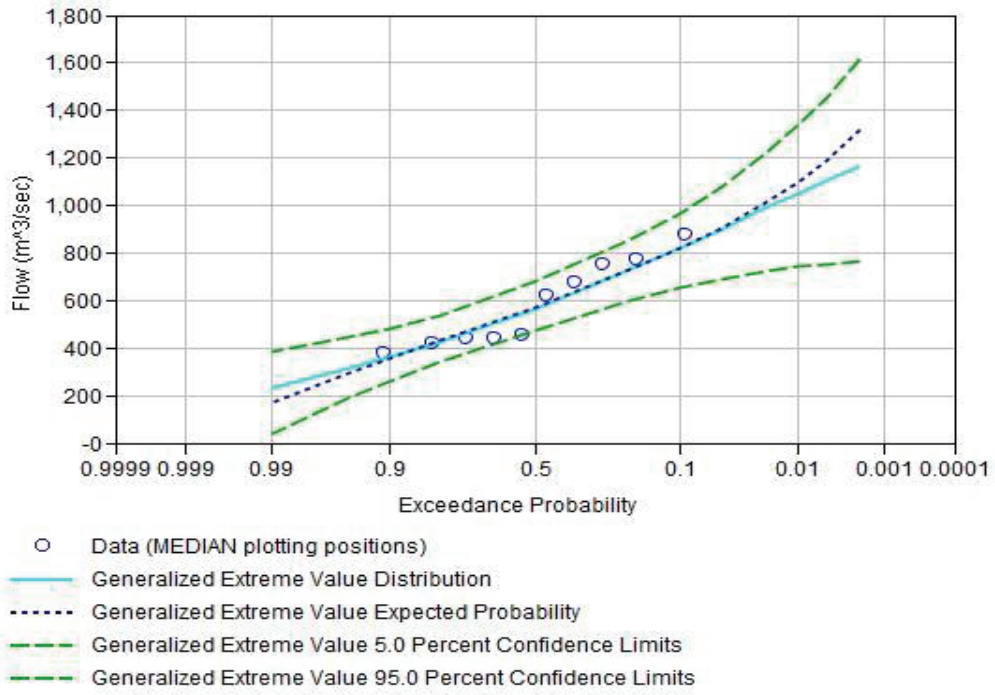

Figure 3.5. Exceedance probability for Pul-Behsod station using HEC-SSP Software

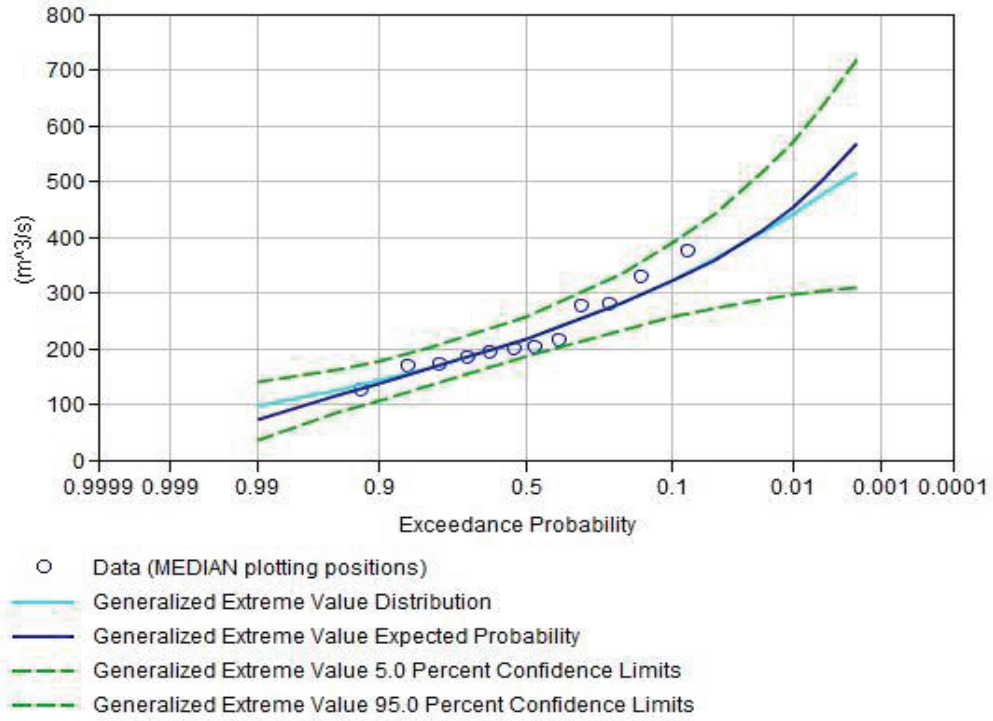

Figure 3.6. Exceedance probability for Pich station using HEC-SSP Software

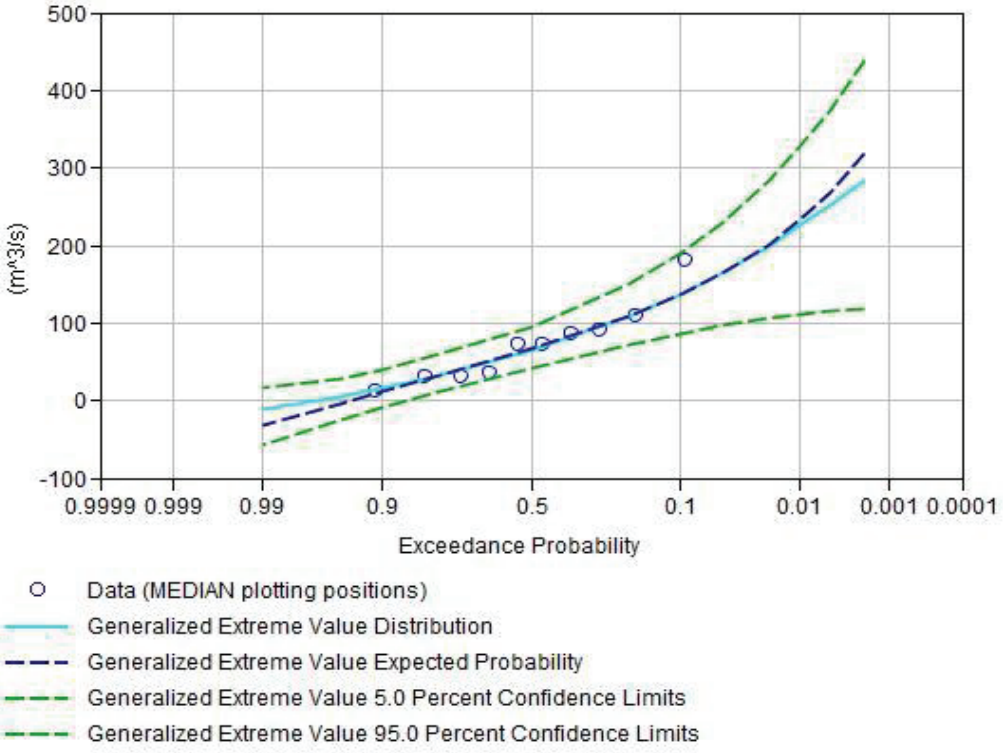

Figure 3.7. Exceedance probability for SorkhRod station using HEC-SSP Software

CHAPTER 4

DESCRIPTION OF THE STUDY AREA AND MATERIALS

This chapter presents a summary of the Kabul River Basin and materials set required to investigate the basin's flood risk. The application of flooding, precipitation, soil type, lithology type, topography, and LULC are covered in detail.

4.1. Kabul River Basin

KRB is situated in the central-east of Afghanistan and lies within 33 ° to 37 ° north latitudes and 67 ° to 74 ° east longitudes (Figure 4.1). The area of the KRB is 92269 km^2, which Afghanistan and Pakistan both share. KRB has a drainage area of 76908 km^2 in the Afghanistan tributary upstream, and the rest of 15361 km^2 is located in Pakistan and discharges into the Indus river. KRB is one of the country's most susceptible regions to flooding catastrophes.

KRB originates in the central highland of the Hindu Kush mountains at an altitude of 7500 m above the mean sea level and reaches the eastern valley at an elevation of 300 m on average above the mean sea level. The KRB basin's geography is mountainous, characterized by barren terrain in the downstream reaches and higher slopes and valleys in its upstream area. According to Najmuddin et al. (2018), on the assessment of LULC change, it was figured out that agriculture, grassland, waterbodies, and urbanization areas increased in the KRB from 2001 to 2010. In contrast, forests, unused land, and snow/ice areas declined. All of these variables and the location of the basin could affect the study area's discharge, flood peaks, and frequency.

Kabul River Basin is the highest populated watershed in the country, accounting for 35% of the country's population and 11% of its overall land area. 59% of KRB's population resides in rural areas near rivers and agricultural land, while 41% live in the cities (World-Bank, 2010). According to the report of the Central Statistical Office of the country, the population of KRB was about 11-12 million in 2015.

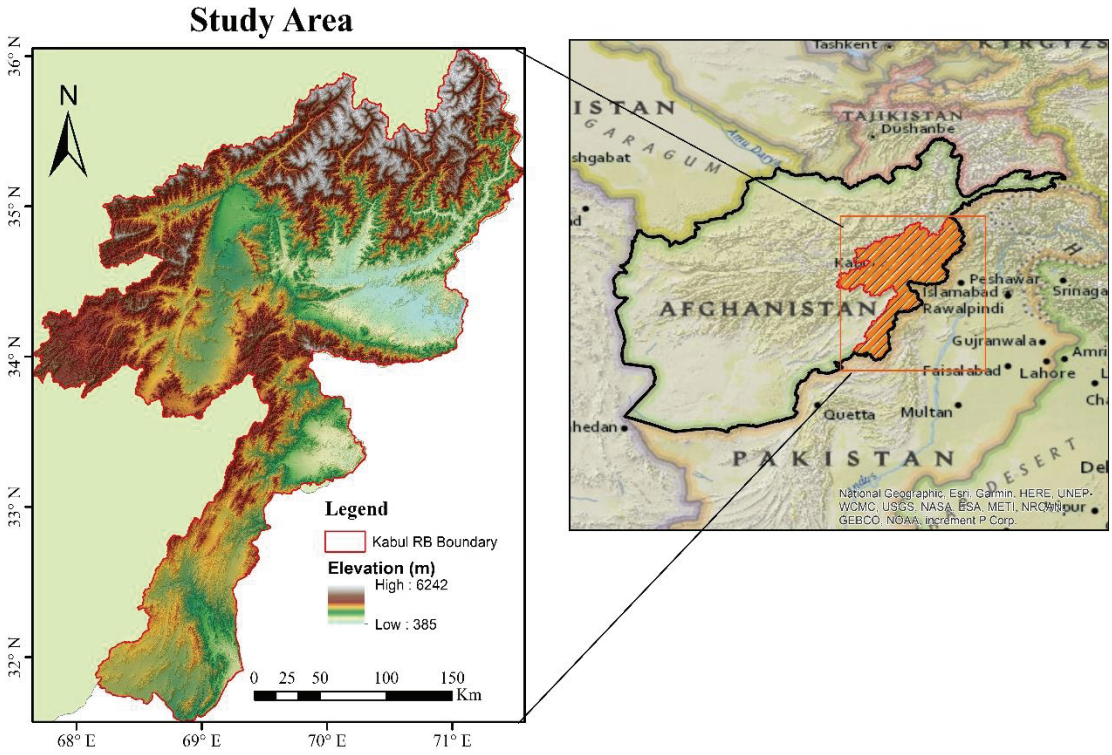

Figure 4.1. Kabul River Basin Map, Afghanistan

KRB is divided into seven watersheds/sub-basins (Kunar, Kabul, Alingar, Shamal, Cack wa Logar Rod, Gomal, and Ghorband wa Panjsher) and covers thirteen administrative provinces. In this watershed, Kabul, Jalalabad, Charikar, Pol-Alam, Mehtarlam, and Asadabad are major cities. KRB has a length of 700 km, 460 of which are located in Afghanistan and remaining 240 km in Pakistan, joining the Indus river.

The glaciers, snow, and monsoon rains in the Hindu Kush mountains, a component of the Himalayas, are the main sources of surface water in KRB (Vick, 2014). The melting of snow and glaciers during summer contributes significantly to the basin's runoff. Typically, more than 72% of the runoff occurs between May and September, and between October and April, 40%. Approximately 12% of Afghanistan's national territory is covered by the KRB, and it also provides 26% of the country's total streamflow (Favre & Kamal, 2004). The average annual water capacity of the surface water of the Kabul catchment is about 17.1 billion cubic meters, which is 34.73 percent of the country's total yearly water, of which about 5.3 billion cubic meters of available water capacity is currently being used in the country, and the rest is leaving the country due lack of water infrastructure basis.

4.1.1. Climate

Kabul River Basin has a semi-arid continental climate with hot summers and cold winters. The weather conditions vary from sub-basin to sub-basin due to the tremendous variation between the altitude, rainfall, and variations in temperature in the higher and lower parts of the KRB. Because of the heterogeneity of the basin, the upstream and downstream areas have different cropping regimes, crop production seasons, and agricultural frequencies.

Annual rainfall in the basin is approximately 450 mm (Sayama et al., 2012) and is highly variable. The maximum precipitation happens in spring (March to May), with highly irregular rainfall patterns in the neighboring areas. The annual average temperature was recorded to be around 9 C^{o} in the KRB. In the summer, the Nangarhar region of the KRB, which is situated in the catchment's downstream zone, experienced temperatures as high as 48 °C while the Chatral Valleys, which are located in the basin's eastern part, recorded temperatures as low as -28 °C. The average maximum and minimum temperatures measured in KRB were 28 °C and 17 °C and with a total average annual precipitation of 327 mm (Akhtar, 2017).

4.1.2. Water Usage in the Kabul River Basin

Water is a valuable resource that is progressively becoming more scarce. Water use has significantly increased globally due to population growth, industry, and urbanization. KRB's water resources are not always in the right place and time to meet present and expected needs for sustainable socio-economic development, flood control, irrigation, industry, domestic use, and power generation due to insufficient water infrastructure and climate conditions. Afghanistan can store water from its infrequent rainy seasons and rapid snow melting by constructing dams and reservoirs for various purposes throughout the year.

Three categories of use of water in KRB have been defined: beneficial water use (e.g., rain-fed crops, forest, and shrubs, rangeland), non-beneficial water use (e.g., losses from watercourse), and controlled or regulated water consumption (e.g., irrigation, livestock, domestic use) (FAO-MEW, 2015).

In Afghanistan, the natural discharge peak happens in the spring and early summer. Over a significant portion of the basin, a minimal flow is seen from late summer to winter. During the minimum-flow season, many rivers lose some of their discharge or are reduced to small, which are typically insufficient to meet agricultural water needs (Petr, 1999).

4.2. Materials

This research has used different datasets for flood risk assessment and analysis. The hydraulic model (HEC-RAS), literature review, and AHP modeling approach using ArcGIS software employed in this study dictated the choice and application of data for identifying potential flood zone, flood risk assessment, mapping, and mitigation strategies.

The data used in this research include LULC, soil type, lithology, and hydro-meteorological data (rainfall, measured flow rate). Additionally, topography data (e.g., DEM, DTM) played an essential role in the analysis. Hydro-meteorological data (rainfall, measured flow rate) from 2008 to 2019 were obtained from the MEW of Afghanistan.

For the identification of potential flood zone in the whole KRB based on the AHP modeling approach using ArcGIS software, ten different types of thematic maps (Elevation, Precipitation, Slope, LU/LC, Geology, Soil, Distance to River channel, NDVI, Curvature, and TWI) have been used.

A hydraulic model has been applied only for the Kunar and lower Kabul sub-basin to assess the flood risk. Recorded flow data, DTM, and LULC data were applied in the HEC-RAS to evaluate flood risk in these sub-catchments. In this work, LULC was downloaded from ESA Sentinel-2 imagery for the year 2021 and used for modeling purposes. The geological map for the research area was obtained from the United States Department of the Interior, which developed the lithology map of Afghanistan (Figure 5.8). Geology of the research area includes a variety of different types of rocks (Limestone and dolomite, Metamorphic rocks, Rhyolite to andesite, Sand, Schist and phyllite, Andesitic tuff, Basalt, Rhyolite, Travertine, Volcanic and sedimentary Rocks, Basalt, Conglomerate, Clay, Sandstone, Diorite, Gabbro, diorite, Gneiss, and Granite).
The soil type of the study area is downloaded from USDA which was developed for Afghanistan.

4.2.1. Terrain Data

DEM data was obtained from the ALOS GDSM (AW3D30), with a 30 m resolution. The Advanced Land Observing Satellite "DAICHI" was used to collect the images for the collection (ALOS). The 30-meter mesh version of the dataset also has elevation precision, which is among the highest in the world (AW3D30).

DEM is used to generate thematic maps (e.g., Slope, altitude, curvature, TWI, and Distance to River channels). Also, DEM has been used as Digital Terrain Model (DTM). DEM has been resampled to 20 m resolution to be used as a 2D flow area and development of mitigation measures in a hydraulic model (HEC-RAS) environment.

4.2.2. River Flow

This study used the maximum annual flow rates of the Kabul River Basin at four stations (Asmar, Pich, Pul-Behsod, Sorkh-Rod) for flood risk mapping and flood frequency analysis with different return periods and mitigation strategies in the HEC-RAS environment for the Kunar, and lower Kabul sub-basins (Table 4.1). Annual flow data from 2009 to 2018 were obtained from the MEW of Afghanistan in SI unit format.

Record of river flow started in 1946 in the country, and data were gathered until the 1980s (Westfall & Latkovich, 1966). The hydrological data network was damaged during the Afghan civil war, which left a significant gap in the hydrological cycle information after collection period. With the financial help of international donors, the monitoring of hydrological data in Afghanistan was restarted in 2003. Table 4.1 shows the specifications of flow rate gauge station of lower Kabul sub-basin and Kunar river.

Table 4.1. Specifications of flow rate station in the Kunar and lower Kabul sub-basin

Station_Name	Latitude (N)	Longitude (E)	Elevation (m)	Drainage Area Km^2
Asmar	34.9	71.2	832	19960
Chaghasarai (Pich)	34.9	71.1	847	3855
Pul-i-Behsod	34.4	70.5	555	36980
Sultanpor((SorkhRod)	34.4	70.3	686	2590

4.2.3. Precipitation Data

Daily series of rainfall data of 25 stations from 2009 to 2018 were obtained from MEW of Afghanistan for Kabul River Basin (Table 4.2). This dataset is used for the determination of potential flood zone in the whole KRB based on the AHP modeling approach using ArcGIS software. Table 4.2 shows characteristics of the meteorological data station in the KRB. Overall, these data play an essential role in predicting, understanding, identifying flood prone zones, and mitigating risk and impacts of floods, and ensuring safety the well-being of communities that are at risk, and making informed decisions about flood preparedness and engineering responses. Table 4.2 illustrates meteorological information regarding the station's characteristics of Kabul RB.

Table 4.2. Characteristics of the meteorological data station in Kabul RB

Station_Name	Latitude (N)	Longitude E	Altitude m	Area (Km^2)
Asmar	34.9	71.2	832	19960
Bagh-i-Lala	35.2	69.2	1698	485
Bagh-i-Omomi	35.1	69.3	1587	205
Chaghasarai	34.9	71.1	847	3855
Doabi	35.3	69.6	2059	789
Keraman	35.3	69.7	2232	110
Khawak	35.6	69.9	2405	369
Maton	33.4	69.9	1177	
Naghlo	36.6	69.7	998	26046
Nawabad	34.8	71.1	796	23960
Nazdik-i-Dowamandi	33.3	69.6	1527	
Nazdik-i-Khawak	35.6	69.9	2407	981
Omarz	35.4	69.6	2042	2240
Payin-i-Qargha	34.6	69.0	1970	1970
Pul-i-Ashawa	35.1	69.1	1624	4020
Pul-i-Behsod	34.4	70.5	555	36980
Pul-i-Islamabad	34.8	70.1	982	1142
Pul-i-Kama	34.5	70.6	558	26005
Pul-i-Qarghayi	34.5	70.2	643	6155
Pul-i-Surkh	34.4	68.8	2216	1305
Qala-i-Malik	34.6	70.0	2211	69
Shokhi	34.9	69.5	1374	10850
Sultanpor	34.4	70.3	686	2590
Tang-i-Gulbahar	35.1	69.3	1625	3565
Tang-i-Sayedan	34.4	69.1	1870	1625

CHAPTER 5

GIS-AHP RESULT AND DISCUSSION

5.1. Flood Susceptibility Modeling

Flooding is a common natural catastrophe on the planet, with enormous negative impacts on the environment, socioeconomic, properties, etc. Afghanistan is a country that is prone to flooding, particularly during the spring and summer months. The country's rugged terrain, combined with a lack of adequate infrastructure and resources, makes it especially vulnerable to the effects of flash floods and heavy rains, which have caused significant damage to agricultural land, homes, and infrastructure.

GIS, RS techniques, and the AHP have tremendously assisted in investigating natural risks, such as flood mapping and flood assessment based on various criteria, purposes, uncertainty, and complexity of the issues. Integration of GIS and AHP approach is beneficial in identifying flood-prone zones. This is due to the complex combination of variables that affect flood risk, including elevation, land use, precipitation, lithology, distance to a river, TWI, NDVI, slope, soil type, LULC, etc.

GIS can be used to generate detailed maps of these factors and overlay them to create a comprehensive picture of the potential for flooding in a given location. Moreover, the AHP technique can be used to rank and prioritize the different factors based on their relative importance in evaluating flood prone-areas and risks. Therefore, the combination of GIS and AHP offers a significant tool for making flood risk judgments and assessments. In this research a GIS-based MCDA model was employed to conduct flood hazard evaluation. The analysis was based on ten flood-hazard criteria as documented in the literature and analyzed in Section 5.1.2.

5.1.1. Multi Criteria Decision Analysis (MCDA) Technique

Analytical Hierarchy Process is a multi criteria decision making method that utilizes hierarchical structures to describe an issue and to develop priorities for alternative solutions according to user assessment and judgment (Malczewski, 2006). AHP is a multi criteria decision analysis technique developed by Dr. Thomas Saaty in the 1970s. AHP assists individuals or groups in deciding on complicated issues by breaking down a problem into a hierarchy of structures and more manageable sub-problems and then comparing the relative importance of each sub-problem (Saaty, 1980). The AHP process can be applied to various functions, including product development, project management, strategic planning, and investment analysis. It is beneficial when there are several criteria or considerations to consider and when a team of people with various viewpoints and perspectives is involved in the decision-making process. AHP is a technique in risk assessment. Many researchers, including (Das, 2018), (Sinha et al., 2008), etc., have used the AHP approach for flood investigation, flood susceptibility, and flood mapping. The variables included in this study are described in Section 5.1.2 along with the methods .utilized to investigate and create each component map

The AHP procedure consists of the following steps (Saaty, 1980):

- Recognize the problem and decide what to do.
- Generate a hierarchical system: Make a list of factors that contribute to the problem.
- Investigate each criterion or sub-criterion compared to every other criterion or sub-criterion.
- Compute Priorities: Using the pairwise comparison outcomes, determine relative weights or priorities of each factor or sub-criterion. The weights are calculated using a mathematical formula that takes the values of the pairwise comparison matrix into account.
- Sensitivity analysis: Analyze the consistency of pairwise matrix of the factor using a consistency ratio. The value of CR should be below 0.1 to be acceptable.
- Make the judgment and decision: Use the calculated weights to make the decision.

5.1.1.1. AHP Model and Weighting

AHP method was applied to calculate the final weights for each flood factor. The pair-wise comparison matrix was computed as the initial phase in the AHP, and each item in the matrix shows relative standing of each element to others. The technique of comparisons per pair is used to determine the parameter weight coefficients. A numerical scale matrix from 1 to 9 (Table 3.2), which was developed by (Saaty, 1980), was applied to assess relative importance of each element and to establish the pair-wise comparison matrix by Equation 5.1. The decision analysis matrix evaluates each alternative using the evaluation criteria. The decision analysis matrix is the following if the problem has n factors and m alternatives:

Let PC represent an m x n pairwise comparison matrix:

$$\mathrm{PC} = \begin{bmatrix} d_{11} & d_{12} & \cdots & d_{1n} \\ d_{21} & d_{22} & \cdots & d_{2n} \\ \vdots & \vdots & \vdots & \vdots \\ d_{m1} & d_{m2} & \cdots & d_{mn} \end{bmatrix} \tag{5.1}$$

where the aspects d_{ij} represent the relationship between both ith alternative and jth factors.Moreover, the weighting factor for each criterion was computed. Also, the normalized pair-wise matrix of the element was generated see (Table 5.2).

Table 5.1. Pair-wise comparison matrix of assigned flood variables

	RF	EL	SL	DTR	TWI	LULC	ST	GT	NDVI	CUR
RF	1	2	2	2	5	3	4	4	6	9
EL	1/2	1	1	2	4	5	4	5	7	9
SL	1/2	1	1	2	4	6	5	4	4	9
DTR	1/2	1/2	1/2	1	4	5	4	5	6	8
TWI	1/5	1/4	1/4	1/4	1	1	4	3	3	7
LULC	1/3	1/5	1/6	1/5	1	1	4	4	5	8
ST	1/4	1/4	1/5	1/4	1/4	1/4	1	1	1	5
GT	1/4	1/5	1/4	1/5	1/3	1/4	1	1	1	3
NDVI	1/6	1/4	1/4	1/4	1/3	1/5	1	1	1	3
CUR	1/10	1/8	1/10	1/8	1/7	1/4	1/5	1/3	1/3	1

RF: Rainfall, EL: Elevation, SL: Slope, DTR: Distance to the river, TWI, LULC, ST: Soil Type, GT: Geology Type, CUR: Curvature.

Table 5.2. Normalized pair-wise comparison matrix and criterion weights coefficient

	RF	EL	SL	DTR	TWI	LULC	ST	GT	NDVI	CUR	W(%)
RF	0.26	0.35	0.35	0.24	0.25	0.14	.14	.14	.17	.15	22
EL	0.13	0.18	0.17	0.24	0.02	0.23	.14	.18	0.2	.2	18
SL	0.13	0.18	0.17	0.24	0.02	0.27	.18	.14	.12	.12	18
DTR	0.13	0.09	0.09	0.12	0.02	0.23	.14	.18	.17	.17	15
TWI	0.05	0.04	0.04	0.03	0.05	0.05	.14	.11	.09	.09	8
LULC	0.09	0.04	0.03	0.02	0.05	0.05	.14	.14	.15	.15	7
ST	0.07	0.04	0.03	0.03	0.01	0.01	.04	.04	.03	.03	3
G	0.07	0.04	0.04	0.02	0.02	0.01	.04	.04	.03	.03	4
NDVI	0.04	0.02	0.04	0.02	0.02	0.01	.04	.04	.03	.01	3
CUR	0.03	0.02	0.02	0.02	0.01	0.01	.01	.01	.01	0.02	2

After calculating the weights for each flood-controlling component, Equations 3.2 and 3.1, developed by (Saaty, 1980), were used to conduct a consistency check to see whether or not the comparison is accurate and consistent. $\lambda max,$ which is the eigenvalue of the 10 x 10 matrix, was found to be 10.9. Equation 3.2 is used to calculate CI as 0.1. CR was calculated to be 0.067 (CR = 0.067 < 0.1), indicating that the consistency of pair-wise comparison element of the matrix is appropriate and sufficient for the assessment.

The criteria/alternatives that have the most influence on flooding extent and dimensions are the ones with the highest weight coefficient. Flood criteria were generated in raster format, and then each element was categorized into one of five common uniform measurement scales, ranging from 1 extremely low sensitivity to flooding to 5 very high susceptibilities to flooding). In Table 5.3, higher rank categorized rating values are associated with more vulnerable areas to flooding, whereas smaller values are identified with less vulnerable regions. Table 5.3. Weights and related feature of thematic layers using AHP Method.

Table 5.3. Weights and related feature of thematic layers using AHP Method.

Influencing Criteria	Classes	Potentiality of flood Risk	Rank	(Wi) %
NDVI	< -0.049	Very High	5	
	-0.049-0.094	High	4	3
	0.094-0.186	Moderate	3	
	0.186-0.335	Low	2	
	> 0.335	Very Low	1	
Rainfall (mm/yr)	< 189	Very Low	1	
	189-264	Low	2	22
	264-339	Moderate	3	
	339-414.6	High	4	
	414.6-489.6	Very High	5	
Curvature	Concave	Very Low	1	
	Flat	Very High	5	2
	Convex	Moderate	3	
Distance to River (m)	< 200	Very High	5	
	200-500	High	4	15
	500-1000	Moderate	3	
	1000-5000	Low	2	
	> 5000	Very Low	1	
Elevation (m)	< 1000	Very High	5	
	1000-1900	High	4	18
	1900-3500	Moderate	3	
	3500-4500	Low	2	
	> 4500	Very Low	1	
Slope (°)	< 10	Very High	5	
	10-15	High	4	
	15-20	Moderate	3	18
	20-35	Low	2	
	> 35	Very Low	1	
TWI	<5	Very Low	1	
	5-7	Low	2	
	7-9.4	Moderate	3	8
	9.4-13	High	4	
	>13	Very High	5	

(Cont. on next page)

Table 5.3 (Cont.).

Influencing Criteria	Classes	Potentiality of flood Risk	Rank	(Wi) %
LULC	Water	Very Low	1	
	Forest	Very Low	1	
	Crops	High	4	
	Urban Areas	Very High	5	
	Flood Vegetation	Low	2	7
	Bare Ground	Moderate	3	
	Snow/Ice	Very Low	1	
	Grass	Very Low	1	
	Scrub/Shrub	Moderate	3	
Soil	Rocky Land with Lithic Cryorthents	Very High	5	
	Rocky Land with Ice-Capped Bare rock	High	4	
	Rocky Land with Lithic Haplocryids	Low	3	
	Calcixeralfs with Xerochrepts	Very Low	1	
	Xerorthents with	Low	2	
	Rocky Land with Lithic Haplocambids	Moderate	3	3
	Torriorthents with Torifluvents	High	4	
	Torifluvents with Torripsamments	Low	2	
	Haplocambids with Torripsamments	Very Low	1	
	Haplocambids with Torriorthents	Low	2	

(Cont. on next page)

Table 5.3 (Cont.).

Influencing Criteria	Classes	Potentiality of flood Risk	Rank	(Wi) %
Lithology	clay and shale	Very High	5	
	conglomerate and sandstone	Very Low		
	limestone & shale	Moderate	3	
	gneiss	High	4	
	granite	Very High	5	
	Fan alluvium and colluvium	Low	2	
	sandstone & siltstone	Very Low	1	
	Volcanic & sedimentary rocks	Moderate	3	
	Basalt	Moderate	3	
	metamorphic rocks-undivided	Moderate	3	
	limestone & dolomite	Low	2	
	schist & phyllite	High	4	
	granodiorite and granosyenite	Moderate	3	4
	siltstone & sandstone	High	4	
	marble & gneiss	High	4	
	diorite & plagiogranite	Very High	5	
	Rhyolite	High	4	
	schist	Low	2	
	Travertine	Very Low	1	
	basaltic andesite & basalt	Moderate	3	
	gabbro & monzonite	High	4	
	granodiorite sandstone & conglomerate	Very Low	1	
	ultramafic intrusions	Moderate	3	
	Basalt lava	High	4	
	gneiss & granite	High	4	
	limestone	Moderate	3	

(Cont. on next page)

Table 5.3 (Cont.).

Influencing Criteria	Classes	Potentiality of flood Risk	Rank	(Wi) %
	Metavolcanic andesitic lava	High	4	
	limestone & sandstone	Moderate	3	
	gabbro & maficmeta volcanics	High	4	
	Lava	Very High	5	
	basalt & sandstone	Moderate	3	
	shale	High	4	
	Andesitic tuff			
	Meta volcanic lava	Moderate	3	
	granodiorite and granite	High	4	
	limestone & chert	Very High	5	
	gabbro & diorite	Moderate	3	

5.1.2. Influencing Flood Factors

Effective criteria on flood potential zones are based on an extensive assessment of the literature review, including precipitation, distance to the channels, slope percent, LU-LC, elevation, geology, soil type, NDVI, TWI, etc. All factors were created and transformed to a raster with 28 x 28 m grid-cells for applying the AHP technique and flood susceptibility map for the whole KRB. AHP method is employed by choosing flooding risk factors, assigning relative rates, and creating a pair-wise comparison matrix.

5.1.2.1. Rainfall

Rainfall is a critical factor in identifying flood-prone areas since it is an important element of the water cycle and a key contributor to flooding. Flooding might occur if the amount of rainfall is greater than capacity of water bodies to store water. Potential of flooding is affected by a number of factors, including intensity and frequency of

precipitation, the local terrain (e.g., steep slope, poor drainage system), landslides, dam failure, and the water management system. Understanding the impact of rainfall on flooding is crucial for effective flood mitigation and risk management strategies.

Precipitation data from 28 rainfall observation stations in (Figure 5.1) in Kabul River Basin were obtained from the MEW of Afghanistan from 2009 to 2019. IDW interpolation technique was applied using ArcGIS to analyze and create a spatial distribution of the annual mean rainfall map of the study area (Figure 5.2). Rainfall raster layer was classified into five categories. The redefined rainfall map was rated from 1 for the least precipitation to 5 for the greatest (Table 5.3).

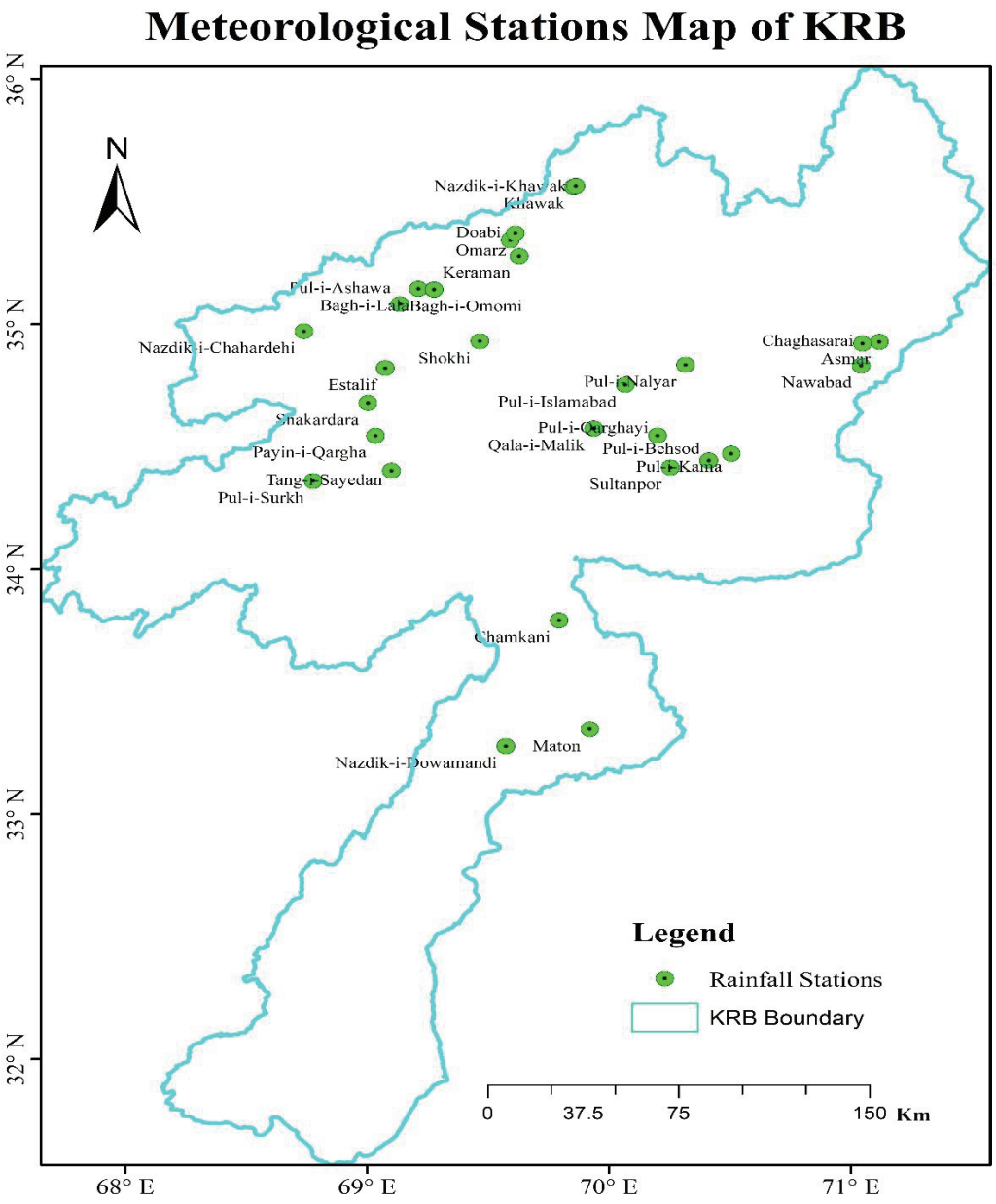

Figure 5.1. Map of Meteorological Stations of KRB

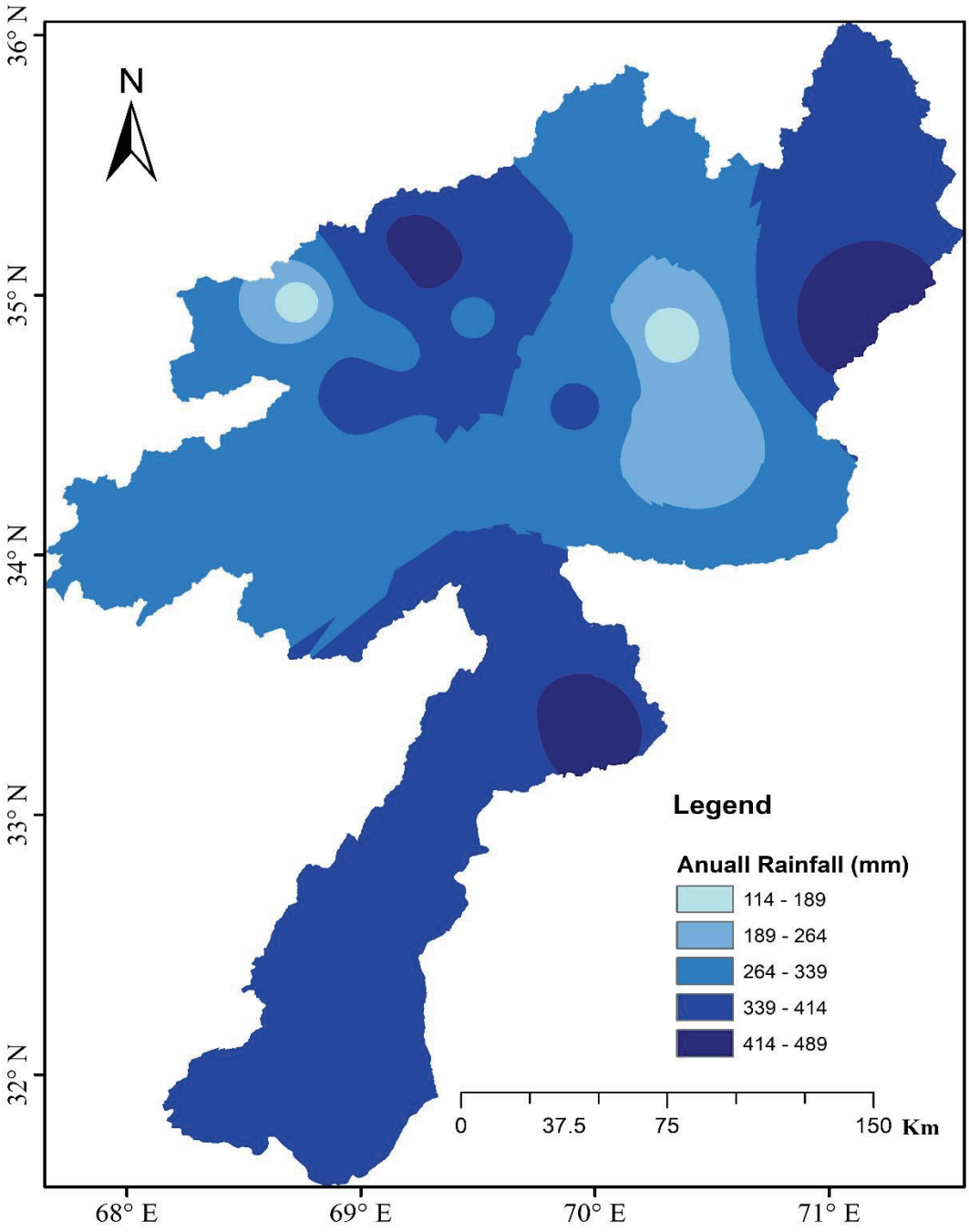

Figure 5.2. Mean Annual Precipitation map of Kabul RB

5.1.2.2. Land Use-Land Cover

LULC is a crucial factor in determining runoff and possible floods in a watershed (Kachouri et al., 2015). LULC has a great impact on infiltration, rate of recharge, evapotranspiration, and interaction between groundwater. On the other hand, runoff is accelerated by bare lands and impermeable surfaces such as roadways and residential areas. Urbanization frequently results in a reduction in lag-time of rainfall, and an increase in peak flow and cumulative flow (Skinner et al.).

Moreover, bare fields are moderately prone to flooding risks. Rain can quickly penetrate the Earth surface and increase velocity and amount of runoff because bare soil cannot effectively absorb or hold water. Bare soil can become compacted, which lowers its capacity to absorb precipitation and can increase the potential for erosion. The lack of vegetative cover also makes the flooding risk worse, which prevents rain from being absorbed (Owuor et al., 2016).

The LULC in the study area were categorized as: croplands, forest, residential areas, flooded vegetation, bare ground, snow, scrub/shrub, and grass. On floodplains, scrub/shrub vegetation can be extremely important since it is the most land cover type in the region. These kinds of plants typically have deep, wide root systems that improve soil stabilization and minimize erosion, reducing the velocity and volume of floodwaters, which can reduce the risk of flooding, especially downstream. Moreover, scrub/shrub vegetation can be an essential part of a natural-based solution for flood-prevention methods, reducing danger and effects of flood in flood-prone locations. LULC layer of KRB is shown in Figure 5.3.

A rating from 1 for the least influential factor to 5 for the most influential criteria was assigned to the LULC layer (Table 5.3). Following are some strategies for managing LU-LC to decrease the impact of floods as a part of mitigation strategies for interested areas:

- Wetlands, forests, and natural vegetation can behave as water sponges by absorbing excess and storing significant amounts of water. To reduce the adverse impacts of floods, land use policies can promote the preservation of native plants in flood-prone locations.

- With the absorption and filtration of storm water, green infrastructure such as rain gardens and permeable pavements can decrease runoff. Green infrastructure can be utilized in metropolitan settings to mitigate the impact of flooding.
- Wetlands and riparian zones, which operate as buffer zones, can act as a natural barrier against floods by minimizing erosion and reducing the flow of water.

LU-LC management can be used to mitigate effects of floods by establishing and maintaining buffer zones, conserving natural vegetation, developing green infrastructure, and promoting sustainable land use techniques. Land use regulations may be essential to promoting these strategies and reducing the effects of floods (European-Directive, 2007).

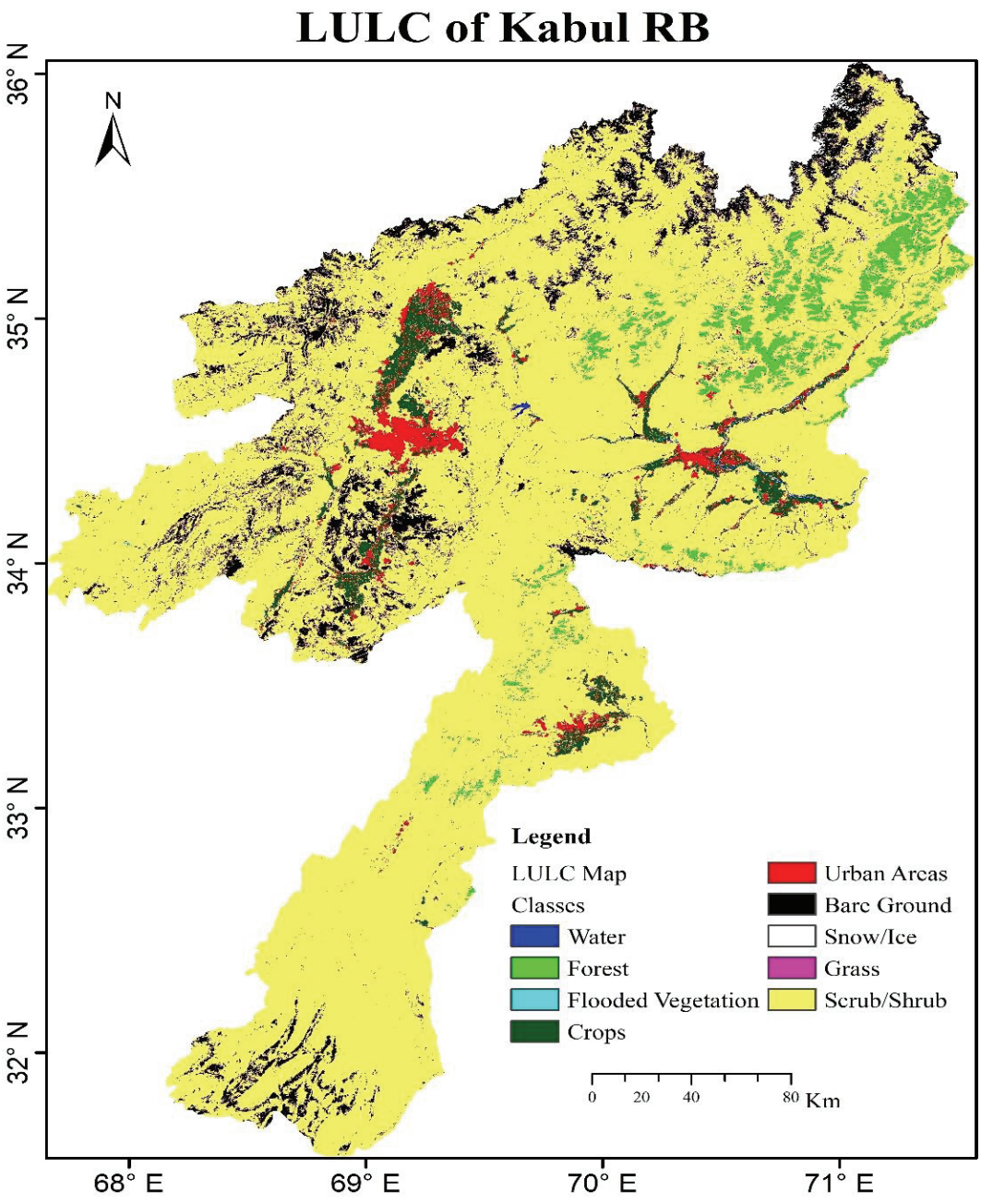

Figure 5.3. LULC Map of Kabul RB

5.1.2.3. Elevation

Several related studies indicate that altitude is one of the major variables determining the possibility of a flood (Grimm et al., 1995). The effects of flooding are significantly influenced by elevation. In general, areas with lower altitudes are more

vulnerable to flooding than areas with higher elevations. This is due to the fact that water naturally flows downstream, and lower-lying zones are more likely to gather and hold water during periods of intense precipitation or flooding. Due to gravitational force, water rapidly flows from highlands to plains, causing inundation in the lower regions (Das, 2019).

The Kabul River Basin's interaction between elevation and flood occurrences indicates that areas with higher altitudes have not been affected by floods, whereas the majority of historical events took place in lower altitudes. Moreover, areas at higher altitudes might be less vulnerable to flash floods, which are sudden, severe flooding occurrences that can happen in places with steep slopes or constrained valleys. A flash flood can be especially deadly because it often happens suddenly and without notice, giving communities little time to leave or take other protective measures.

By analyzing the level of previous flood occurrences in KRB, elevation grid of the research region was created using 28 m resolution DEM, and classified into five groups, as shown in Figure 5.4. Low-lying regions were given a maximum rating of 5 since they were thought to be more vulnerable to floods than higher-elevation areas. A rating score from 1 to 5 was assigned for elevation criteria to show the Potentiality for flood susceptibility (Table 5.3).

Flooding at high elevations in Afghanistan is a rare event, but it can occur for a number of reasons, including severe rain and snowmelt, while in the low-lying area, it is a major concern in the KRB. The steep terrain and lack of sufficient infrastructure increase the impact of floods, causing major damage to houses, property, and infrastructure and human casualties. Afghanistan is home to numerous glaciers, some of which are in danger of exploding as a result of climate change, which is intensifying their melting. Rapid water flows from glacial lakes can result in catastrophic floods downstream. The government and international organizations must act to minimize the impact of floods and deal with their causal factors (e.g., the threat of glaciers and snow-melting).

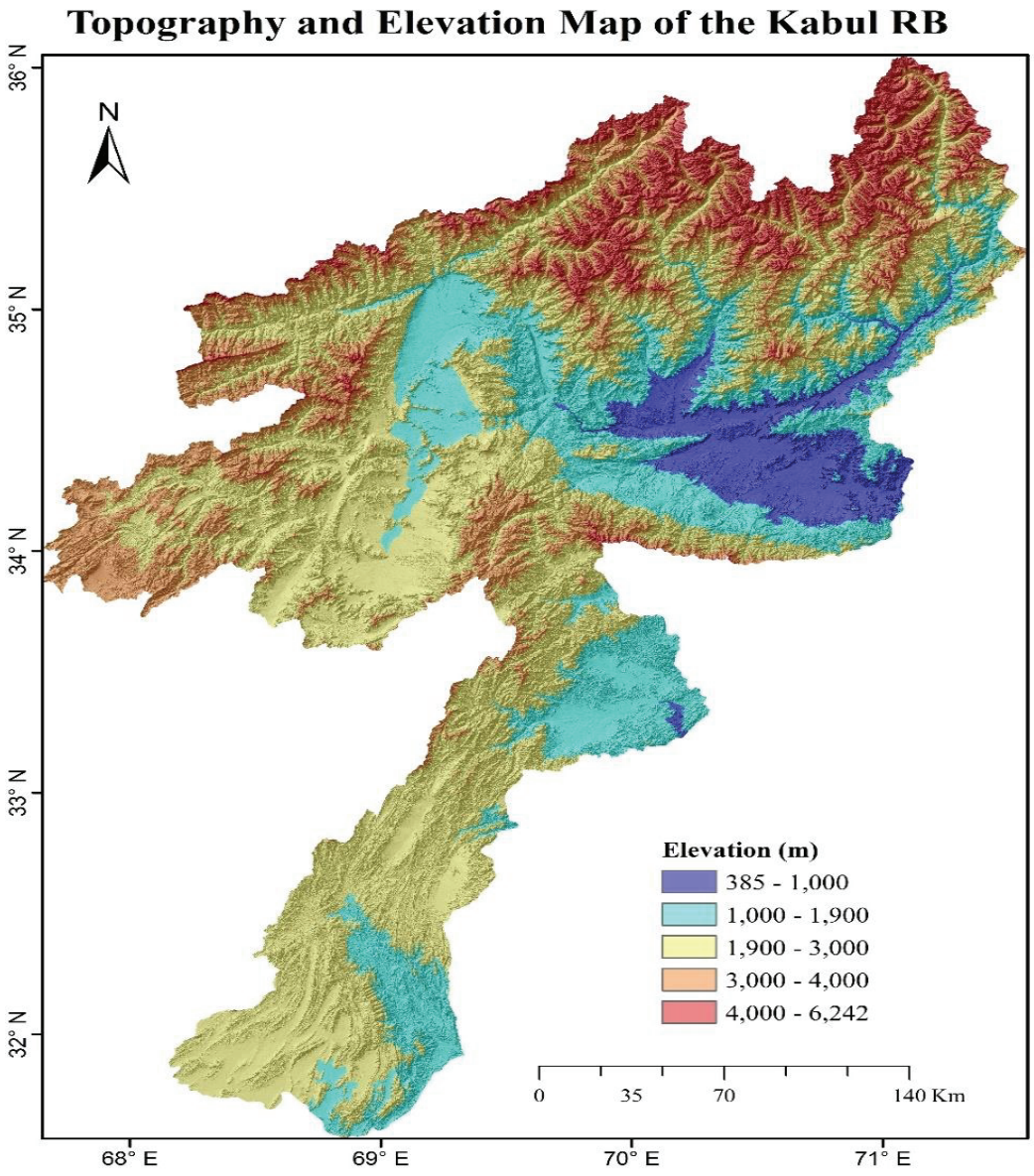

Figure 5.4. Elevation map of KRB

Elevation level generated by ArcGIS model happens to be the most informative component. This demonstrates during periods of intense rainfall, floods tend to occur most frequently in low-lying, shallow areas surrounding rivers (Figure 5.4).

5.1.2.4. Slope

In any geomorphic environment, runoff and accumulation of water process depend on ground slope (Fernández & Lutz, 2010). It affects the amount of ground runoff and infiltration since water tries to flow from higher to lower altitudes. Flooding can be significantly impacted by slope of topography. A steep slope can increase the velocity and the force with which water flows, hence raising the risk of flash flooding. Rain that falls on a steep gradient flows downstream more quickly and has less time to seep into the ground or be absorbed by vegetation. Flooding is more likely to happen in low altitude, flat, and slightly sloping (0–18°) locations (Termeh et al., 2018). As a consequence, rivers, streams, and other water bodies downstream and lower slopes accumulate more water, which raises the risk of floods.

A moderate and gentle slope can help by decreasing the water flow and enhancing ground infiltration. This can improve rivers' and other water bodies' ability to manage excess water without flooding while also lowering the risk of flash floods. Furthermore, slope of ground can influence direction of water movement. If slope is angled towards a specific region, water will be directed there, raises the likelihood of flooding. Flooding in KRB can be considerably impacted by the slope of the area. The Kabul watershed is situated in the Hindu Kush Mountains, with steep slopes and narrow valleys. The risk of flash floods can increase due to the steep slopes' potential to accelerate and intensify water flow. The water runoff from the steep slopes can rapidly accumulate in the narrow valleys during extreme precipitation, resulting in flash floods that can be extremely damaging. Also, the areas with steep slopes have the potential to cause landslides that would block rivers and streams, resulting in flooding both downstream as well as upstream.

In addition, the Kabul River Basin's steep slopes may contribute to soil erosion and river and stream sedimentation. This might change how rivers flow and increase the chance of riverbank erosion, which might make floods catastrophic. It is essential to take the impact of slope on flooding into account. In contrast, developing flood prevention and management techniques in the area, including the establishment of a flood defenses system and other flood control structures, as well as land use planning to limit the danger of flooding since the KRB is located in steep terrain.

Using terrain data from the watershed's comprehensive 28 m resolution DEM, slope of the research area was obtained using ArcMap (Figure 5.5). slope parameters were

categorized into five groups according to how the slope relates to previous flood occurrences. As a result, the gently/moderately sloping regions of the watershed were given the ratings of 5, 4, and 3, respectively, since they are thought to be areas that are more susceptible to flooding than high steep slopes (Table 5.3).

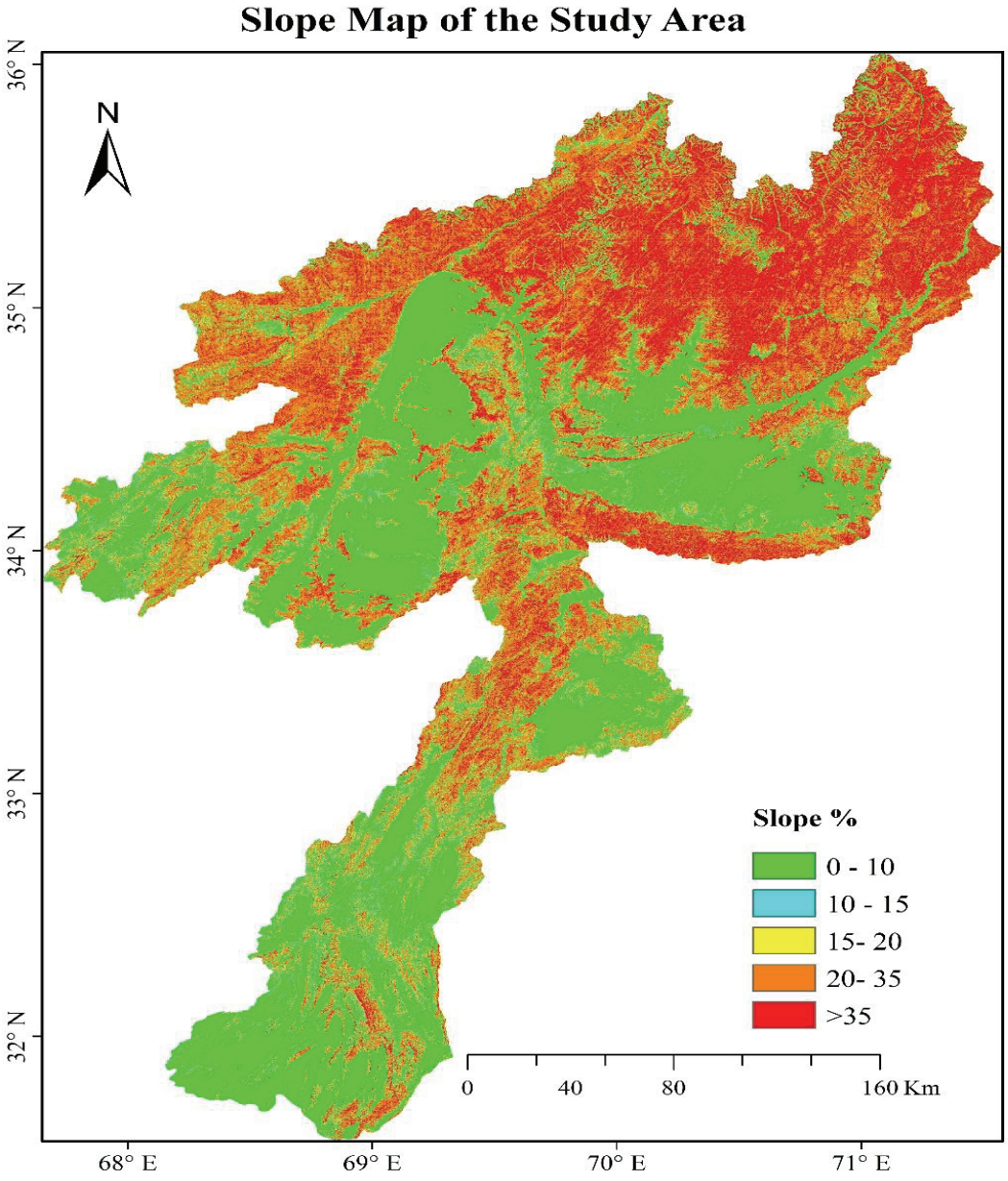

Figure 5.5. Slope Map of Kabul RB

5.1.2.5. Normalized-Difference-Vegetation Index (NDVI)

NDVI is widely used to assess vegetation as a flood control factor since it reduces runoff and functions as an obstacle. The NDVI is an index based on the earth's surface reflectance. Furthermore, The NDVI scale has values between -1 and +1. In contrast to a lower number, which suggests limited vegetation, a larger NDVI score indicates a good plant canopy. NDVI is frequently used to assess the growth and well-being of vegetation, as well as to evaluate the risk of flooding. Healthy and dense vegetation can absorb much more precipitation, reducing runoff and increasing water infiltration into the ground. It can assist in decreasing the probability of flooding.

Moreover, locations with a greater risk of flooding can identify using NDVI. For instance, regions with low NDVI values may be more susceptible to flooding and have less vegetative cover. High NDVI rates may represent a sign of healthy vegetation and reduced flood risk.

NDVI is calculated by ArcGIS software as a ratio between the near-infrared (NIR) and red (R) values from Landsat 8 imagery to evaluate vegetation density and greenness using equation 5.2. Landsat 8 imagery was downloaded for the year 2021 to evaluate NDVI for KRB. Figure 5.6 illustrate NDVI map of Kabul RB, which ranges from -0.5 to 0.78. Equation 5.2 shows the method for calculation of the normalized difference vegetation index

$$NDVI = \frac{(Band\ 5 - Band\ 4)}{(Band\ 5 + Band\ 4)} \tag{5.2}$$

As a consequence, the watersheds with lower NDVI values received scores of 5, 4, and 3, respectively, since it is considered to be locations that are vulnerable to flooding due to a lack of healthy and dense vegetation. On the other hand, the places with a higher NDVI value which shows more greenness and dense vegetation, are rated 2 and 1 (Table 5.3).

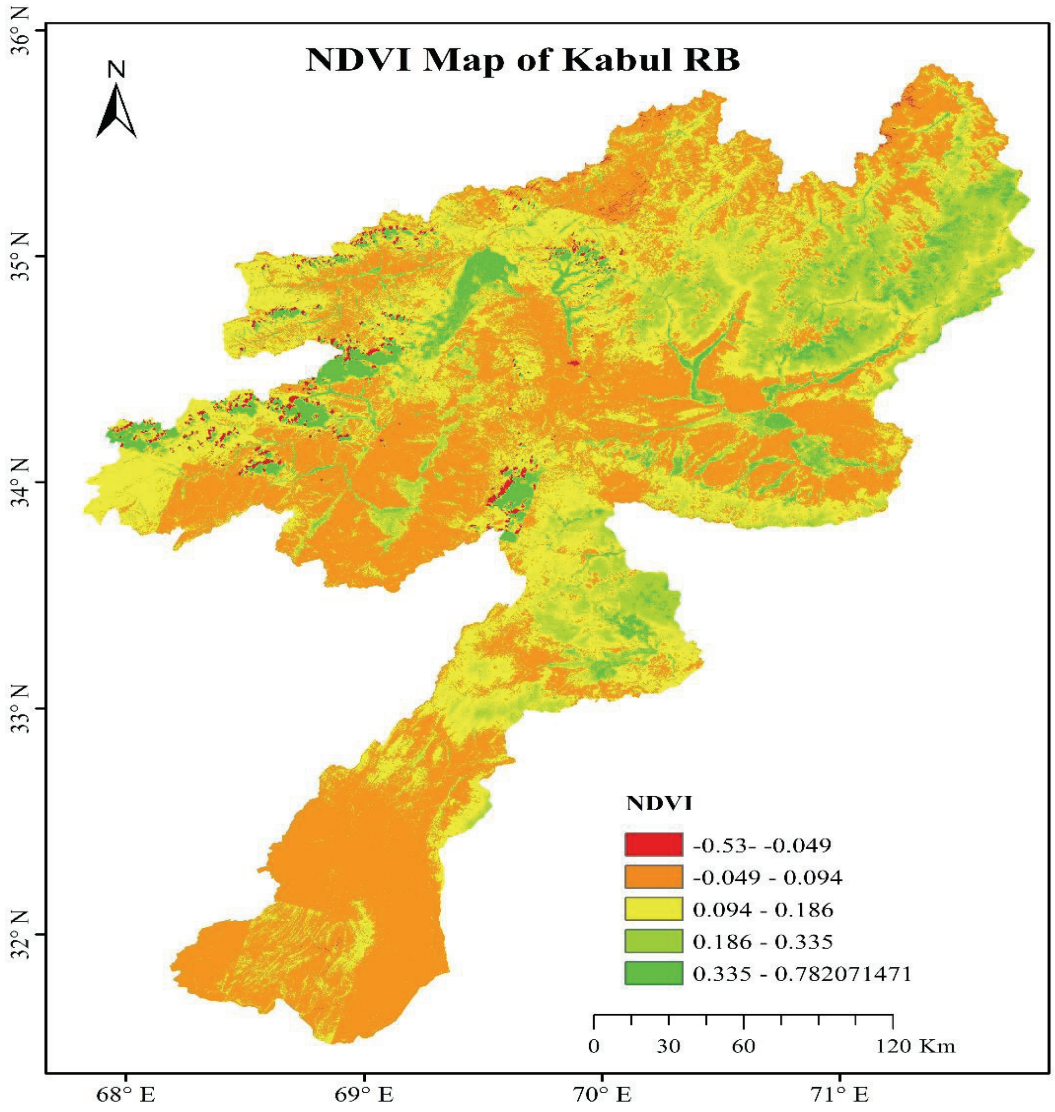

Figure 5.6. NDVI map of Kabul RB

5.1.2.6. Distance to Stream Channels

The distance to stream channels and river overflows can have major causes of flooding. The potential of experiencing a river system flood event is greatly increased by position relative to the stream channel (Fernández & Lutz, 2010; Predick & Turner, 2008). Heavy discharges frequently result in a rapid rise in river level during intense precipitation, which causes floods in the surrounding area. Thus, areas located near waterways face frequent flooding (Pham et al., 2020).

This is due to the fact that excess water needs somewhere to go when there is a substantial amount of rainfall or snowmelt. The water naturally flows downhill towards the nearest water body, which may be a stream channel, whether the ground is inclined or flat. The water may exceed its banks and flood neighboring areas if the watercourse system has reached its capacity or if there are obstructions (such as debris or other constructions) in the path. The effect of distance from river systems on flooding can change depending on many variables, like size and slope of the catchment, volume, and intensity of rainfall, and state of the actual stream channel. Even when a property is far from a river system, it may still be at risk of flooding if it's located in a low-lying area that is susceptible to flooding. Generally, in regions far from the river channel, there is less possibility of flooding. Although it is not the only element that causes flood risk, the distance to stream channels is an important one to take into account when estimating the possibility of flooding in a specific location.

Kabul River Basin is prone to frequent floods during the monsoon months; hence the distance to stream channels can have a large impact on flooding in the catchment. The basin is situated in a narrow valley with steep hillsides, which makes it especially susceptible to flooding. In the basin's river systems and tributaries, water can quickly accumulate during periods of intense precipitation, leading to overflows that flood neighboring areas. So, one of the most vital factors in finding how susceptible a property or location is to flood is its closeness to a stream channel.

Flooding in Kabul River Basin can also be influenced by the state of the actual stream courses. Anthropogenic, such as LU-LC, and erosion processes, have changed and extended over the natural channels throughout time. In turn, this may make the channels shallower and narrower, worsening the effects of floods during periods with significant surface runoff. Areas close to the river systems are deemed to be serious flood-hazard zones.

Using terrain data from the catchment's comprehensive 28 m resolution DEM, the distance to stream channels, which are more at risk of flooding in the research area, was estimated using ArcMap (Figure 5.7). Higher hazards and higher values are allocated for shorter distances, whereas lower risks and lower values are assigned for longer distances (Table 5.3).

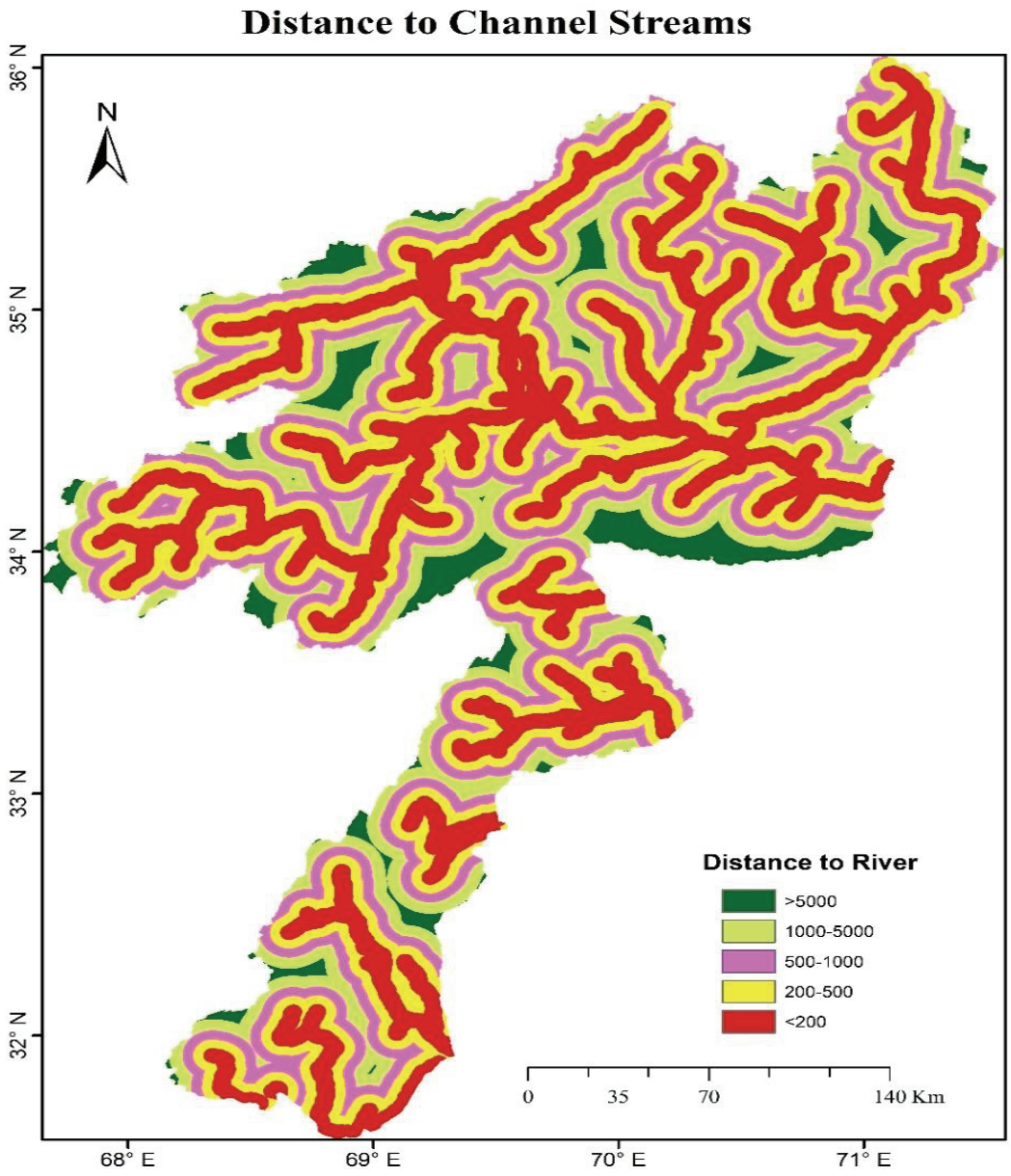

Figure 5.7. Thematic map of distance from stream channels

5.1.2.7. Lithology Formation

Flooding can also be influenced by lithology or the kind of rock and sediment that are available in a region. Geological formations in a region are crucial since they possess the potential to increase or decrease the size of flood occurrences. Depending on the conductivity and porosity, geological features of a region have an impact on runoff and infiltration either directly or indirectly (Rahmati, Pourghasemi, & Zeinivand, 2016). Geology predominates in studies of flood vulnerability because of the various lithological strata' sensitivities to active hydrological processes. The temporal and geographic

diversity of watersheds hydrology and sediment production are assumed to be significantly influenced by lithology (Miller et al., 1990). Furthermore, the permeability and erodibility of the torrential geological structures are natural elements that are crucial for determining flood risk (Stefanidis & Stathis, 2013).

Lithology can have a significant impact on flooding and its velocity. The following are some possibilities that lithology/geology may affect flooding risk (Srivastava et al., 2014):

- Water movement through the earth may be impacted by the lithology's permeability. Sandstone and gravel are examples of rocks and sediments that permit water to pass through them more freely. This may result in less surface water and a reduced danger of floods. In contrast, less permeable rocks and sediments, such as clay or shale, can block water from infiltrating, increasing surface water flow and increasing the potential of floods.
- The flow of surface water can also be impacted by the lithology's surface properties. Smooth and impermeable rocks and sediments, like some varieties of limestone, can increase surface runoff and raise the danger of flooding.

The geological map of the watershed was generated from Afghanistan's geologic age and lithology map, which was developed by USGS for Afghanistan (Doebrich, 2006) (Figure 5.8Error! Reference source not found.**).** Geology of KRB is various; for example, 16% of i ts sandstone and siltstone, 14% is gneiss, 6% is fan-alluvium, 14% conglomerate, 10% clay- shale, 4% limestone, dolomites 4% granite, etc. The lithology map’s ranking was given 1 to 5 based on the potential that increases flood risk (Table 5.3).

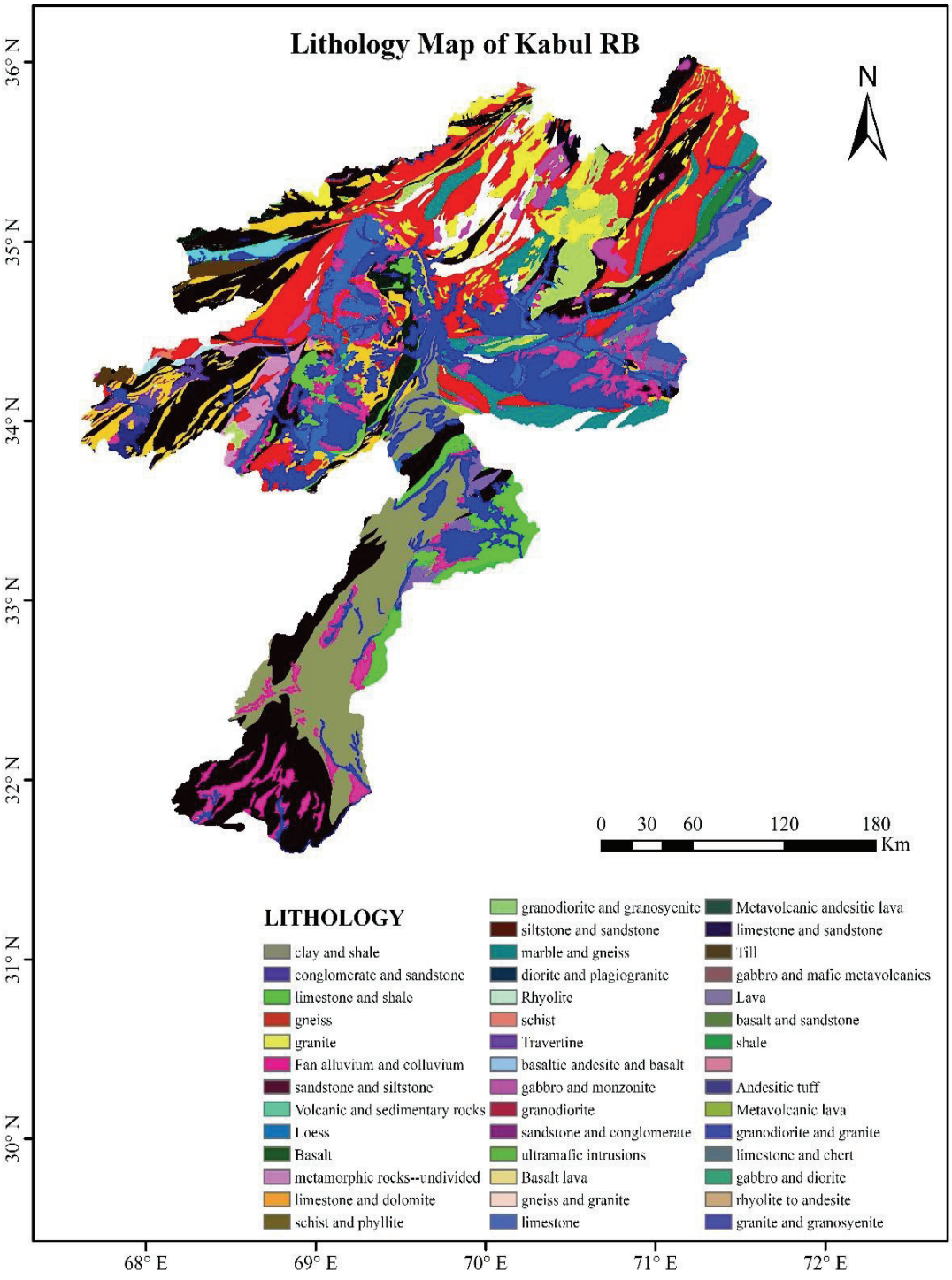

Figure 5.8. Geology Map of Kabul RB

5.1.2.8. Topographic Wetness Index

TWI specifies areas and dimensions of saturated areas prone to flow, and it estimates the effects of the local terrain on runoff process (Wilson & Gallant, 2000). TWI was developed in combination with the runoff model (Beven & Kirkby, 1979). TWI explains the water flow accumulating at a certain site in relation to a specific watershed (Pourali et al., 2016).

The TWI can be used to indicate regions that are more susceptible to floods since they are likely to have high soil moisture content. For instance, locations with high TWI values can have low-lying topography, shallow groundwater, or soils that are not well drained, all of which might make floods more possible. Policymakers and authorities can make well-informed decisions concerning land use and development through the use of TWI to identify areas at hazard for flooding. For instance, they might decide to restrict development in places with a high TWI value or put policies in place to improve the landscape's ability to absorb water, such as building green infrastructure or recreating wetlands. The TWI formula is expressed by Equation 5.3:

$$TWI = \ln\left(\frac{A_s}{tan\beta}\right) \tag{5.3}$$

A_s is the upslope watershed area, and β is local-slope angle in degree.

The TWI's accuracy is determined by the surface characteristics. The 28x28 m DEM is used to create a raster model of TWI and to specify flood-prone regions that are in danger of flooding based on this index (Figure 5.9). In order to estimate and develop an appropriate TWI, various slope values and flow routing methods were used. The resulting TWI models were then validated using existing watercourses such as a wetland area and observations using satellite images and remote sensing techniques during a flood event. Higher hazards and higher values are allocated for larger TWI values, whereas lower risks and lower values are assigned for smaller TWI values (Table 5.3).

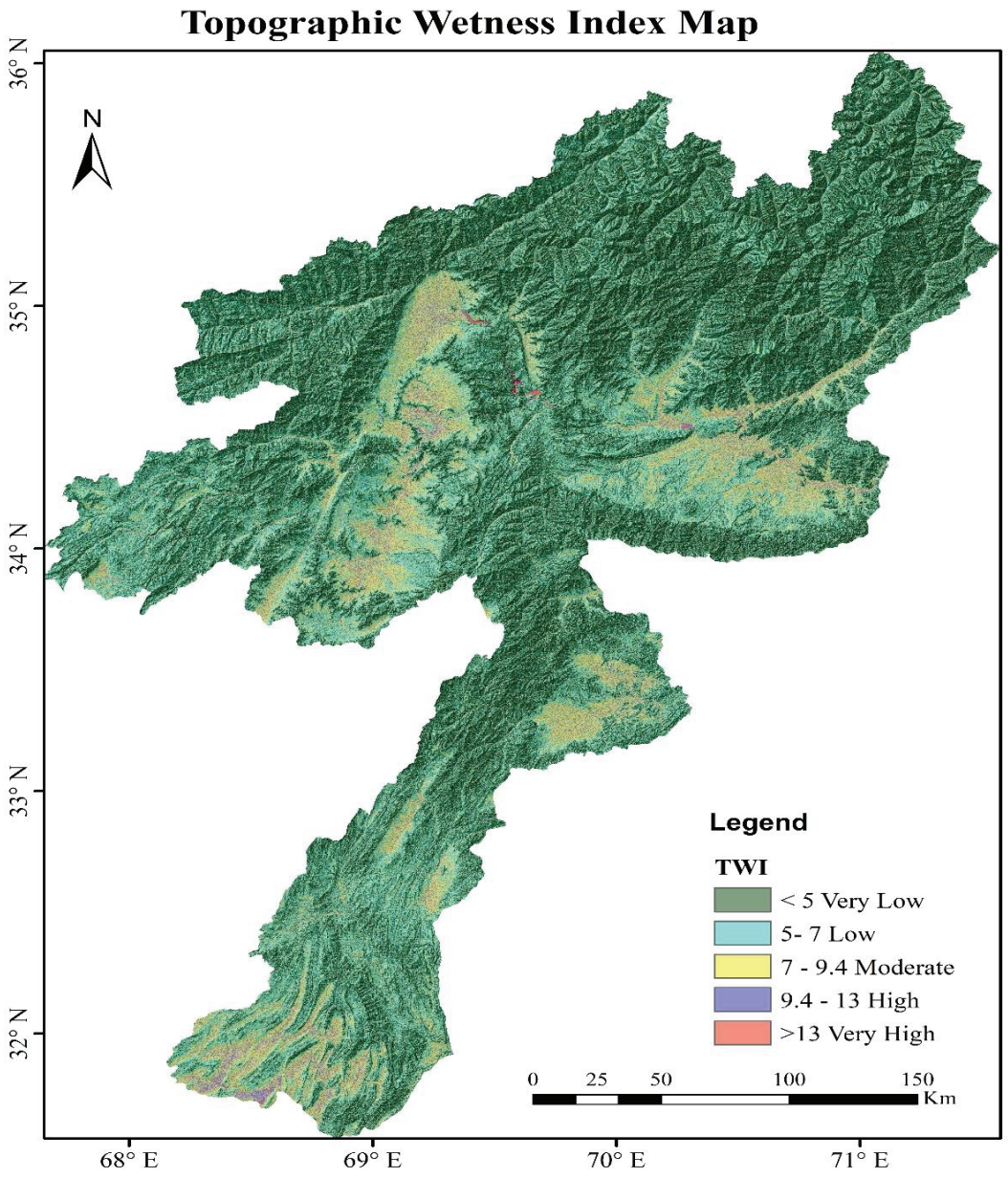

Figure 5.9. TWI Map of KRB

All in all, the Topographic Wetness Index is an effective tool for predicting the potential of flooding, as well as disaster response and preparedness attempts.

5.1.2.9. Soil Type

Soil texture has a major impact on flood events as it influences how soils can hold and receive water. The development of surface run-off and flooding processes is governed by soil texture since soil characteristics mostly determine water infiltration (Cosby et al., 1984). The texture of the soil is crucial for assessing how rapidly water can be absorbed as well as how much water the soil can hold, which impacts the possibility of flooding.

Many factors, including soil texture, might influence how flooding risk occurs and increases. The following are some ways that soil texture may impact flooding (Patel et al., 2021; Ponnamperuma, 1984):

- Infiltration rate: The amount of water that may infiltrate the soil depends on structure of soil, such as (Soil compaction, vegetation, texture, etc.). Sandy soils have a greater infiltration capacity due to their larger pores, which enable water to pass easily through them. On the other hand, clay has a low rate of infiltration due to its smaller pores, which are susceptible to rapid saturation and surface runoff. Also, during precipitation events, rocks can increase the quantity of surface runoff. Water may not be capable of infiltration into the soil rapidly enough if the terrain is covered with rocks, resulting in more surface runoff. Kabul River Basin is mostly covered by rock, which can increase the chance of flooding, especially flash floods.
- Erosion: During a flooding occurrence, rocks can potentially enhance the risk of erosion. The instability that rocks can create in water when it is running over the ground can accelerate erosion and soil loss.
- Surface runoff: is the result of excess precipitation flowing over the surface of the earth since it is not capable of absorbing all of the water. The soil's composition and texture, together with the frequency and duration of rainfall, all have an impact on the amount of surface runoff which define the extent and risk of flooding. KRB soil data obtained from USDA-SCS (Figure 5.110).

Higher hazards and higher values are allocated for soil texture with low permeability, whereas lower risks and lower values are assigned for soil type with high permeability based on the 1 to 5 rating score (Table 5.3).

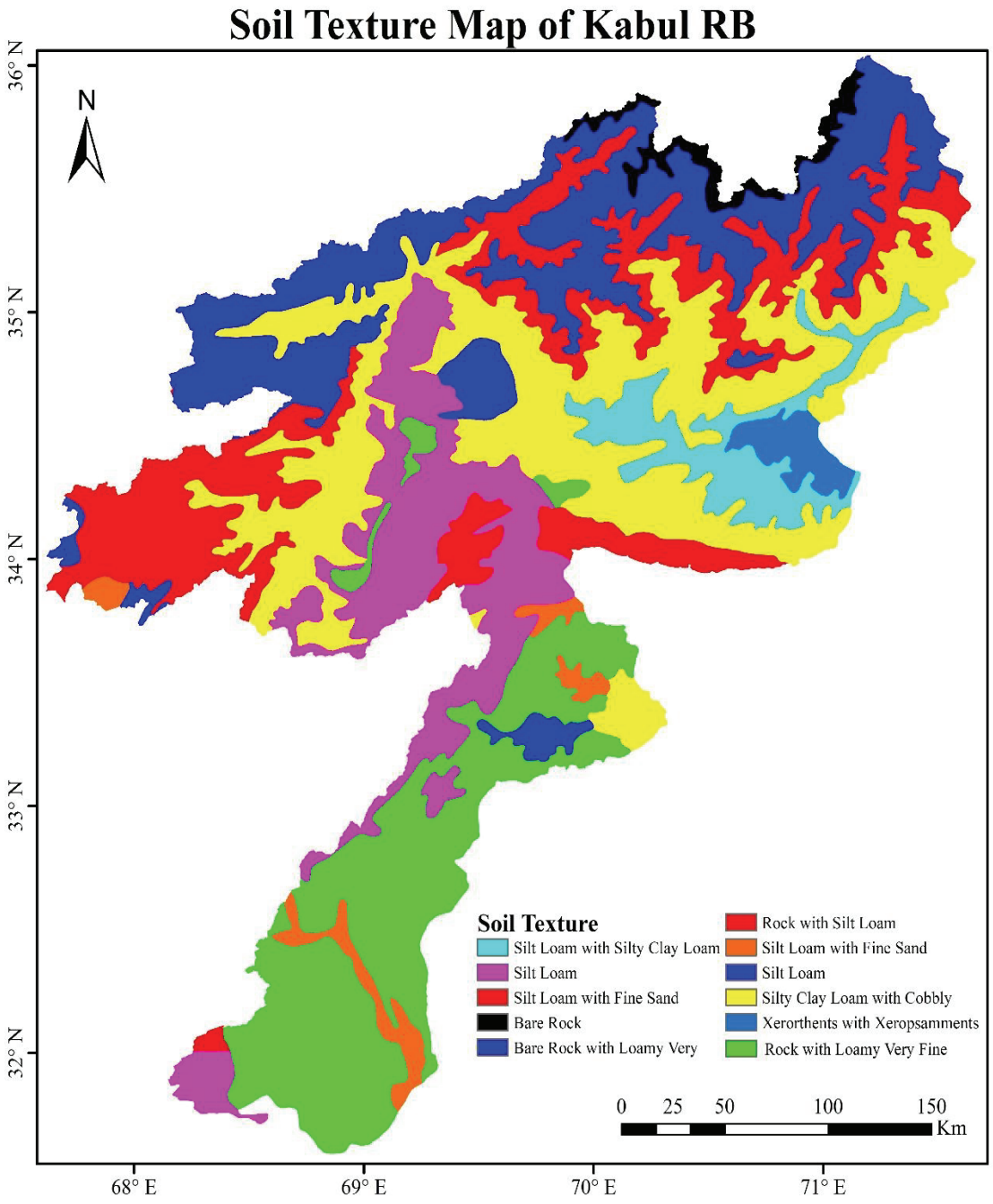

Figure 5.10. Kabul River Basin Soil Texture Map (USDA)

5.1.2.10. Curvature

Curvature represents morphology of the ground in a specific location and shows the degree of slope surface distortion (Wang et al., 2020). The curvature of the terrain can significantly affect the flooding process. High curvature areas experience faster runoff than relatively flat areas. One of the main causes of this is that water flows more quickly

downhill when it is channeled by curved surfaces rather than plain ones. This could result in a greater volume of water accumulating in low-lying regions, which may accelerate the risk of flooding.

Water movement through underground aquifers and drainage systems can also be influenced by curvature of ground. During heavy rainfall events, areas with high curvature may have more complex drainage patterns that are more difficult to predict and manage. Curvature is classified into three types (convex, concave, and flat regions) (Mojaddadi et al., 2017).

Curvature layer of KRB, which indicates direction of the maximum slope, is an influential element in flood occurrence. Curvature was computed from DEM and classified into three groups (convex, concave, and flat areas) using ArcGIS software (Figure 5.11). In a cell with a negative slope, the surface is upwardly convex, which will delay the flow. On the other hand, a positive slope shows that surface of that cell is upwardly concave, which can cause the flow to be accelerated.

Higher flood hazards and higher values are allocated for areas with flat Curvature, whereas areas with lower risk of flooding are assigned for concave and convex curvature based on the 1 to 5 scale (Table 5.3).

In general, the curvature of the land surface can be useful in evaluation of flood risk and in developing flood management plans. Decision-makers can more accurately predict and get prepared for potential future flood events by knowing the effect of curvature on the flooding process.

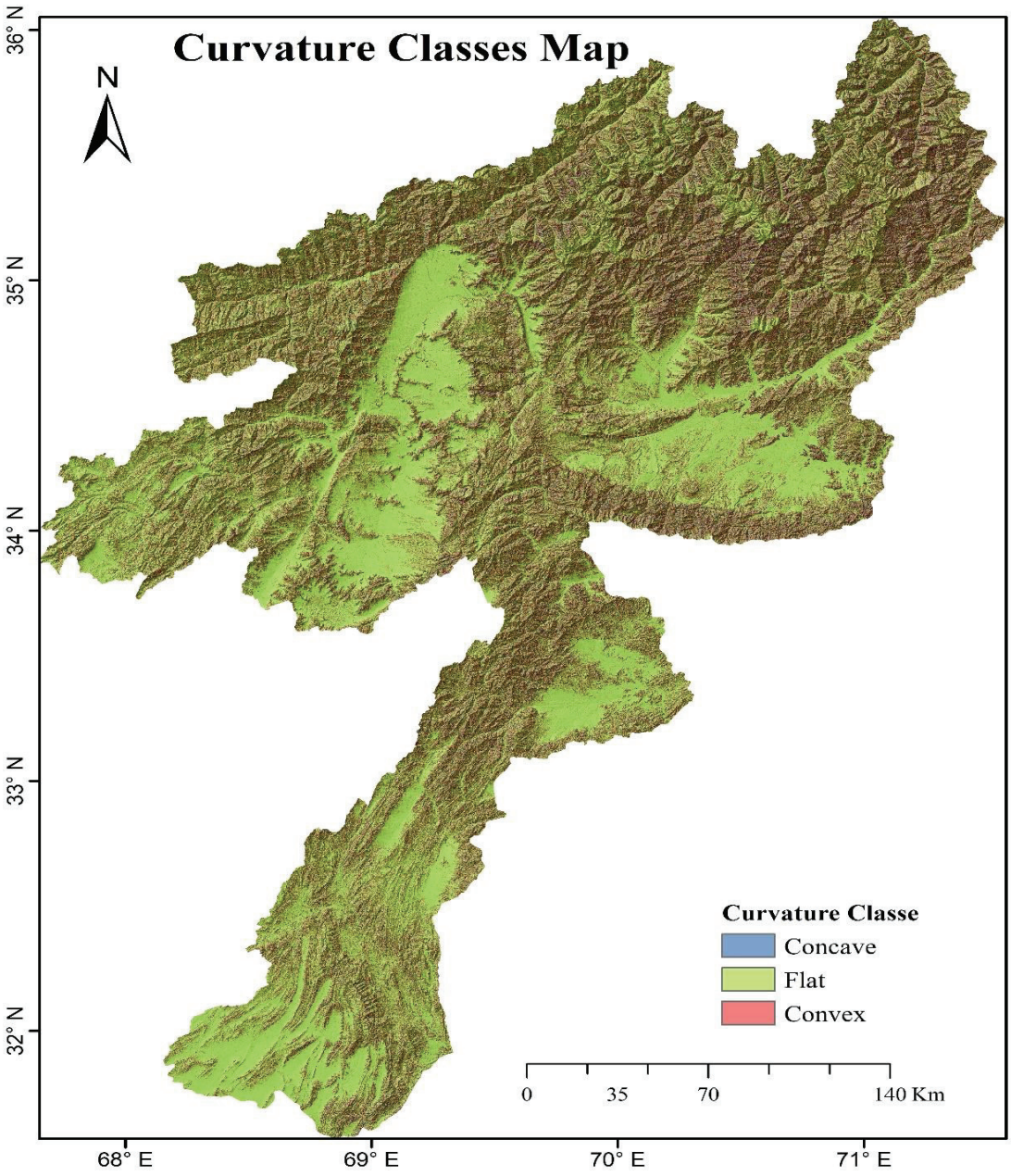

Figure 5.11. Curvature Map of the Kabul River Basin

After generating each flood-controlling criteria in raster format, each component was classed into five categories, ranging from 1 as very low vulnerability and 5 as very high vulnerabilities to flooding. Regions more vulnerable to flood correlate to a greater classified value of 5, while areas less susceptible to flooding correspond to a lesser value of 1 (Table 5.3). The evaluation of past studies and the analysis of the KRB local environment contributed to the classification of all factors into various groups.

5.1.3. Flood Vulnerability Map of KRB

By integrating flood-controlling factors/criteria, a flood susceptibility map of KRB has been generated (Figure 5.12) using Equation 5.4 on the basis of AHP decision-making method results. The following Equation 5.4 has been employed with the support of ArcGIS to produce the flood hazard zone (FHZ). Based on the weighted overlay integration technique, Kabul River Basin was categorized into four flood vulnerability zones: very high (5), high (4), low (2), and very low (1).

Equation 5.4 represent weighted overlay integration technique to obtain the flood hazard zones.

$$\begin{aligned} \mathrm{FHPZ} = {} & \mathrm{E_W E_{NR}} + \mathrm{LULC_W LULC_{NR}} \\ & + \mathrm{Slope_W Slope_{NR}} \\ & + \mathrm{R_w R_{NR}} + \mathrm{G_w G_{NR}} \\ & + \mathrm{NDVI_w NDVI_{NR}} \\ & + \mathrm{C_w C_{NR}} + \mathrm{DTR_w DTR_{NR}} \\ & + \mathrm{Soil_w Soil_{NR}} \\ & + \mathrm{TWI_w TWI_{NR}} \end{aligned} \tag{5.4}$$

Where W represents the individual criteria/factor weights, and NR rating factor, respectively. E is the elevation, R is the rainfall, G is the geology, NDVI, C is the curvature, LULC, and TWI, respectively.

All the layers were combined in the ArcGIS using the Weighted Overlay Combination WLC technique to prepare flood zones in the whole KRB. Flood hazard potential zone (FHPZ) was determined, and area for each vulnerability class is shown in Table 5.4.

Table 5.4. Susceptibility to flooding, affected area, and percentage

Flood risk class	Area	
	Km^2	Percent (%)
Very High	56.2	0.08
High	17768.4	25.15
Low	51689.8	73.17
Very Low	1129.7	1.60
Total	70644.2	100

The results show that the basin has a high susceptibility to floods in around 25% of the area. A low to extremely low vulnerability to floods is recognized in the remaining 75% of the research zone. Based on flood susceptibility map (Figure 5.12), majority of the research area's eastern and western, southwestern, and central regions are more susceptible to floods. The provinces of Kunar, Laghman, Logar, Maidan Wardak, Nangarhar, Nuristan, Paktya, Panjshir, Kabul, Kapisa, Khost, and Parwan were found to be the most susceptible to flooding (Figure 5.13).

These regions are primarily characterized by low altitude, generally flat slopes, low permeability, significant rainfall accumulation, and higher TWI. In contrast, regions with low vulnerability to floods are characterized by higher-slopes and altitudes, formation of low flow, distance from river channels, high soil permeability, and higher NDVI.

According to the outcomes, TWI, elevation, slope, and distance from stream channels are the four vital variables for the assessment of flood in the current study work respectively. In the research area, where the elevation and slope toward the watershed outlet are reduced, the risk level happens to be highest (Figure 5.12).

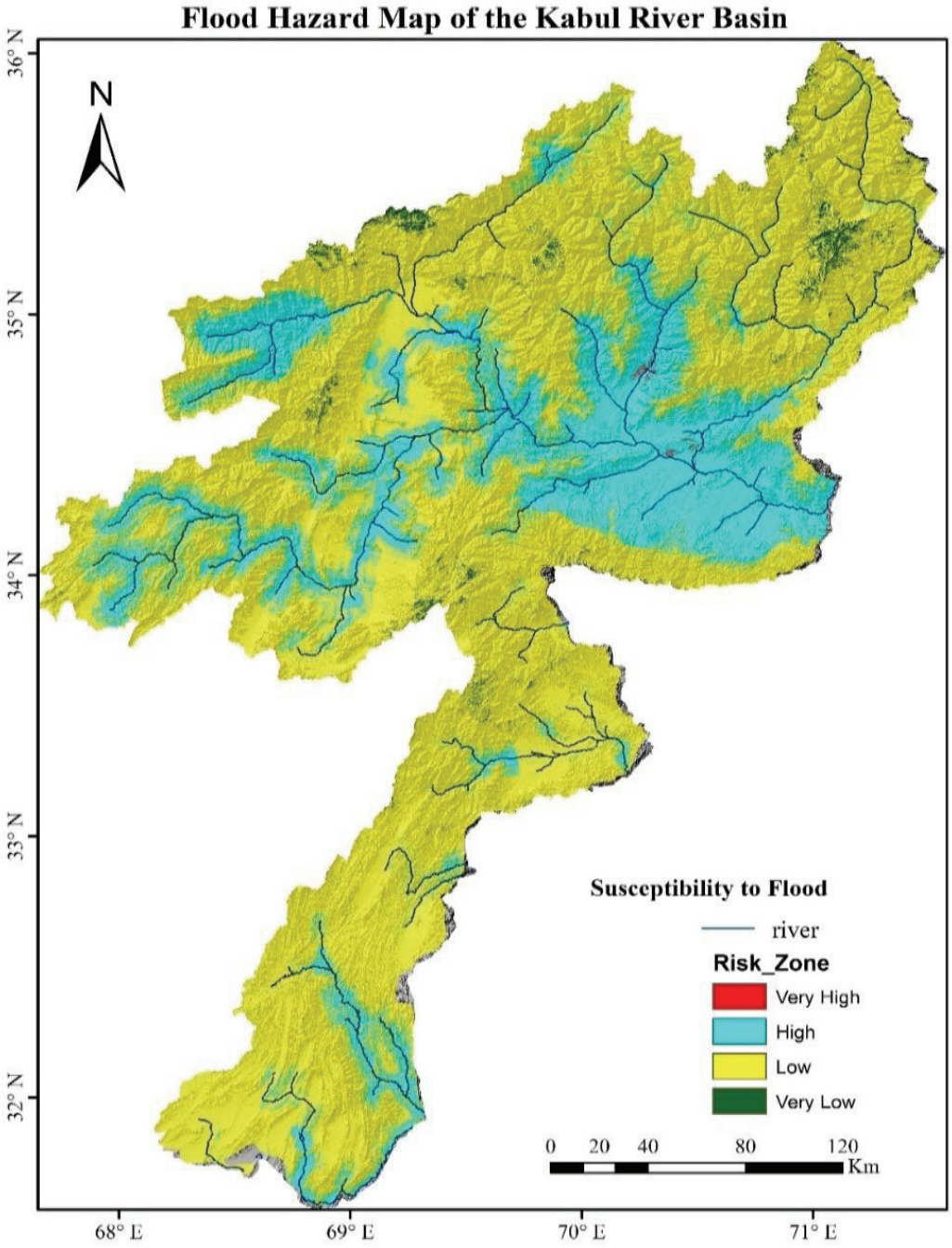

Figure 5.12. KRB Flood Risk Map

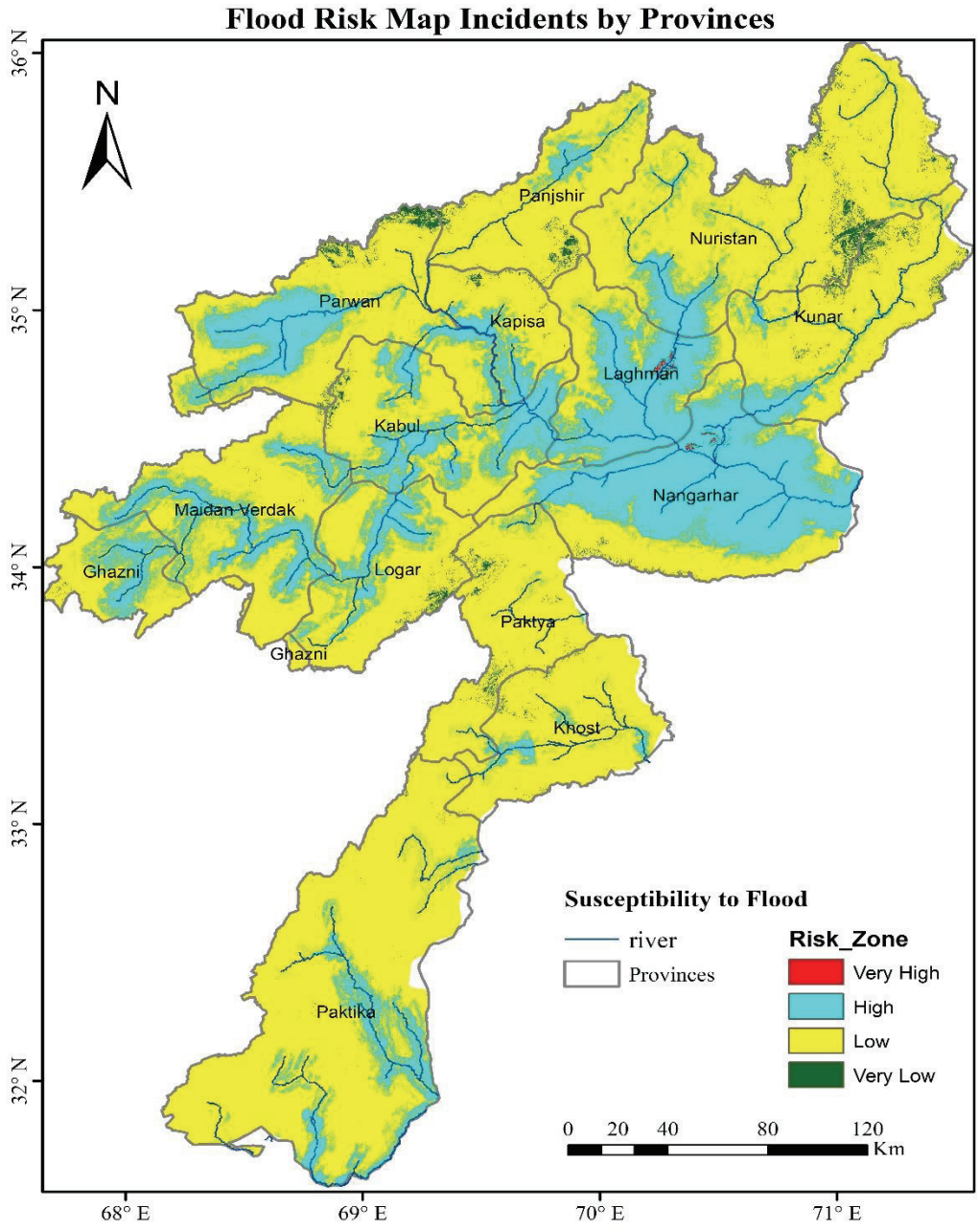

Figure 5.13. Flood Susceptibility Map Incidents by Provinces

5.1.4. Validation

Model validation is important for deciding whether the output of the model accurately reflects the situation on the ground. Model outcome can be compared to actual flood events observed to conduct model validation. Historical flood zones were utilized as a validation set to assess the reliability of the prediction techniques.

In this research, the flood vulnerability map was further validated using historical floods that occurred in the years 2013, 2020, and 2022, respectively. Data on previous flood incidents were collected from OCHA (OCHA, 2013; UNOCHA, 2020, 2022) for Afghanistan. Based on the data from the OCHA investigation and flood hazard assessment for Afghanistan, Kabul River Basin's eastern and western, southwestern, and central regions have been affected by floods. According to validation, the majority of the flooding occurred in areas that can be characterized as being very flood-sensitive. (Figure 5.14, Figure 5.15, Figure 5.16).

The final flood inundation map (Figure 5.12) generated using the AHP-GIS method was compared to the flood event from the year 2013 (Figure 5.14). The resulting map shows that areas having a high sensitivity to flooding are where significant flooding has happened in 2013 flood event. This outcome demonstrated accuracy of flood risk created using data from 2013 flood event for validation. As the GIS-AHP technique is based on the judgment and opinion of experts, the actual validity percentage may change.

In Figure 5.14 (a), the 2013 flood-event happened in most part of provinces of KRB, such as Nangarhar, Kabul, Kunar, Laghman, Khost, Paktya, Logar, Parwan, Nuristan, Panjshir, and Kapisa. The borders of these provinces demonstrate the 2013 flood occurrence in the basin.

The results of the GIS-AHP model and the past flood events in the basin indicate that highly vulnerable locations to flood hazards are identical. This indicates that the past flood occurrence on the ground collected from UNOCHA and flood risk map developed by integration of GIS-AHP method coincided well.

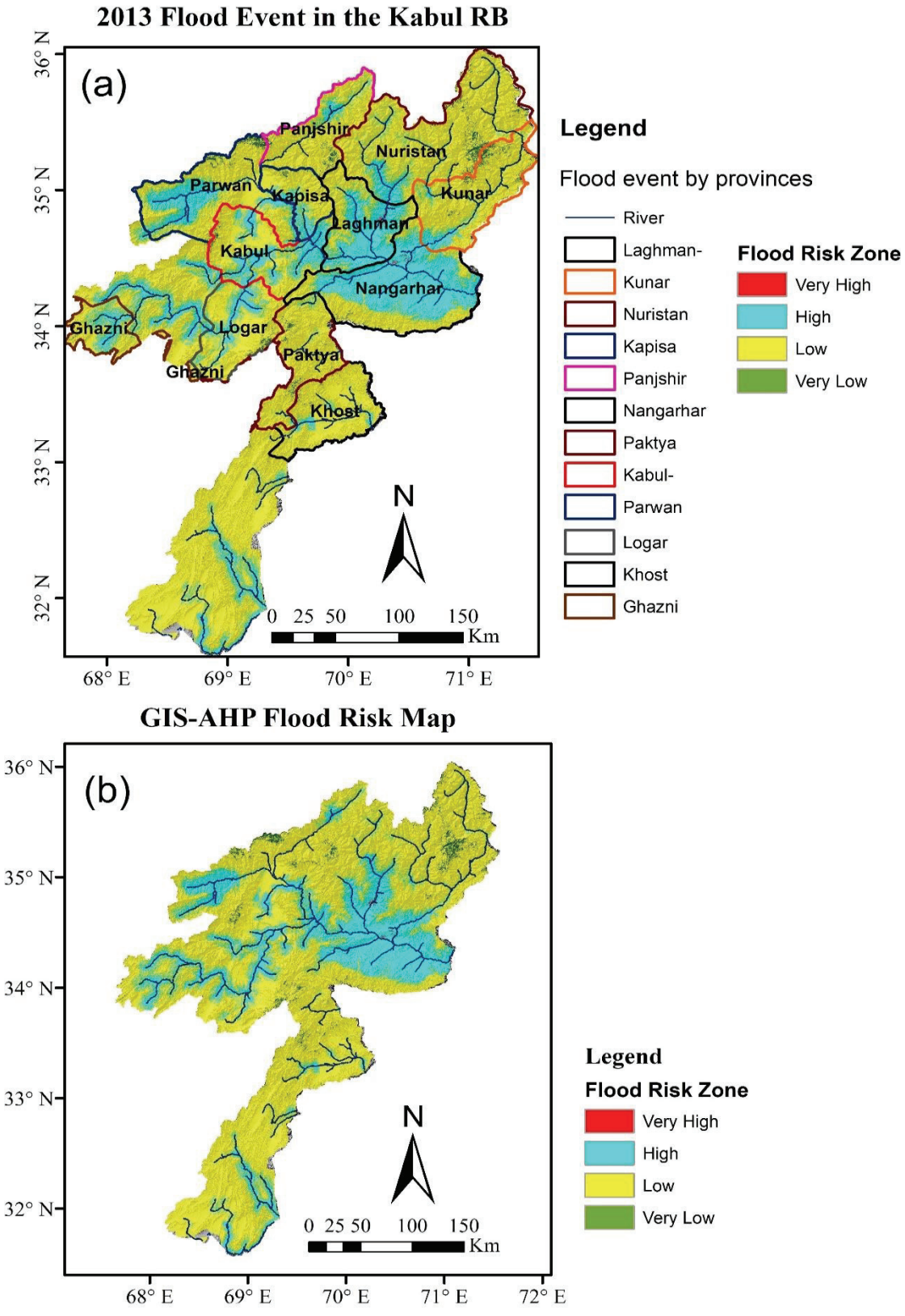

Figure 5.14. (a) 2013 flood event (OCHA, 2013), (b) flood risk map by GIS-AHP

Also, the 2020 inundation-map Figure 5.15 (a) was used to validate the flood hazard zone created using the MCDA technique. The comparison shows that in some provinces of the Kabul River Basin, such as Kabul, Kunar, Laghman, Nangarhar, Paktya, and Khost, floods had been happened (Figure 5.15). The borders of these provinces demonstrate the 2020 flood occurrence in the basin.

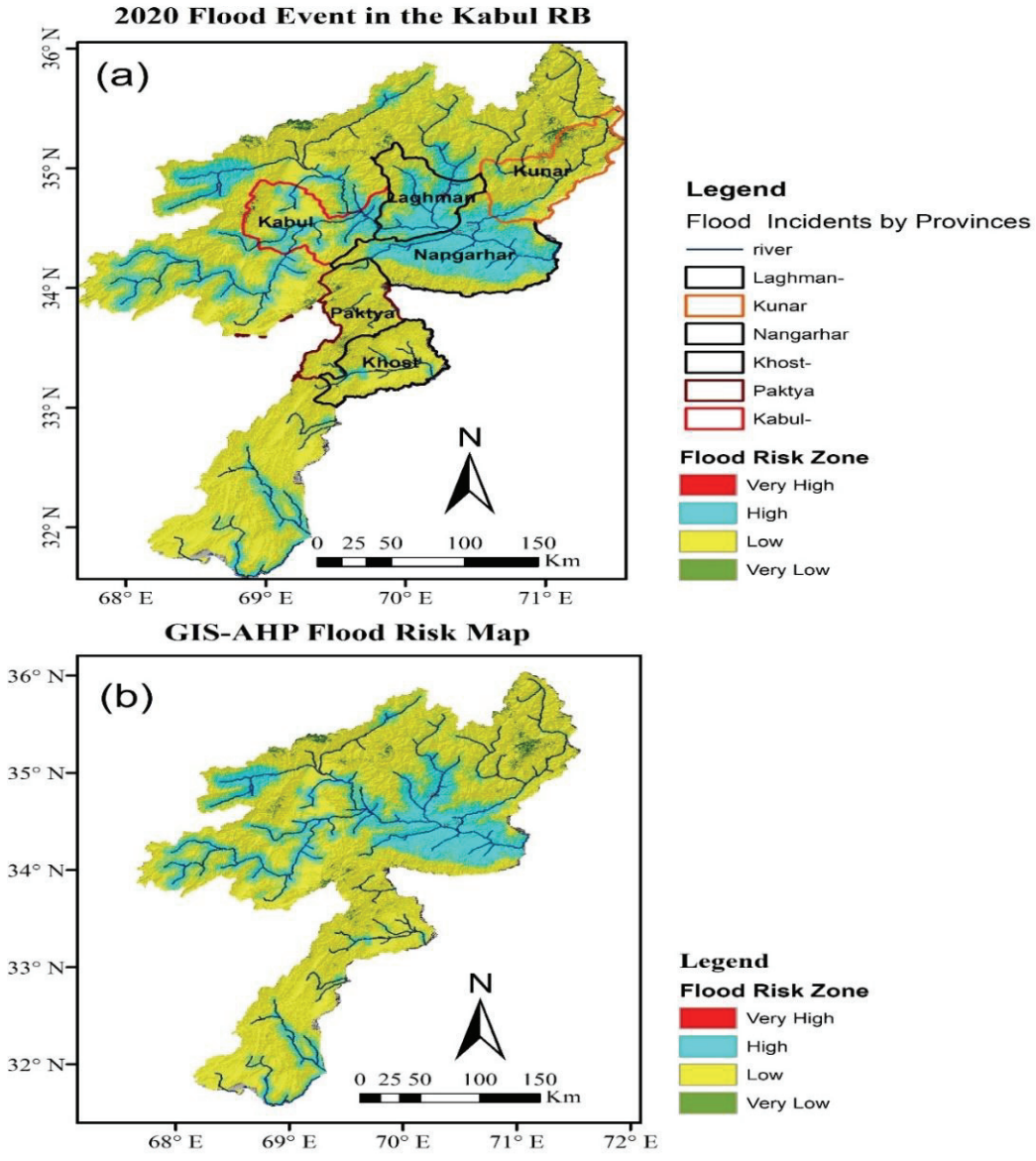

Figure 5.15. (a) 2020 Flood event (UNOCHA, 2020), (b) flood map by GIS-AHP

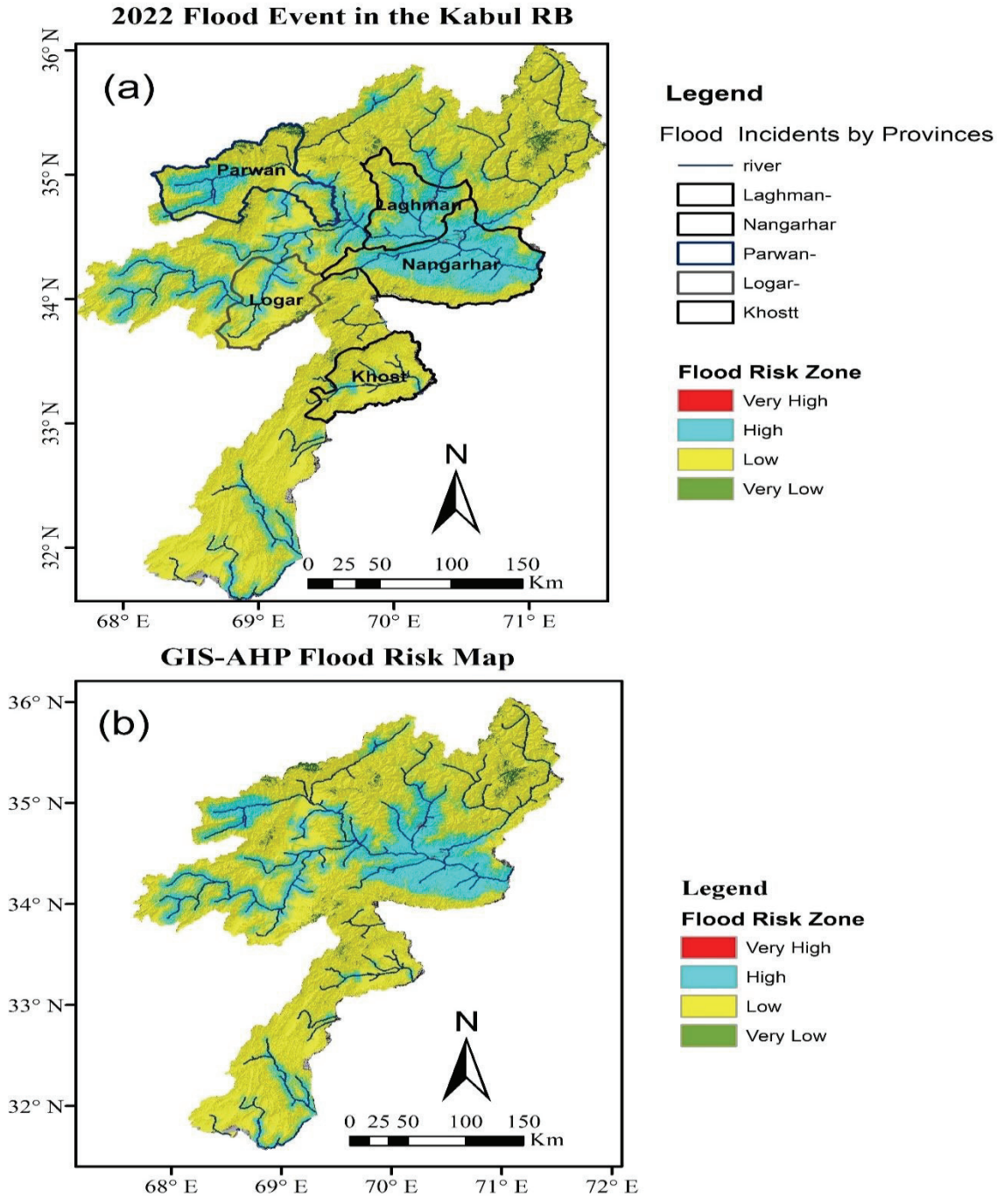

Figure 5.16. (a) 2022 Flood Incident (UNOCHA, 2022), (b) flood map by GIS-AHP

Additionally, the flood hazard zone generated using GIS-AHP technique was validated using the flood inundation map for 2022, shown in Figure 5.16 (a). The comparison demonstrates that flooding has occurred in various provinces of the Kabul River Basin, including Laghman, Nangarhar, Parwan, Logar, and Khost. (Figure 5.15 (a)). These provinces' borders show how the basin experienced flooding in 2022.

The assessment shows that evaluated flood hazard areas are acceptable and match past flood events. Flood hazard zones can indicate how well flood vulnerability models and flood conditioning factors estimate the occurrence of floods. In this research-work, the vulnerability of flood maps was compared to the flood in the validation dataset.

CHAPTER 6

HEC-RAS ANALYSIS & DISCUSSIONS OF THE RESULTS

A hydraulic study assesses the reactions and motions of fluids in channels and other hydraulic structures. The hydraulic analysis is used to design functional and effective hydraulic structures, as well as to evaluate how water reacts under various circumstances by determining parameters (e.g., flow rate, velocity, depth, inundated areas, etc.). The accuracy of the input data, including flow information, quality of topographic data, and land cover, is crucial to this kind of research.

A flood inundation map is generated by the hydraulic analysis and flood risk assessment for the lower Kabul and Kunar sub-basin, whose location is presented in Figure 6.1.

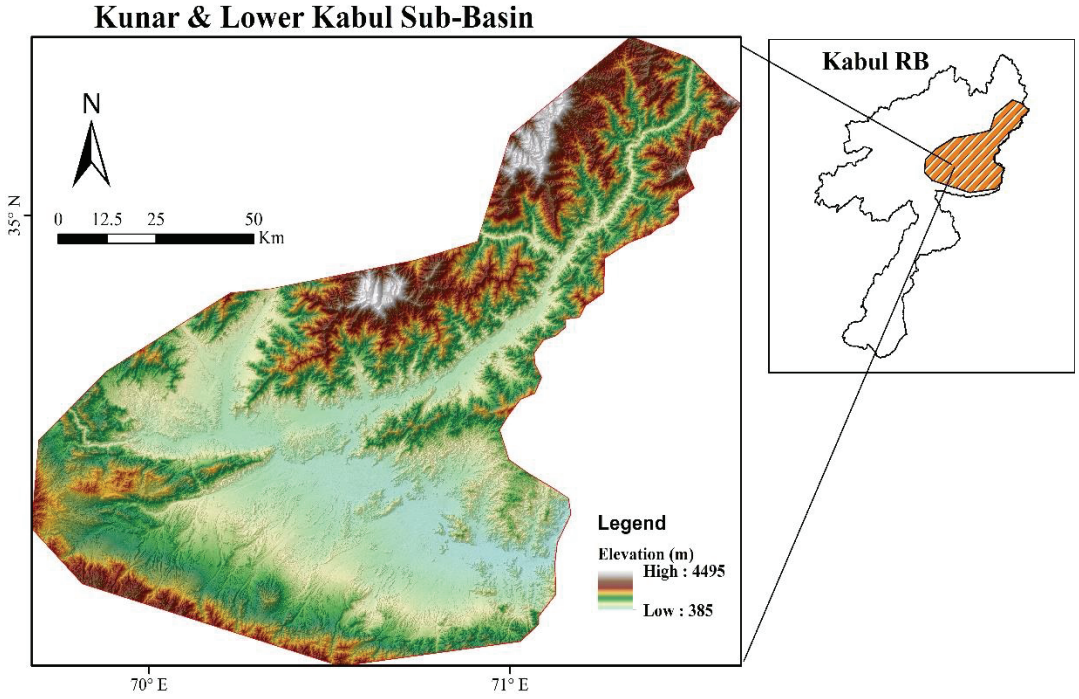

Figure 6.1. Lower Kabul and Kunar sub-basin

6.1. Application of HEC RAS 2D

HEC-RAS model was employed in this work to carry out hydraulic modeling. The software's 2D hydraulic modeling was used to create flood hazard maps for the lower Kabul and Kunar sub-basin and propose the related flood mitigation strategies.

The HEC-RAS model needs a variety of input data for implementing and simulation of model, and these data vary depending on purpose of assessment that is being performed. Primary goal of this work is to evaluate several viable solutions as mitigation actions and to identify the flooded regions in order to prevent floods in the hazardous areas near the river. This research utilizes hydraulic modeling to find effective flood prevention measures for watersheds by first identifying the maximum flow inundated risk map and then developing an inundation map with 500-year return periods. DTM with a resolution of 20 m and land cover are data sources applied in this work for HEC-RAS model. A DTM is a topographic representation of the bare Earth, which includes boundaries and terrain elevations spaced uniformly along a grid.

Roughness is one of the most important variables in hydraulic modeling, which is being used to calculate the flow rate. Manning roughness coefficient shape files were generated using ESRI 2010 land cover data with 10-meter resolution.

In the present investigation, two inflow hydrographs were used individually to produce two flood extents, including a flood map of the maximum flow discharge and map of 500- years of design flood events. Actual maximum flow hydrographs were used as the boundary parameter for constructing the inundated flood map in the basin. Flood map for the 500-year flood period was developed using the peak discharge from the environment of HECSSP program output and used for mitigation measures and flood extent.

First, the inundation map of the research area is produced using the 72 hours' inflow hydrograph of the maximum flow as boundary conditions, which has a peak discharge of 2697.5 m^3/s at Asmar station, 878.5 m^3/s at Behsod, 181 m^3/s at SorkhRod, and 374 m^3/s at the Pich gauging station respectively (Figure 6.2). It has peak flow rates of 4837 m^3/s at Asmar, 1207 m^3/s at Pul-Behsod, 1501 m^3/s at SorkhRod, and 654 m^3/s at the Pich station, respectively (Figure 6.3).

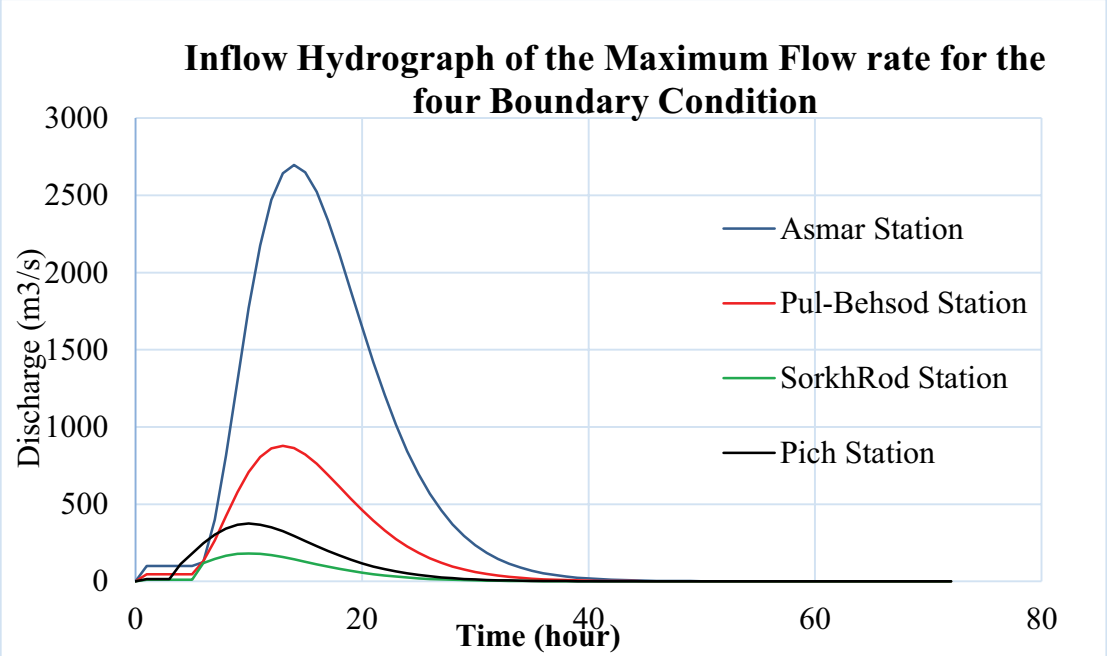

Figure 6.2. Inflow Hydrograph of the maximum flow rate KRB

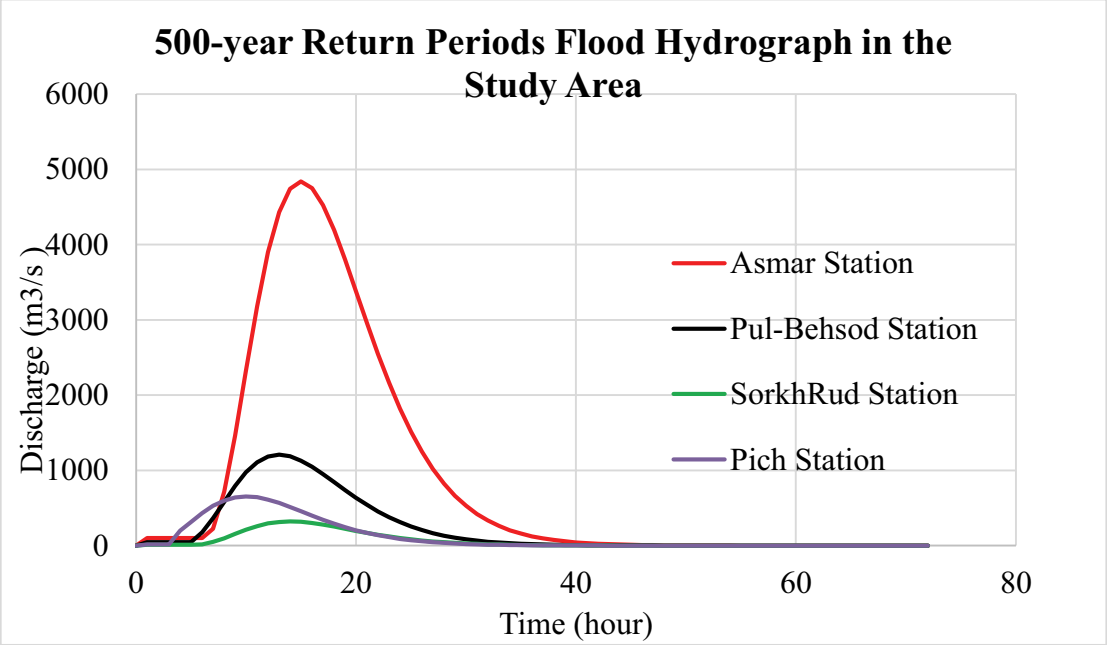

Figure 6.3. 500-year Return Periods Flood Hydrograph KRB

6.1.1. Development of the 2D Computational Mesh

In HEC-RAS, mesh construction is the process of developing a computational grid or mesh for the flow area that subdivides the research area into discrete components or cells. Equations that describe the flow of water through the system are numerically solved using this mesh. In the HEC-RAS system, cells might have three, four, and up to eight edges.

In this study, a two-dimensional computational mesh with 100 x100 m cell size was generated for a 2D flow region, yielding 2480781 computational cells. Upstream, downstream and properties of the 2-D flow are mapped in (Figure 6.4).

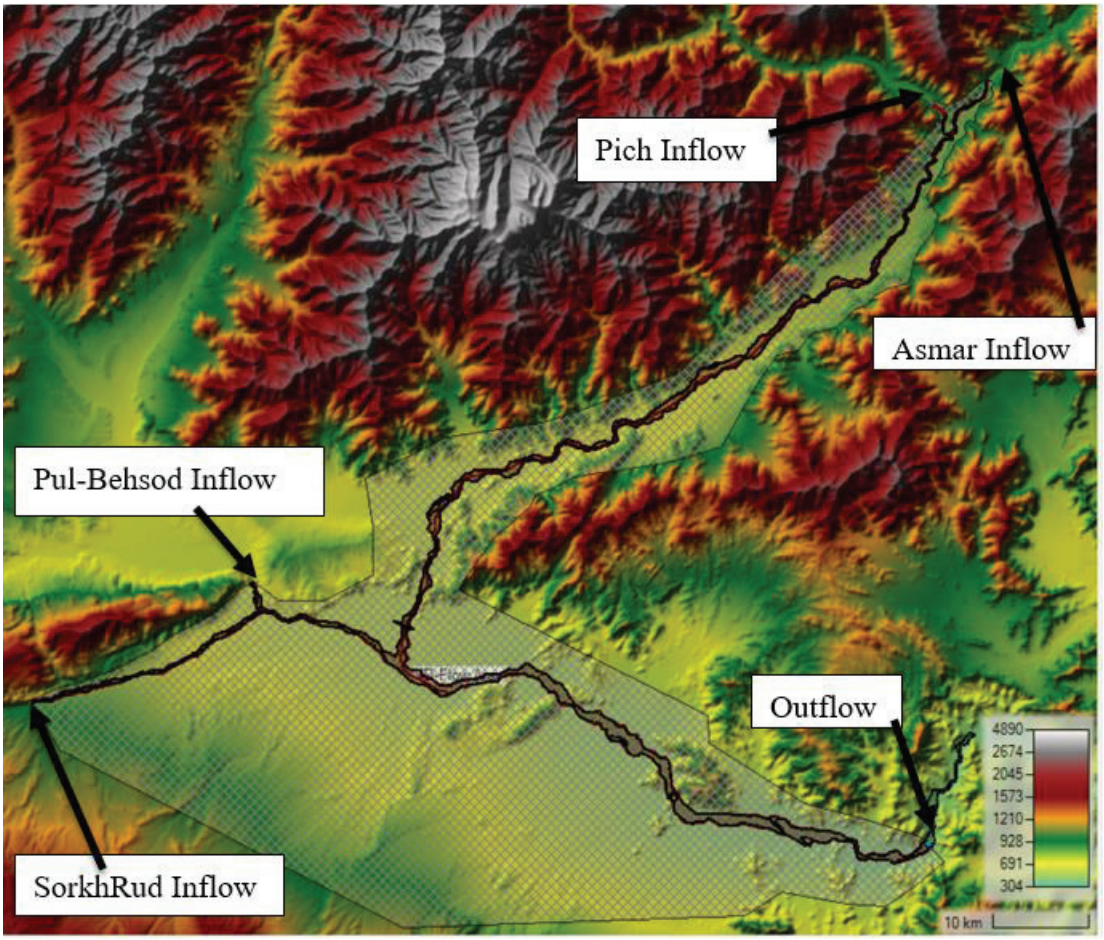

Figure 6.4. HEC RAS 2-D Flow Area and Boundary Conditions of Study Area

In addition, river's main channel is refined with a 10 x 10 m cell size, and break-line is developed in the river center for indication of path of water motion and ground level (Figure 6.5). The flow will first move into the channel center using the break lines feature, then the whole channel, and finally into the areas which considered as possible inundated areas.

In HEC-RAS, areas of the computational mesh that need a higher resolution for precise hydraulic modeling are referred to as refinement zones. In order to achieve this goal, the main channel of the river was chosen as the region of interest, and the appropriate cell size was created as 10 x 10 meters for a more accurate representation of the ground surface and water movement path (Figure 6.5). Refinement zones have the advantage of tremendously enhancing the precision of hydraulic simulation in locations where the flow is complicated or fluctuates greatly. By improving the mesh resolution in certain areas, HEC-RAS is more capable of analyzing the flow characteristics and accurately predicting water surface heights, depth, and velocities (HEC-RAS, 2016).

The geometry of the stream or river channel is defined by the break lines characteristic. A break-line is a polyline that divides a terrain surface or river cross-section into more manageable parts of various elevations. For a correct representation of the geometrical parameters and water movement through the channel, the break line is used as a guide by HEC-RAS to interpolate elevations between the points on the break line (HEC-RAS, 2016) (Figure 6.5). Break lines are very effective in characterizing the geometry of channels with asymmetrical or non-uniform slopes.

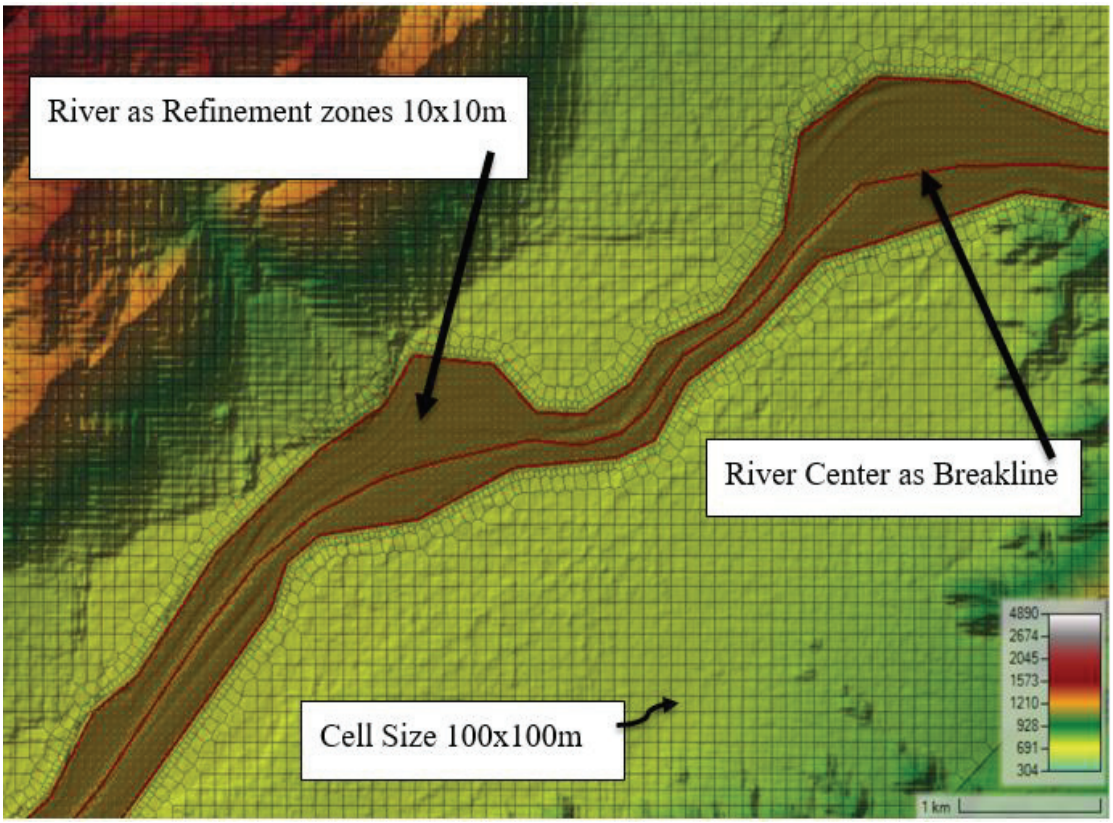

Figure 6.5. Development of 2D flow area, break-lines, and refinement zones

In conclusion, the purpose of the break lines and refinement features in HEC-RAS is to characterize the channel geometry and movement of water through the channel more accurately by segmenting the topography into smaller sections at various elevations.

6.1.2. Roughness Coefficient

The roughness Coefficient is one of the vital variables in hydraulic analysis (n), which is used for evaluating a channel's or a ground surface's resistance to flow. A greater roughness coefficient shows a rougher surface and higher flow resistance. The Manning value is influenced by the type of waterway, the type of soil, vegetation, as well as the structure of the earth's materials (Chow et al., 1988b).

HEC-RAS model enables the allocation of Manning's n values. ESRI 2020 land use land cover data with the 10-meter resolution was used to generate a roughness coefficient for the study area in the HEC-RAS environment (Figure 6.6). ESRI land cover data was linked with the 2-D geometry data set of the study area for simulation.

Roughness was assigned for each land cover type base on the HEC-RAS manual and the USGS of NLCD (Dewitz, 2016; HEC-RAS, 2016) (Table 3.3). The accurate area for the main channel was defined and created using the classification polygons in the HEC RAS environment for the land cover layer.

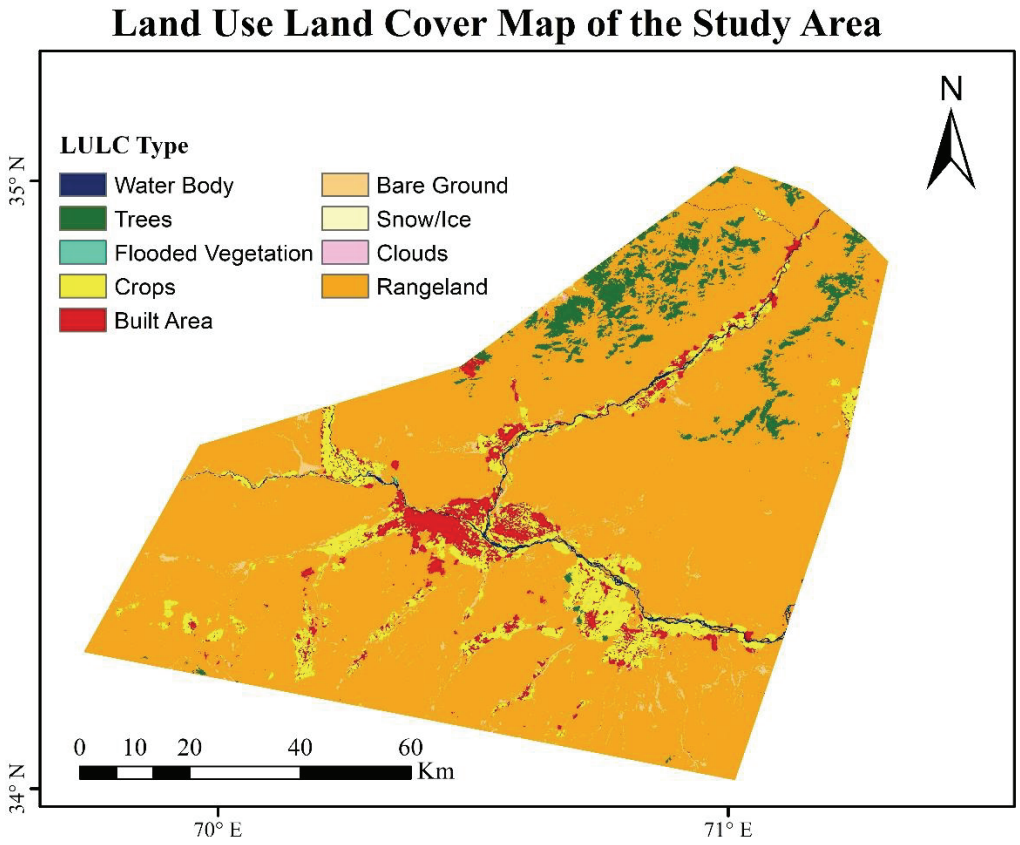

Figure 6.6. Land Cover Data for Manning's Roughness Coefficient

6.1.3. Calibration of HEC-RAS Model

The procedure of modifying model parameters is known as calibration in the HEC-RAS system, such as hydraulic structure coefficients and roughness or manning's n value, to ensure it accurately represents observed data. To increase the consistency between the simulated and observed or historical flood extents, model parameters, including channel and floodplain roughness coefficients, hydraulic boundary conditions, and topography, have been adjusted through several trials. In this research, manning's n values were assigned as calibration parameters using the ESRI 2020 land cover of the

study area. The performance of the model was assessed by referencing the extent of the simulated map with the corresponding observed or historical flood event map. Roughness type is shown in Figure 6.7.

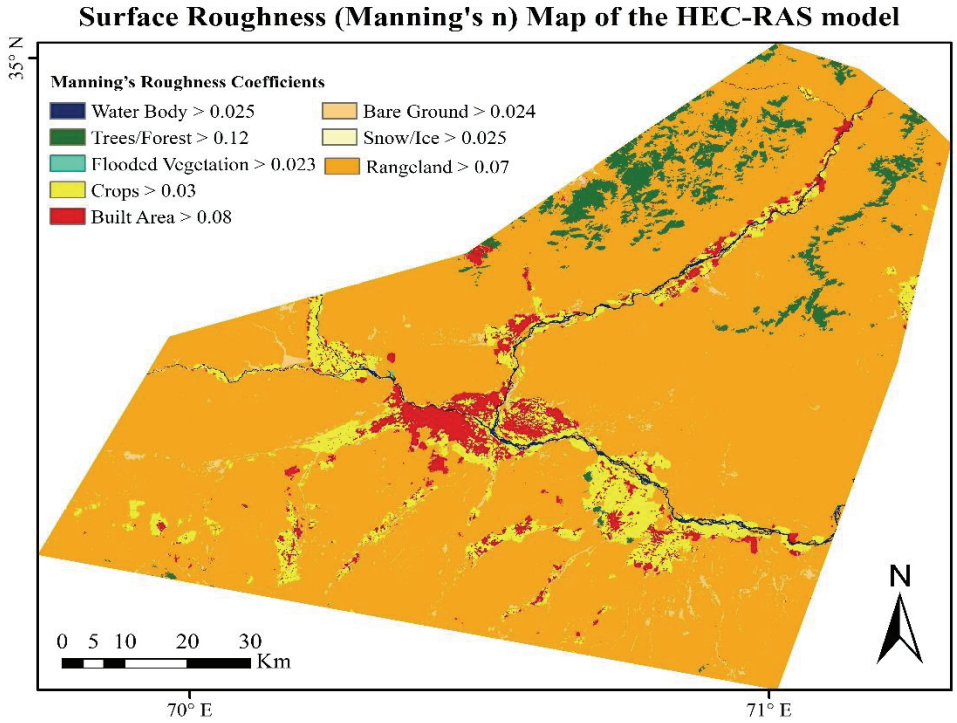

Figure 6.7. Surface/Manning's Roughness Coefficients Map of the Study Area

6.1.4. Flood Risk Maps

After creating a 2D flow area (Figure 6.4), computing Manning's roughness coefficient (Figure 6.7), and determining boundary conditions (Figure 6.2 and Figure 6.3), two-dimensional hydrodynamic analyses were performed for the maximum flow which happened in the basin using the HEC-RAS software. The flood hydrograph (Figure 6.2) was used as the upstream boundary condition for the actual flow in the model to calculate the unsteady flow using the Diffusion Wave equation. The Diffusion Wave equation provides better accuracy and numerical stability.

The Courant time step is used for the model to provide acceptable stability and precision. The model simulation in the current study is initially run with a time step of 30 second. The flow hydrograph simulation takes approximately 62 hours to complete.

The Diffusive Wave Equation computation approach was used to simulate the HEC-RAS flood model for an actual event and a 500-year design occurrence. For the 500-year return period, the highest simulated depth is 18 meters, while it is approximately 16 meters for the actual flow occurrence (see Figure 6.8 and Figure 6.9).

Furthermore, the flood velocity profile for the flood plain and main river channel in the Kama area was displayed in Figure 6.12 and Figure 6.13 for the actual vs. 500-year design event flood. The maximum velocity in this area for the 500-year design event is approximately 5 m/s, whereas the actual flow hydrograph is about 4 m/s (Figure 6.12 and Figure 6.13).

The simulation's findings indicate that 98 km^2 of the flood plain was inundated during a real flood event, while only 122 km^2 were submerged throughout the 500-year return period flood. The outcome shows that agricultural lands are mostly inundated during 500-year-design event floods around the main river stream, while the settlement areas are inundated in the Kama region and some parts of Nangarhar city, which is closer to the mainstream channel.

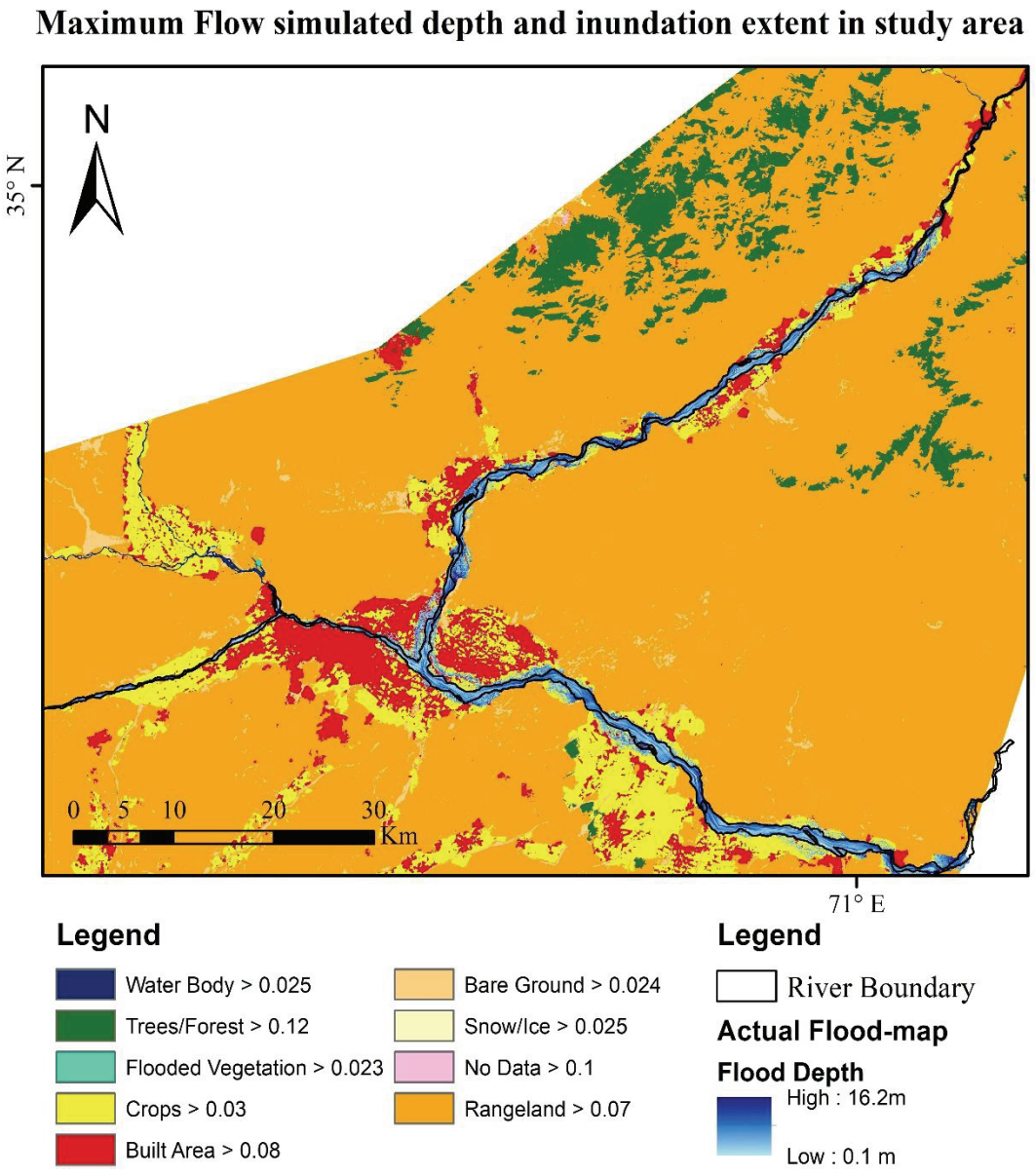

Figure 6.8. Flood depth and inundation using maximum actual flow

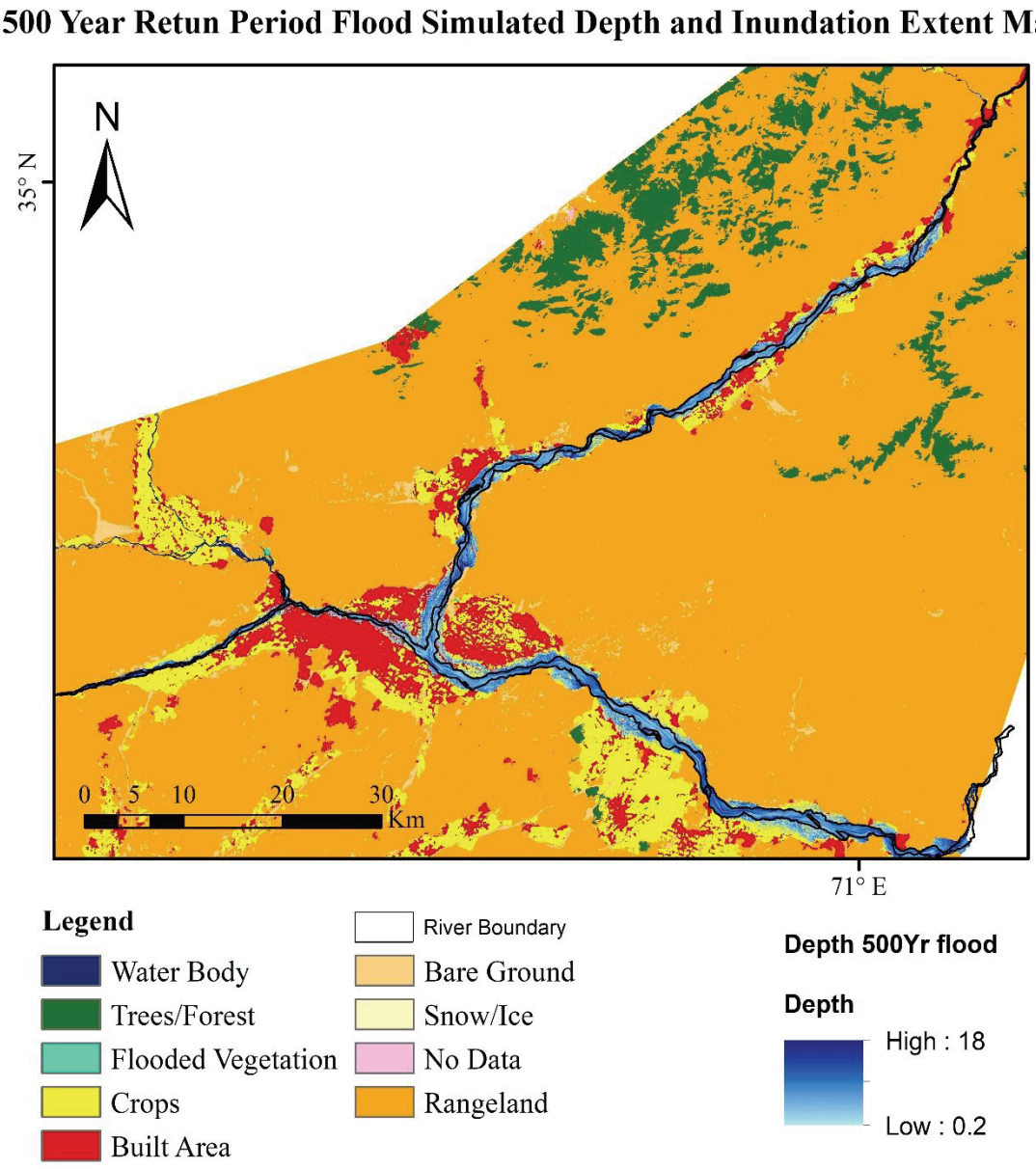

Figure 6.9. Flood inundation and depth using 500 year return period

Flood scenarios for residential locations (Nangarhar and Kama) are shown in Figure 6.10 and Figure 6.11, which show the actual flood map and a predicted 500-year flood event, respectively. In the two figures, there is a distinct difference in the extent of the inundated areas. The actual flood map displays the regions that were devastated by the highest flow occurrence. However, the 500-year flood event is a significantly larger and more catastrophic flood. This incident has the potential to bring extremely severe flooding across a much greater area.

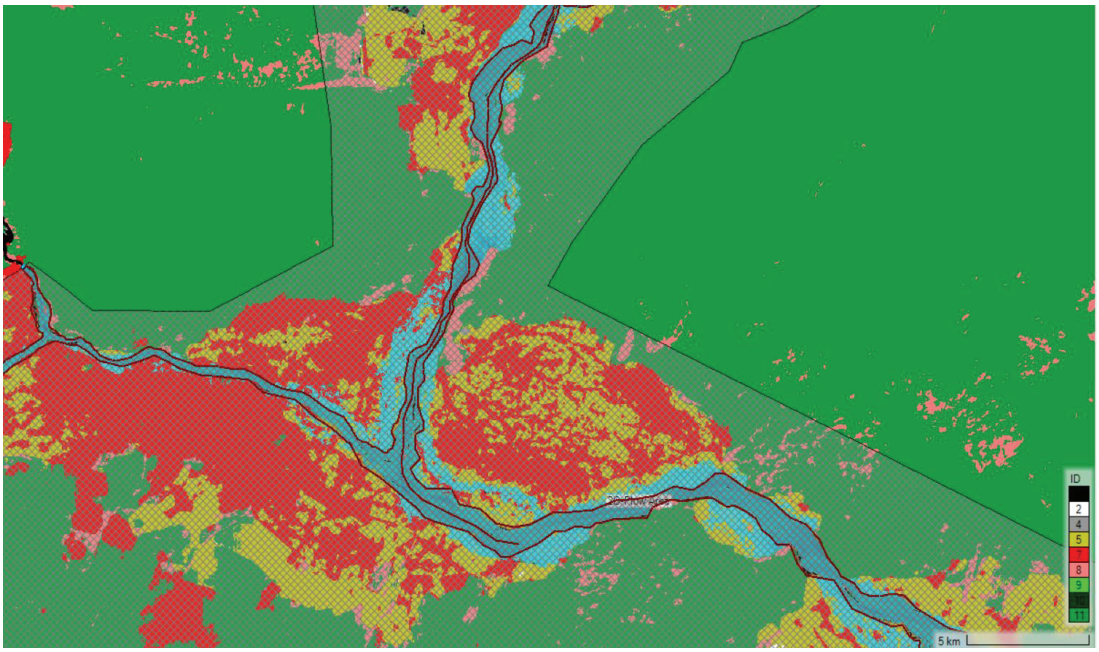

Figure 6.10. Actual inundated map

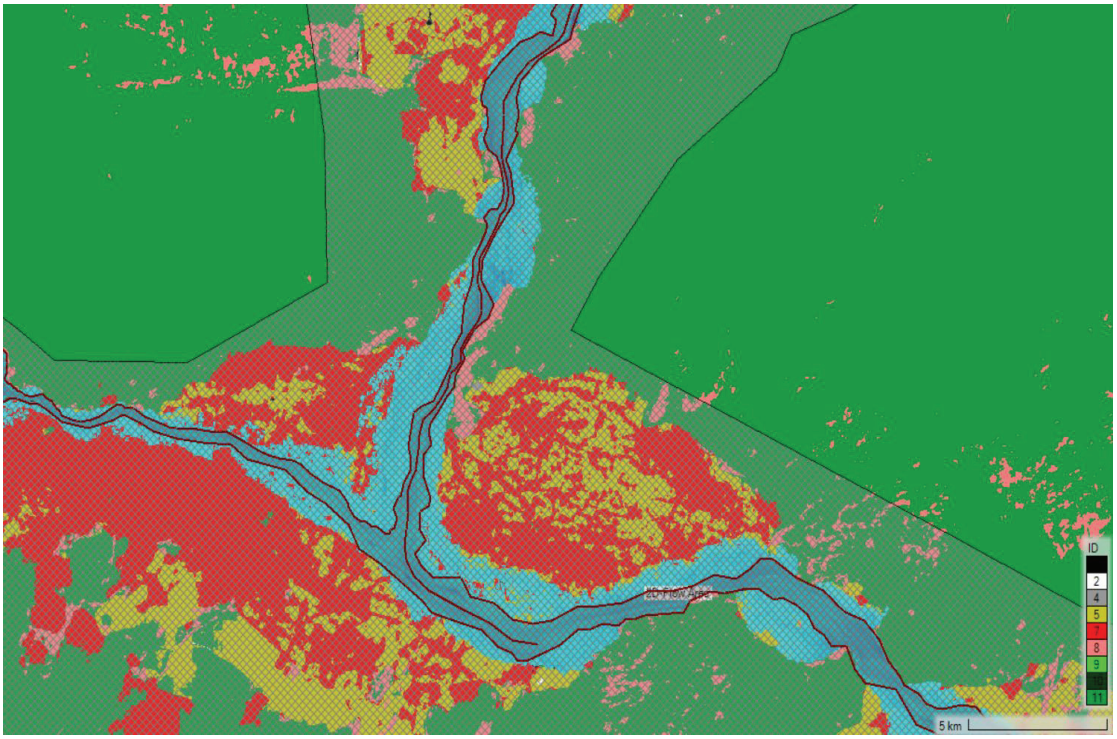

Figure 6.11. 500-year flood event map

The contrast between the two flood scenarios indicates how crucial it is to acknowledge and plan for potential flooding situations. Effective management and planning can mitigate the damage that flooding causes to both humans and the environment.

The velocity of profiles in the Kama region has been shown in Figure 6.12 and Figure 6.13, respectively. Velocity of the 500-year design flood is larger than the actual flow, which happened in recent years in work area. It is vital to recognize that even though a flood's velocity is lower than that of a 500-year flood event, it can still cause major damage and should be regarded seriously. Being knowledgeable about flood dangers and having a strategy in place for emergencies are both beneficial.

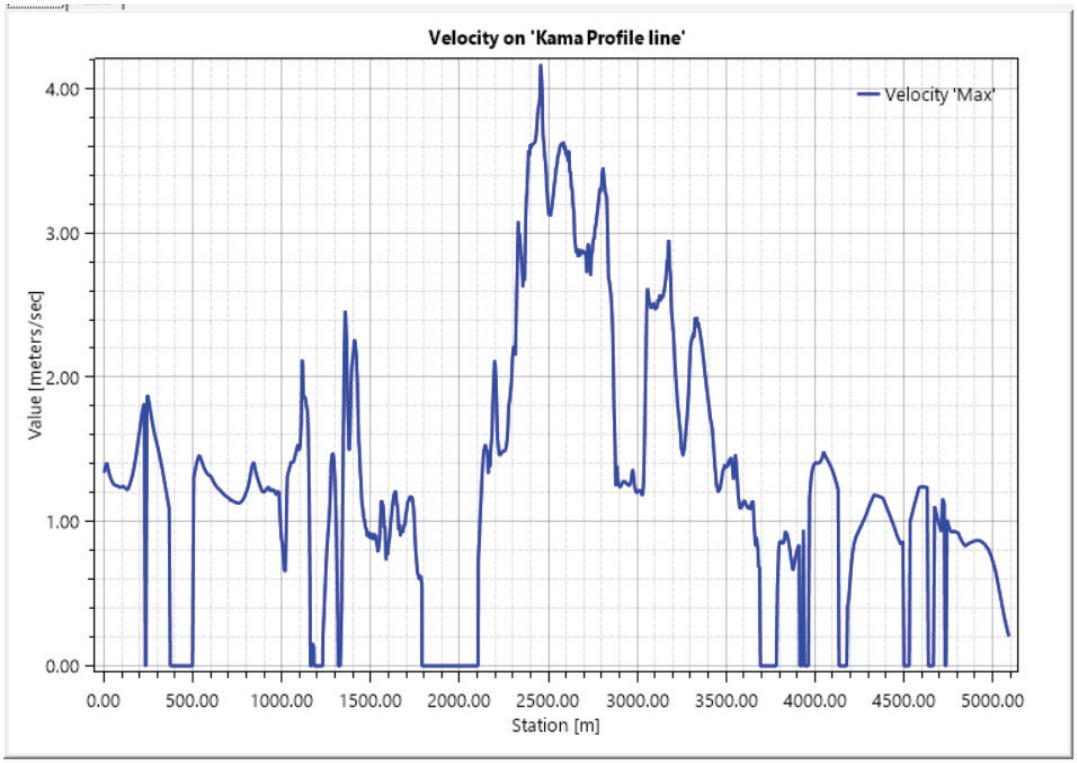

Figure 6.12. velocity profile for the actual flow hydrograph in the Kama area

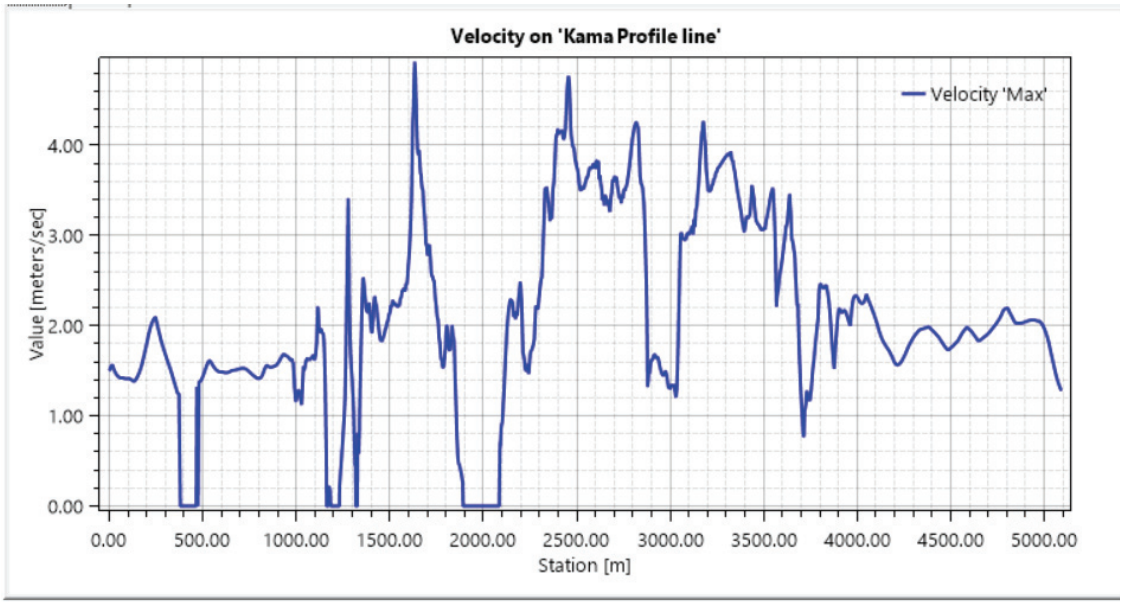

Figure 6.13. velocity profile for the 500-yer design event in Kama area

Figure 6.15 indicates depth profile for the actual flow hydrograph in Kama area, and Figure 6.14 shows depth profile for the 500-yer design event in Kama area. Almost 1 meter is the difference in depth in the specific location.

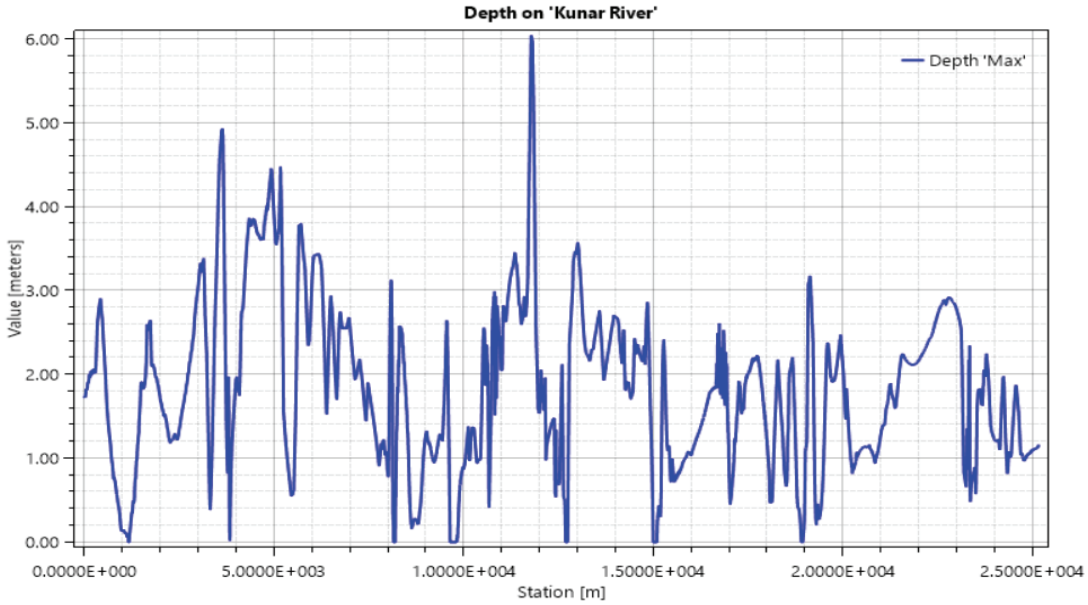

Figure 6.14. Depth profile for the actual flow hydrograph in Kama area

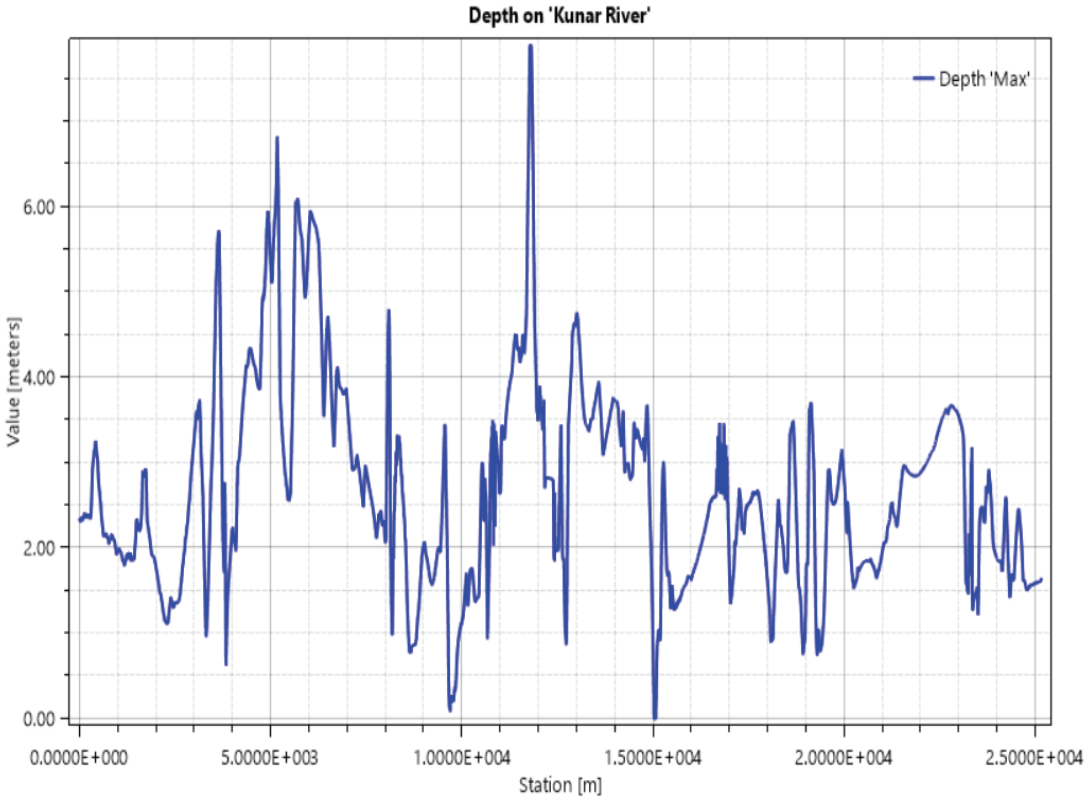

Figure 6.15. Depth profile for the 500-yer design event in Kama area

6.2. Flood Mitigation Strategies

In this section of the research, HEC-RAS is applied to generate flood structural mitigation strategies for the study work. Structural protection for flood control can include constructing flood embankments, reservoirs, levees, floodwalls, channel restoration, diversion plans, etc. For implementation of mitigation measures as described in the literature review, the maximum discharge value of the 500-year design event was utilized as a flow hydrograph, as shown in Figure 6.3 obtained by HEC-SSP program as 4837 m^3/s at Asmar, 1128.78 at Pul-Behsod, 320.7 at SorkRod, and 654 at Pich station respectively.

To determine the most suitable remedial actions, each solution proposed was related to a flood map constructed for a 500 design value.

6.2.1. Alternative 1: Restoration of the River

River modification or restoration refers to improving or reconstructing the natural processes and functions of a river system, as well as removing debris and sediments from streams and river beds. This procedure is frequently employed to keep the channel's capacity at a sustainable level and reduce flooding by enhancing the river.

The Kunar river system is well known for experiencing significant sedimentation issues as flash floods frequently happen in the basin, which carries a huge amount of rock and debris.

This mitigation measure used maximum flow of a 500-design hydrograph to analyze function that river improvement performs in protecting vulnerable areas from flooding. The digital model of elevation or terrain has been modified to optimize or restore the river capacity. Since there are no records of the river's depth in the research area, the river channel was restored using a range of trail depths. Eventually, river depth was increased by 1 meter in Nangarhar city and 1.5 meters in the Kama district, which are the vulnerable locations to flooding in the study area.

After the implementation of river restoration, there was a small improvement in the total flooded area, which decreased from 122 km^2 to 120 km^2. A flood map derived from a 500-year flood shows that inundated area has not reduced much, and the extent of the inundation map is nearly identical.

Debris and sediment removal from a river can also be expensive, time-consuming, and have potentially harmful environmental effects; therefore, doing so might not be sufficient to stop floods, especially during times of intense precipitation or melting snow.

6.2.2. Alternative 2: Building a Dam on the Kunar River

A reservoir/dam is an artificial infrastructure that is used to store rainwater runoff and discharge. A storage dam is employed for sediment accumulation, irrigation, electricity, and as a flood mitigation control system. A reservoir normally consists of an embankment with a controlled outflow and/or spillway, which is used to control storm-water runoff and minimize the effects of flash floods and also can decrease river erosion (Yanmaz, 2018). The implementation of a flood dam in an appropriate site is an effective mechanism due to its capacity to hold significant flood water behind its reservoir.

In this alternative the flow of a 500-year design graph has been used to assess the effectiveness of the developed embankment in protecting the inundated and risky areas (Figure 6.16).

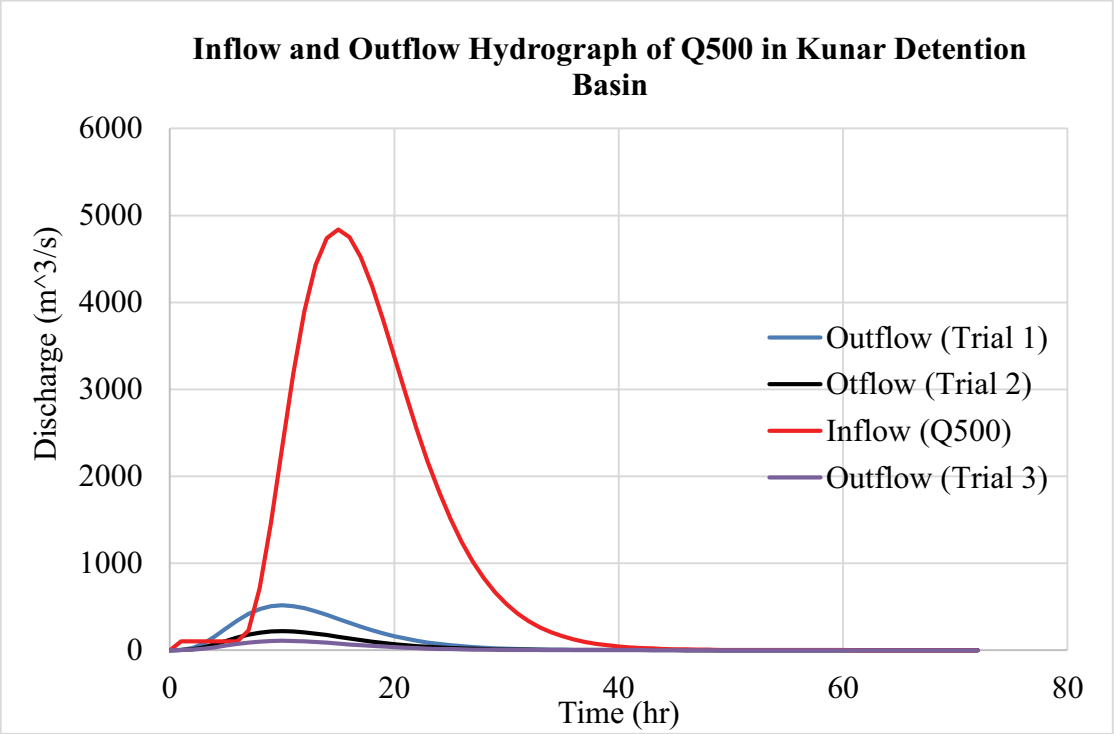

Figure 6.16. Q-500 and flow hydrographs of various trials in the upper Kunar dam

In order to prevent flash floods and storm-water runoff, a dam was constructed in the Kunar river's upstream sections. The placement of the proposed reservoir was selected based on local suggestions and spatial topographic assessments. According to site investigations, the upper part of Kunar River is appropriate for the reservoir location (Figure 6.17).

The size of the proposed dam employed in this alternative was determined through a series of trials to find the ones that would best protect the inundated area from the maximum flood design event. Figure 6.18 demonstrate the suggested dimensions of the reservoir used in this assessment.

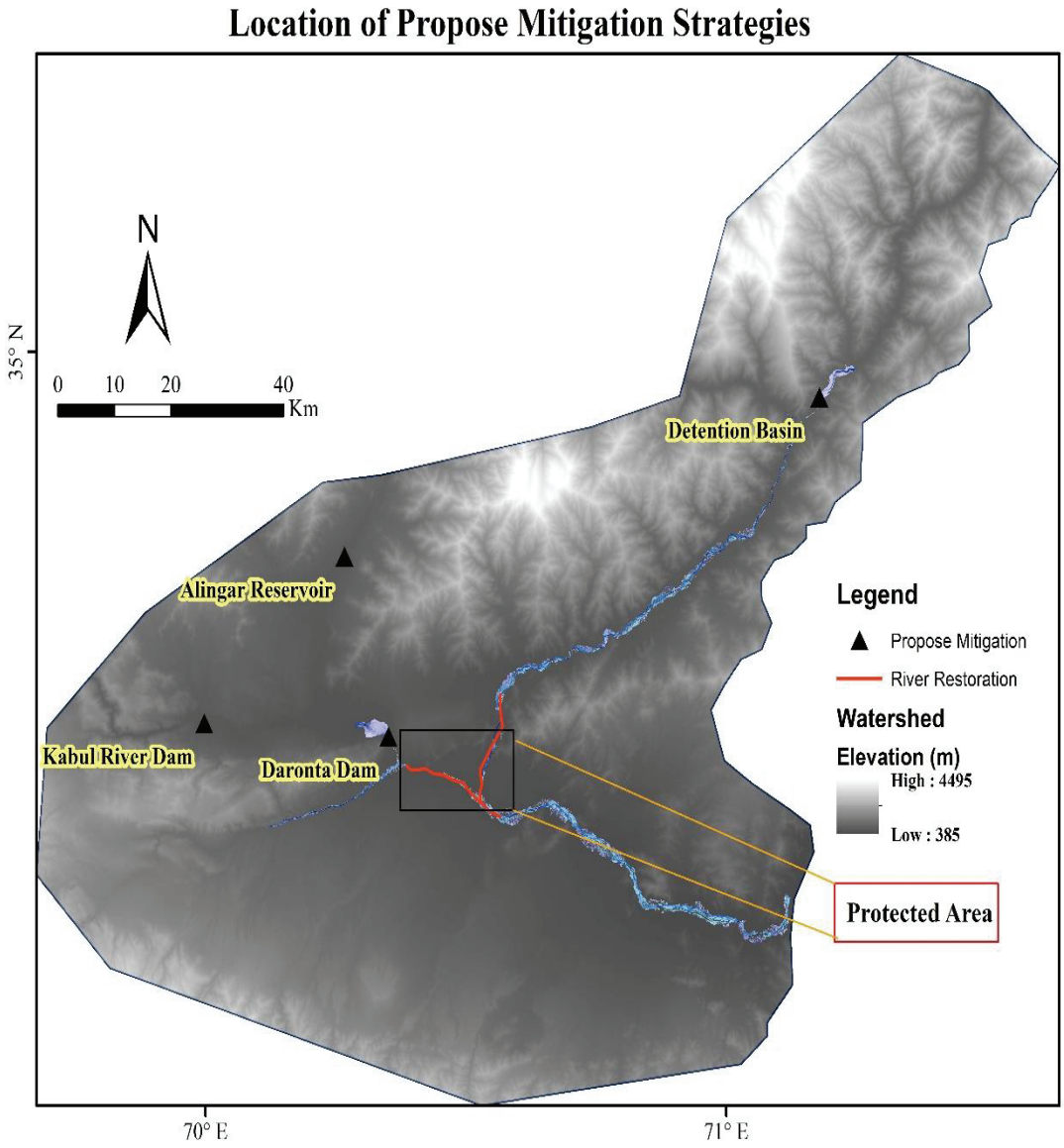

Figure 6.17. Propose mitigation measure type and location

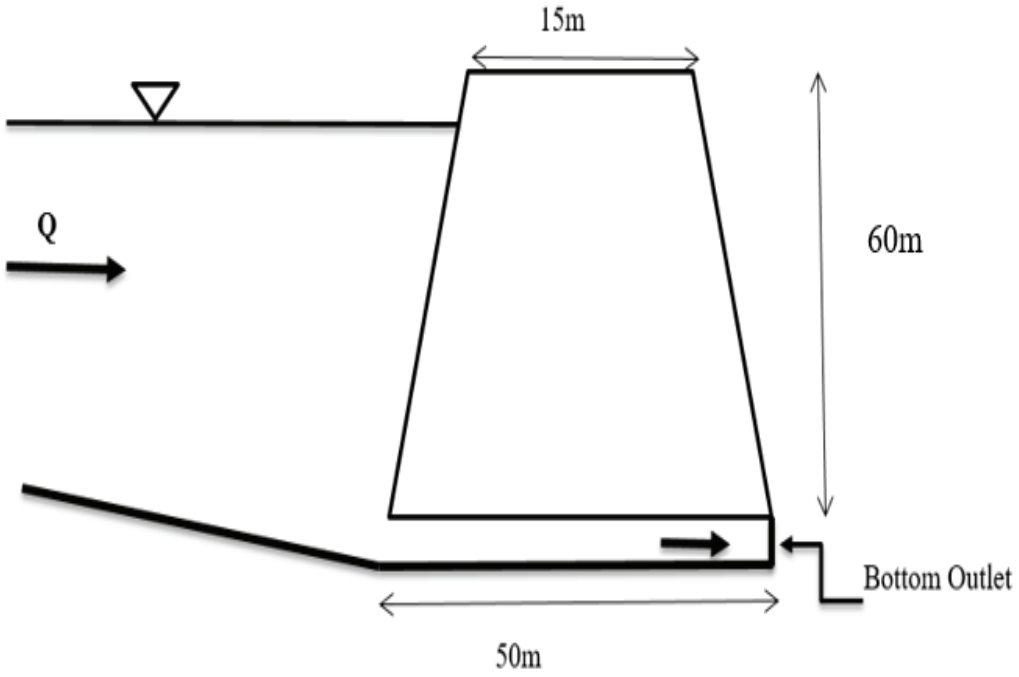

Figure 6.18. Proposed dam in the upper Kunar River

After performing the simulation, the overall inundated area was reduced from 122 km^2 to 44 km^2. Most of the inundated areas are located in the lower Kabul sab-basin, which is downstream of Kunar, Pich, Kabul main river, and Srokhrod river. So a large reservoir on the upstream part of the Kunar river can significantly control flash floods and storm-water runoff. Flooded areas along the main river of Kunar to Kama district reduced from 57 km^2 to 18 $km^{2,}$ which is the inflow of the Pich river to the main river.

Figure 6.19 indicates the depth of water behind the proposed reservoir on the main river of Kunar, with a 57.8-meter maximum height.

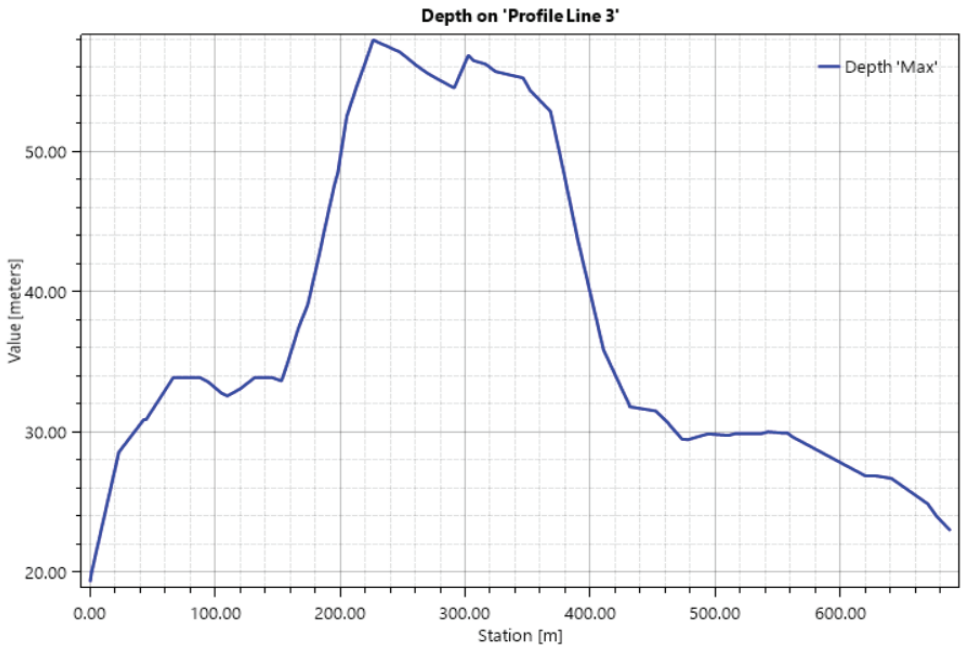

Figure 6.19. Depth of water behind the proposed dam on the main river of Kunar

Based on the result of this alternative on the Kunar main river, the settlement area and agricultural land have been protected from flooding during heavy precipitation and flash floods on both sides of the Kunar river (see Figure 6.17). The total flooded areas decreased almost by 50% in the lower Kabul sub-basin, which is downstream of the Kunar river. Furthermore, an outflow hydrograph with a peak flow of 515 m3/s was observed, causing major downstream inundation for an agricultural area in the lower Kabul sub-basin.

Another experiment was utilized to reduce flood-locations in the lower Kabul sub-basin by reducing cross-section of the bottom outlet of the dam from 3 to 1.5 m. The outflow hydrograph of the peak flow is reduced to 220 m3/s, which considerably impacts flood management on both sides of the Kunar river and in the lower Kabul sub-basin.

Figure 6.16 Indicates Q500 and discharge hydrographs of various tests in the upper Kunar reservoir. A reservoir can hold water and release it in a controllable way, which helps to reduce flood peaks and flow rates in the study area.

6.2.3. Alternative 3: Rehabilitation of Darunta Dam

The issue of the floods in the lower Kabul sub-basin can also be resolved in another way. Improving the capacity of Daronta dam can significantly help flood control by providing extra water storage capacity during periods of intense precipitation or snowmelt (see Figure 6.17). This can minimize the potential of flooding in the lower Kabul sub-basin by allowing the reservoir to hold back more water and discharge it gradually over time. By applying this alternative, the flow of Pul-Behsod, which is about 1207 m^3/s can be held there and released gradually to protect the lower Kabul sub-basin. Also, another embankment dam on the Alingar River, or the main Kabul river, which is upstream to the Daronta dam (Figure 6.17) and lower Kabul sub-basin, is also thought to store or hold the flow that is recorded at Pul-Behsod as 1207 m^3/s.

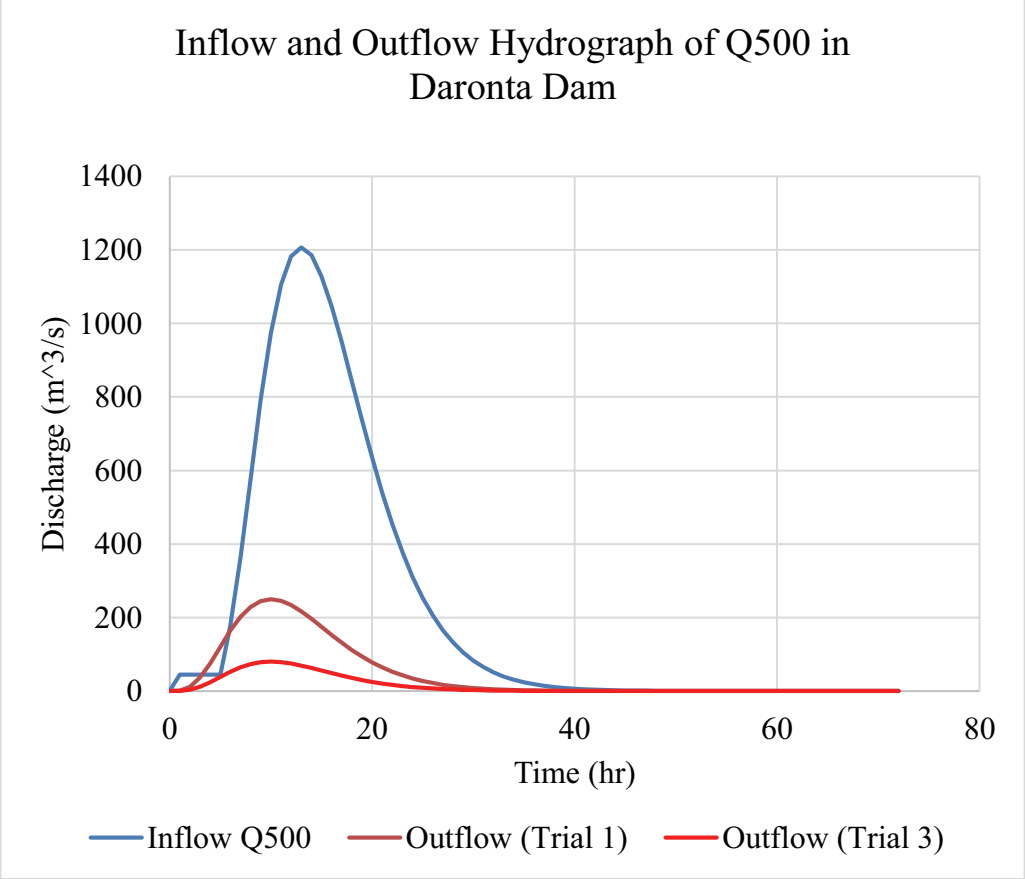

Figure 6.20. Q-500 and outflow hydrographs of various tests in the Darunta dam

Overall, proper planning, evaluation, and cooperation are necessary for the rehabilitation of a dam for flood control. Yet, with the appropriate technique, it can be a useful tool to reduce and mitigate economic flood risks and protect infrastructures and surrounding neighborhoods.

It is indeed crucial to remember, though, that improving a dam's capacity is not typically the most effective strategy for preventing flooding. Other flood control strategies, such as constructing levees or floodwalls or enhancing local drainage systems, could occasionally be more effective. Since the flow in the basin is frequently a flash flood, it cannot be controlled by levees or flood walls; therefore, Daronta Dam is the ideal location to be improved as a storage area and hold 1207 m^3/s of flow and release it gradually to protect downstream areas. Both alternatives 2 and 3 can reduce inundated area to 31.7 km^2 from 122 km^2.

To implement this solution, another dam will need to be constructed in the Alingar river or main Kabul river basin to store 1207 m^3/s flow on upstream part of the dam, which can be the best remedial solution since most of the flow discharging from Alingar river due to lack of reservoir.

CHAPTER 7

SUMMARY AND CONCLUSIONS

7.1. Summary

In summary, this study employed remotely sensed data, precipitation, discharge, ArcGIS, and hydraulic HEC-RAS software to analyze, to identify flood-prone areas. In this research, two study regions have been used: 1) the entire Kabul River Basin implementing the GIS-AHP Multi-Criteria Analysis approach, 2) HEC-RAS program was utilized to model river flow in Kunar and lower Kabul sub-basin based on GIS-AHP result in the risky areas. In this framework, Kunar and lower Kabul sub-basin flow and flood modeling were conducted to understand the flow and flood response of KRB, to simulate flow, find flood extent, and to consider structural mitigation preventions to reduce flood risk against the occurrences of longer recurrence interval.

Safety and the ability to manage a region sustainably are crucial concerns for authorities and planners. This objective can be reached by conducting detailed analysis and assessment in order to be able to act appropriately in the event of risky or hazardous occurrences to reduce the consequences and damages.

7.2. Conclusions

Flooding is a complex and challenging natural hazard for the population, environment, and socioeconomic development, which is difficult to predict and control like any other natural hazard. Still, its impacts can be minimized by structural (e.g., reservoir, detention basin. Channel restoration, levees and etc.) and non-structural (flood mapping, flood directive, identification of flood-prone areas and etc.) approaches.

The first approach in flood mapping and assessment is delineation of regions that are vulnerable to flooding. In this research, flood vulnerability was zoned across the entire KRB, Afghanistan, using GIS-AHP technique. The delineation of flood-prone areas involves integrating flood causal factors into a GIS using a WLC technique. The methodology takes into account ten parameters based on literature reviews accessibility

in arid and semi-arid regions that are relevant to the risk of flooding, including elevation, slope, distance to stream channels, NDVI, TWI, geology type, soil texture, LULC, curvature, and rainfall. Using weighted linear combination (WLC), final maps of locations at risk of floods were produced. The outcomes were validated using a comparison of the final maps' designated areas of hazard with an occurrence of historic flooding that had been documented in the research area.

The validation's findings demonstrate that flood zone of GIS-AHP is consistent with past events, which happened in 2013,2020, and 2022 years. Based on the MCDA flood Probability approach using GIS-AHP in Kabul River Basin of Afghanistan, the risk level zone map was precisely generated. Majority of work area's eastern, western, southwestern, and central regions are more vulnerable to floods or can be considered as high-risk zone where covered mostly by agricultural land and residential area (majority in rural areas and minority in urban areas).

A significant percentage of the catchment area was identified as being at a low to extremely low risk of floods. The watershed as a whole is considered part of 74% no-risk and low-risk zones. Regions of very high risk and high occupy 26% of KRB as a whole. About 1% of the catchment is covered by very high-risk zones, whereas high areas make up 25% of it. Moreover, outcome shows that TWI, altitude, slope, precipitation, and distance to stream channels are five vital variables for the assessment of flood.

Findings make it clear that 25% of KRB is mostly situated in high-risk zones with a higher probability of flooding. These places are generally on low-lying terrain and close to large or minor stream channels. The use of GIS-AHP to define flood hazard zones has proven to be reasonable since it is based on adopted and distinctive criteria that can significantly influence the occurrence of floods with a high hazard index.

As a consequence, flood risks are mapped and delineated, which is the first phase in establishing flood vulnerability management policies and identifying locations where there is or may be a considerable risk of flooding. Furthermore, the results of this analysis require the basin administration, regional planner, and authorities to implement austerity measures in response to unregulated development, particularly in high-risk locations near water bodies and blocking watercourses.

In this section of the study, flood risk and mitigation alternatives for the lower Kabul sub-basin River and the main Kunar River were established based on GIS-AHP results, along with model analyses for alternative approaches. Using the HEC-RAS program, all of the simulations were generated in 2D. The research aimed to evaluate the

current circumstances and flow modeling in the river, identify the inundation zones, and propose hydraulically practical solutions to the issues.

Using hydrological data collected from Asmar, Pul-Behsod, Pich, and SorkhRod gauge stations, designed hydrographs were produced by assessment of flood frequency of data to establish design flood occurrence. A simulation of a flood model was performed for maximum flood events and 500-year return periods.

The research area was protected from maximum flow discharge of a 500-year flood design event using a variety of mitigation techniques after a 500-year flood map was constructed. These techniques were assessed using the same input hydrograph. This assessment investigated a total of three alternatives based on practicality and financial factors. However, it has been found that river restoration in the Kunar River is useless in reducing floods since it takes a long time, has an adverse effect on the environment, is expensive, and does not help flood control greatly. Flooded areas decreased from 122 km^2 to 120 km^2 using river restoration mitigation measures.

Alternative 2, which is construction of a reservoir on the upper main Kunar river, and alternative three which is the rehabilitation of Darunta dam, achieved outstanding development in flood control compared to alternative one which is the restoration of the lower Kabul river in the Nangarhar city and lower Kunar river located in the Kama district. The alternatives included repairing and enhancing the Daronta Dam, building a reservoir on upstream of the Kunar River, and enhancing the riverbed by clearing sediment and debris from it nearby the Nangarhar City and the Kama District, which are more prone to flooding.

The entire area that was flooded decreased from 122 km^2 to 44 km^2 as a result of applying all available alternatives together, and all of this inundated area is located inside the river channel.

By implementing alternative two, which is construction and assessment of a reservoir, the settlement areas and agricultural land are protected on both banks of the river, and the extent and depth of flooding along the main Kunar River significantly decreased. Also, the development zones and agricultural areas in the lower Kabul sub-basin, which is downstream of the Kunar River, were controlled during the highest flow of a 500-year return period.

7.3. Limitations

Limitations of research work are identified as limits relating to the data availability:

- River Geometry: The cross sections of rivers are a crucial part of hydraulic models. Cross-sections are employed in HEC-RAS modeling to describe the geometry of rivers, including their channel, width, depth, and slope, as well as their floodplain at particular locations along the river. The hydraulic characteristics of the channel, including flow rate and water depth, and velocity, are computed using this data.
- Lack of long precipitation and discharge data: The scarcity of long-term precipitation and discharge data in the study area is considered a limitation for hydraulic analysis. Accurate rainfall and discharge data are critical for analyzing hydraulic processes in a watershed, monitoring floods and droughts, and effectively directing water resources.

7.4. Recommendations for Further Investigation

This work might serve as a useful resource for academics who wish to investigate flooding and related topics in greater detail and at various scales, particularly for arid and semi-arid locations like Afghanistan. The research recommended the following suggestions for future studies:

- Using high-resolution terrain topography: For HEC-RAS modeling, high-resolution terrain data is crucial because it presents important points on the topography of the river channel and floodplain. The quality and dependability of HEC-RAS modeling outputs can be increased with accurate topographical data, resulting in more efficient floodplain planning and evaluation of flood hazards.
- It is highly recommended that more meteorological and hydrological stations be constructed in the basin to get better outcomes.
- Further investigation should be done with complete river cross sections, high-resolution terrain topography, and meteorological data in the catchment area to check the overall accuracy.
- Consider applying climate change forecasts to flood mapping models to assess how the changing climate will affect the danger of flooding. This will contribute

to the creation of suitable adaptation strategies by government officials and planners to minimize the susceptibility of flooding.

- In the present research, hydraulic modeling was applied only for Kunar and the lower Kabul sub-basin to model river flow and flood assessment. A hydraulic model is recommended to be done for other sub-basins of the Kabul River Basin.

LIST OF REFERENCES

Abbas, A., Amjath-Babu, T., Kächele, H., & Müller, K. (2015). Non-structural flood risk mitigation under developing country conditions: an analysis on the determinants of willingness to pay for flood insurance in rural Pakistan. *Natural hazards, 75*(3), 2119-2135.

Abbott, M. B., Bathurst, J. C., Cunge, J. A., O'Connell, P. E., & Rasmussen, J. (1986). An introduction to the European Hydrological System—Systeme Hydrologique Europeen,"SHE", 1: History and philosophy of a physically-based, distributed modelling system. *Journal of Hydrology, 87*(1-2), 45-59.

Afshari, S., Tavakoly, A. A., Rajib, M. A., Zheng, X., Follum, M. L., Omranian, E., & Fekete, B. M. (2018). Comparison of new generation low-complexity flood inundation mapping tools with a hydrodynamic model. *Journal of Hydrology, 556*, 539-556.

Akhtar, F. (2017). *Water availability and demand analysis in the Kabul River Basin, Afghanistan.* Universitäts-und Landesbibliothek Bonn,

Andjelkovic, I. (2001). *Guidelines on non-structural measures in urban flood management*. Retrieved from

Apel, H., Thieken, A. H., Merz, B., & Blöschl, G. (2006). A probabilistic modelling system for assessing flood risks. *Natural hazards, 38*(1), 79-100.

ASDC, A. A. S. D. IMMAP (Web, map, dashboard, infographic). *Afghanistan. Available online at: http://asdc. immap. org/.(Verified on 16 June 2019)*.

AW3D30. *High-Resolution Topography Data and Tools. The ALOS Global Digital Surface Model (AW3D30)* Retrieved from: https://portal.opentopography.org/raster?opentopoID=OTALOS.112016.4326.2

Bathrellos, G., Karymbalis, E., Skilodimou, H., Gaki-Papanastassiou, K., & Baltas, E. (2016). Urban flood hazard assessment in the basin of Athens Metropolitan city, Greece. *Environmental Earth Sciences, 75*(4), 1-14.

Beirlant, J., Goegebeur, Y., Segers, J., & Teugels, J. L. (2004). *Statistics of extremes: theory and applications* (Vol. 558): John Wiley & Sons.

Benson, M. A. (1968). Uniform flood-frequency estimating methods for federal agencies. *Water Resources Research, 4*(5), 891-908.

Beven, K. J., & Kirkby, M. J. (1979). A physically based, variable contributing area model of basin hydrology/Un modèle à base physique de zone d'appel variable de l'hydrologie du bassin versant. *Hydrological Sciences Journal, 24*(1), 43-69.

Bhandari, M., Nyaupane, N., Mote, S. R., Kalra, A., & Ahmad, S. (2017). *2D Unsteady Routing and Flood Inundation Mapping for Lower Region of Brazos River Watershed*.

Brunner, G. (2018). Benchmarking of the HEC-RAS two-dimensional hydraulic modeling capabilities. *US Army Corps of Engineers: Davis, CA, USA*, 1-137.

Brunner, G. W. (2002). *Hec-ras (river analysis system).* Paper presented at the North American water and environment congress & destructive water.

Budiyono, Y., Aerts, J., Brinkman, J., Marfai, M. A., & Ward, P. (2015). Flood risk assessment for delta mega-cities: a case study of Jakarta. *Natural hazards, 75*(1), 389-413.

Chakraborty, A., & Joshi, P. (2016). Mapping disaster vulnerability in India using analytical hierarchy process. *Geomatics, Natural Hazards and Risk, 7*(1), 308-325.

Chandio, I. A., Matori, A. N. B., WanYusof, K. B., Talpur, M. A. H., Balogun, A.-L., & Lawal, D. U. (2013). GIS-based analytic hierarchy process as a multicriteria decision analysis instrument: a review. *Arabian Journal of Geosciences, 6*(8), 3059-3066.

Chanson, H. (2004). Hydraulics of open channel flow.

Chebana, F., Charron, C., Ouarda, T. B., & Martel, B. (2014). Regional frequency analysis at ungauged sites with the generalized additive model. *Journal of Hydrometeorology, 15*(6), 2418-2428.

Chow, V., Maidment, D., & Mays, L. (1988a). *Applied Hydrology, McGraw-Hill Book Company, New York*.

Chow, V., Maidment, D., & Mays, L. (1988b). Applied Hydrology, McGraw-Hill Book Company, New York. In.

Cigler, B. A. (1996). Coping with Floods: Lessons from the 1990s. *Disaster Management in the US and Canada*, 191-213.

Cook, A., & Merwade, V. (2009). Effect of topographic data, geometric configuration and modeling approach on flood inundation mapping. *Journal of Hydrology, 377*(1-2), 131-142.

Cosby, B., Hornberger, G., Clapp, R., & Ginn, T. (1984). A statistical exploration of the relationships of soil moisture characteristics to the physical properties of soils. *Water Resources Research, 20*(6), 682-690.

Das, S. (2019). Geospatial mapping of flood susceptibility and hydro-geomorphic response to the floods in Ulhas basin, India. *Remote Sensing Applications: Society and Environment, 14*, 60-74.

Dewitz, J. (2016). National Land Cover Database. *US Geological Survey Data Release: Sioux Falls, SD, USA*.

Doebrich, J. L., Wahl, R.R., Ludington, S.D., Chirico, P.G., Wandrey, C.J., Bohannon, R.G., Orris, G.J., Bliss, J.D.,. (2006). Geologic age and lithology of Afghanistan: U.S. Geological Survey data release. Retrieved from https://www.sciencebase.gov/catalog/item/60d3a6a2d34e12a1b009d0cc

Douben, K. J. (2006). Characteristics of river floods and flooding: a global overview, 1985–2003. *Irrigation and Drainage: The journal of the International Commission on Irrigation and Drainage, 55*(S1), S9-S21.

Dunne, T., & Leopold, L. (1978). Calculation of flood hazard. *Dunne, T. and Leopold, LB, Water in environmental planning, San Francisco, WH Freeman and Co, CA*.

Dutta, D. (2003). Flood disaster trends in Asia in the last 30 years. *International Centre for Urban Safety Engineering. Institute of Industrial Science. University of Tokyo. ICUS/INCEDE Newsletter, 3*(1), 1-5.

Dutta, D., Teng, J., Vaze, J., Lerat, J., Hughes, J., & Marvanek, S. (2013). Storage-based approaches to build floodplain inundation modelling capability in river system models for water resources planning and accounting. *Journal of Hydrology, 504*, 12-28.

Dyhouse, G., Hatchett, J., & Benn, J. (2003). *Floodplain modeling using HEC-RAS*: Haestad press.

Eckstein, D., Künzel, V., & Schäfer, L. (2021). Global climate risk index 2021. *Who Suffers Most from Extreme Weather Events*, 2000-2019.

El Kadi Abderrezzak, K., Paquier, A., & Mignot, E. (2009). Modelling flash flood propagation in urban areas using a two-dimensional numerical model. *Natural hazards, 50*(3), 433-460.

Erena, S. H., Worku, H., & De Paola, F. (2018). Flood hazard mapping using FLO-2D and local management strategies of Dire Dawa city, Ethiopia. *Journal of Hydrology: Regional Studies, 19*, 224-239.

European-Directive. (2007). 60/EC of the European Parliament and of the Council of 23 October 2007 on the assessment and management of flood risks. *Brussels: European Commission*.

Faisal, I., Kabir, M., & Nishat, A. (1999). Non-structural flood mitigation measures for Dhaka City. *Urban water, 1*(2), 145-153.

FAO-MEW. (2015). Water Availability and Management in FAO and Afghanistan.Ministry of Energy and Water.

Favre, A., & Kamal, G. M. (2004). "Watershed atlas of Afghanistan".Kabul: Government of Afghanistan, Ministry of Irrigation." Water Resources and Environment.

Fendler, R. (2008). Floods and safety of establishments and installations containing hazardous substances. *Natural hazards, 46*(2), 257-263.

Fernández, D., & Lutz, M. A. (2010). Urban flood hazard zoning in Tucumán Province, Argentina, using GIS and multicriteria decision analysis. *Engineering Geology, 111*(1-4), 90-98.

Gallegos, H. A., Schubert, J. E., & Sanders, B. F. (2009). Two-dimensional, high-resolution modeling of urban dam-break flooding: A case study of Baldwin Hills, California. *Advances in water resources, 32*(8), 1323-1335.

Ghosh, A., & Kar, S. K. (2018). Application of analytical hierarchy process (AHP) for flood risk assessment: a case study in Malda district of West Bengal, India. *Natural hazards, 94*(1), 349-368.

Giustarini, L., Chini, M., Hostache, R., Pappenberger, F., & Matgen, P. (2015). Flood hazard mapping combining hydrodynamic modeling and multi annual remote sensing data. *Remote Sensing, 7*(10), 14200-14226.

Golden, B. L., Wasil, E. A., & Levy, D. E. (1989). Applications of the analytic hierarchy process: A categorized, annotated bibliography. In *The analytic hierarchy process* (pp. 37-58): Springer.

Grimm, M. M., Wohl, E. E., & Jarrett, R. D. (1995). Coarse-sediment distribution as evidence of an elevation limit for flash flooding, Bear Creek, Colorado. *Geomorphology, 14*(3), 199-210.

Hagen, E., & Lu, X. (2011). Let us create flood hazard maps for developing countries. *Natural hazards, 58*(3), 841-843.

Hajkowicz, S., & Collins, K. (2007). A review of multiple criteria analysis for water resource planning and management. *Water resources management, 21*(9), 1553-1566.

Haltas, I., Yildirim, E., Oztas, F., & Demir, I. (2021). A comprehensive flood event specification and inventory: 1930–2020 Turkey case study. *International Journal of Disaster Risk Reduction, 56*, 102086.

Hazarika, N., Barman, D., Das, A., Sarma, A., & Borah, S. (2018). Assessing and mapping flood hazard, vulnerability and risk in the Upper Brahmaputra River valley using stakeholders' knowledge and multicriteria evaluation (MCE). *Journal of flood risk management, 11*, S700-S716.

HEC-RAS. (2016). *HEC-RAS, River Analysis System, Hydraulic Reference Manual*.

HEC-SSP. (2019). *U.S. Army Corps of Engineers, Hydrologic Engineering Center's (HEC) Statistical Software Package (HEC-SSP) Version 2.2.*

Heidari, A. (2009). Structural master plan of flood mitigation measures. *Natural Hazards and Earth System Sciences, 9*(1), 61-75.

Hirabayashi, Y., Mahendran, R., Koirala, S., Konoshima, L., Yamazaki, D., Watanabe, S., . . . Kanae, S. (2013). Global flood risk under climate change. *Nature climate change, 3*(9), 816-821.

Hosking, J. R. M., & Wallis, J. R. (1997). *Regional frequency analysis*.

Hosseinali, F., & Alesheikh, A. A. (2008). Weighting spatial information in GIS for copper mining exploration. *American Journal of Applied Sciences, 5*(9), 1187-1198.

Hu, S., Cheng, X., Zhou, D., & Zhang, H. (2017). GIS-based flood risk assessment in suburban areas: A case study of the Fangshan District, Beijing. *Natural hazards, 87*(3), 1525-1543.

Hunter, N. M., Horritt, M. S., Bates, P. D., Wilson, M. D., & Werner, M. G. (2005). An adaptive time step solution for raster-based storage cell modelling of floodplain inundation. *Advances in water resources, 28*(9), 975-991.

IPCC. (2014). IPCC Fifth Assessment Report—Synthesis Report. In: IPCC New York, NY, USA.

Kachouri, S., Achour, H., Abida, H., & Bouaziz, S. (2015). Soil erosion hazard mapping using Analytic Hierarchy Process and logistic regression: a case study of Haffouz watershed, central Tunisia. *Arabian Journal of Geosciences, 8*, 4257-4268.

Katz, R. W. (1999). Extreme value theory for precipitation: sensitivity analysis for climate change. *Advances in water resources, 23*(2), 133-139.

Kazakis, N., Kougias, I., & Patsialis, T. (2015). Assessment of flood hazard areas at a regional scale using an index-based approach and Analytical Hierarchy Process: Application in Rhodope–Evros region, Greece. *Science of the Total Environment, 538*, 555-563.

Khan, A. N. (2011). Analysis of flood causes and associated socio-economic damages in the Hindukush region. *Natural hazards, 59*(3), 1239-1260.

Khattak, M. S., Anwar, F., Saeed, T. U., Sharif, M., Sheraz, K., & Ahmed, A. (2016). Floodplain mapping using HEC-RAS and ArcGIS: a case study of Kabul River. *Arabian Journal for Science and Engineering, 41*(4), 1375-1390.

Khosravi, K., Nohani, E., Maroufinia, E., & Pourghasemi, H. R. (2016). A GIS-based flood susceptibility assessment and its mapping in Iran: a comparison between

frequency ratio and weights-of-evidence bivariate statistical models with multi-criteria decision-making technique. *Natural hazards, 83*(2), 947-987.

Kidson, R., & Richards, K. (2005). Flood frequency analysis: assumptions and alternatives. *Progress in Physical Geography, 29*(3), 392-410.

Kite, G. W. (1977). Frequency and risk analysis in hydrology.

Kjellgren, S. (2013). Exploring local risk managers' use of flood hazard maps for risk communication purposes in Baden-Württemberg. *Natural Hazards and Earth System Sciences, 13*(7), 1857-1872.

Kron, W. (2005). Flood risk= hazard• values• vulnerability. *Water international, 30*(1), 58-68.

Kundzewicz, Z. W. (2002). Non-structural flood protection and sustainability. *Water international, 27*(1), 3-13.

Levy, J. K. (2005). Multiple criteria decision making and decision support systems for flood risk management. *Stochastic Environmental Research and Risk Assessment, 19*(6), 438-447.

Li, Y., Martinis, S., Wieland, M., Schlaffer, S., & Natsuaki, R. (2019). Urban flood mapping using SAR intensity and interferometric coherence via Bayesian network fusion. *Remote Sensing, 11*(19), 2231.

Lin, L., Di, L., Yu, E. G., Kang, L., Shrestha, R., Rahman, M. S., . . . Zhang, C. (2016). *A review of remote sensing in flood assessment.* Paper presented at the 2016 Fifth International Conference on Agro-Geoinformatics (Agro-Geoinformatics).

Malczewski, J. (2006). GIS-based multicriteria decision analysis: a survey of the literature. *International Journal of Geographical Information Science, 20*(7), 703-726.

Manavalan, R. (2017). SAR image analysis techniques for flood area mapping-literature survey. *Earth Science Informatics, 10*(1), 1-14.

Marriott, S. (1992). Textural analysis and modelling of a flood deposit: River Severn, UK. *Earth Surface Processes and Landforms, 17*(7), 687-697.

Martina, M., Todini, E., & Libralon, A. (2006). A Bayesian decision approach to rainfall thresholds based flood warning. *Hydrology and Earth System Sciences, 10*(3), 413-426.

Mayar, M. A., Asady, H., & Nelson, J. (2020). River flow analyses for flood projection in the Kabul River Basin. *Central Asian Journal of Water Research (CAJWR) Центральноазиатский журнал исследований водных ресурсов, 6*(1), 1-17.

Merritt, W. S., Letcher, R. A., & Jakeman, A. J. (2003). A review of erosion and sediment transport models. *Environmental modelling & software, 18*(8-9), 761-799.

Merz, B., Kreibich, H., Schwarze, R., & Thieken, A. (2010). Review article" Assessment of economic flood damage". *Natural Hazards and Earth System Sciences, 10*(8), 1697-1724.

Mignot, E., Paquier, A., & Haider, S. (2006). Modeling floods in a dense urban area using 2D shallow water equations. *Journal of Hydrology, 327*(1-2), 186-199.

Mihu-Pintilie, A., Cîmpianu, C. I., Stoleriu, C. C., Pérez, M. N., & Paveluc, L. E. (2019). Using high-density LiDAR data and 2D streamflow hydraulic modeling to improve urban flood hazard maps: A HEC-RAS multi-scenario approach. *Water, 11*(9), 1832.

Miller, J. R., Ritter, D. F., & Kochel, R. C. (1990). Morphometric assessment of lithologic controls on drainage basin evolution in the Crawford Upland, south-central Indiana. *American Journal of Science, 290*(5), 569-599.

Mojaddadi, H., Pradhan, B., Nampak, H., Ahmad, N., & Ghazali, A. H. b. (2017). Ensemble machine-learning-based geospatial approach for flood risk assessment using multi-sensor remote-sensing data and GIS. *Geomatics, Natural Hazards and Risk, 8*(2), 1080-1102.

Munich-Re. (1997). Flooding and insurance. In: Munich Reinsurance Company, Munich, Germany.

Mysiak, J., Testella, F., Bonaiuto, M., Carrus, G., De Dominicis, S., Ganucci Cancellieri, U., . . . Grifoni, P. (2013). Flood risk management in Italy: challenges and opportunities for the implementation of the EU Floods Directive (2007/60/EC). *Natural Hazards and Earth System Sciences, 13*(11), 2883-2890.

Najmuddin, O., Deng, X., & Bhattacharya, R. (2018). The dynamics of land use/cover and the statistical assessment of cropland change drivers in the Kabul River Basin, Afghanistan. *Sustainability, 10*(2), 423.

Nasiri, H., Boloorani, A. D., Sabokbar, H. A. F., Jafari, H. R., Hamzeh, M., & Rafii, Y. (2013). Determining the most suitable areas for artificial groundwater recharge via an integrated PROMETHEE II-AHP method in GIS environment (case study: Garabaygan Basin, Iran). *Environmental monitoring and assessment, 185*(1), 707-718.

NERC. (1999). National Environment Research Council (NERC),1999: Flood Studies Report, (in five volumes)
Wallingford: Institute of Hydrology.

O'Brien, G., O'keefe, P., Rose, J., & Wisner, B. (2006). Climate change and disaster management. *Disasters, 30*(1), 64-80.

OCHA. (2013). Afghanistan: Overview of Natural Disasters, Natural disaster incidents as recorded by OCHA (Office for the Coordination of Humanitarian Affairs)Field Offices and IOM from 1 January to 31 December 2013. Retrieved from https://reliefweb.int/map/afghanistan/afghanistan-overview-natural-disasters-natural-disaster-incidents-recorded-ocha-0

Ouma, Y. O., & Tateishi, R. (2014). Urban flood vulnerability and risk mapping using integrated multi-parametric AHP and GIS: methodological overview and case study assessment. *Water, 6*(6), 1515-1545.

Owuor, S. O., Butterbach-Bahl, K., Guzha, A. C., Rufino, M. C., Pelster, D. E., Díaz-Pinés, E., & Breuer, L. (2016). Groundwater recharge rates and surface runoff response to land use and land cover changes in semi-arid environments. *Ecological Processes, 5*(1), 1-21.

Papaioannou, G., Vasiliades, L., & Loukas, A. (2015). Multi-criteria analysis framework for potential flood prone areas mapping. *Water resources management, 29*(2), 399-418.

Patel, K. F., Fansler, S. J., Campbell, T. P., Bond-Lamberty, B., Smith, A. P., RoyChowdhury, T., . . . Bailey, V. L. (2021). Soil texture and environmental conditions influence the biogeochemical responses of soils to drought and flooding. *Communications Earth & Environment, 2*(1), 127.

Pathirana, A., Tsegaye, S., Gersonius, B., & Vairavamoorthy, K. (2011). A simple 2-D inundation model for incorporating flood damage in urban drainage planning. *Hydrology and Earth System Sciences, 15*(8), 2747-2761.

Petr, T. (1999). *Fish and fisheries at higher altitudes: Asia* (Vol. 385): Food & Agriculture Org.

Pham, B. T., Avand, M., Janizadeh, S., Phong, T. V., Al-Ansari, N., Ho, L. S., . . . Bozchaloei, S. K. (2020). GIS based hybrid computational approaches for flash flood susceptibility assessment. *Water, 12*(3), 683.

Pinho, J., Ferreira, R., Vieira, L., & Schwanenberg, D. (2015). Comparison between two hydrodynamic models for flooding simulations at river Lima basin. *Water resources management, 29*(2), 431-444.

Ponnamperuma, F. (1984). *Effects of flooding on soils* (Vol. 10): Academic Press New York.

Pourali, S., Arrowsmith, C., Chrisman, N., Matkan, A., & Mitchell, D. (2016). Topography wetness index application in flood-risk-based land use planning. *Applied Spatial Analysis and Policy, 9*, 39-54.

Pourghasemi, H. R., Pradhan, B., & Gokceoglu, C. (2012). Application of fuzzy logic and analytical hierarchy process (AHP) to landslide susceptibility mapping at Haraz watershed, Iran. *Natural hazards, 63*(2), 965-996.

Predick, K. I., & Turner, M. G. (2008). Landscape configuration and flood frequency influence invasive shrubs in floodplain forests of the Wisconsin River (USA). *Journal of Ecology, 96*(1), 91-102.

Quiroga, V. M., Popescu, I. a., Solomatine, D., & Bociort, L. (2013). Cloud and cluster computing in uncertainty analysis of integrated flood models. *Journal of Hydroinformatics, 15*(1), 55-70.

Quirogaa, V. M., Kurea, S., Udoa, K., & Manoa, A. (2016). Application of 2D numerical simulation for the analysis of the February 2014 Bolivian Amazonia flood: Application of the new HEC-RAS version 5. *Ribagua, 3*(1), 25-33.

Rahmati, O., Pourghasemi, H. R., & Melesse, A. M. (2016). Application of GIS-based data driven random forest and maximum entropy models for groundwater potential mapping: a case study at Mehran Region, Iran. *Catena, 137*, 360-372.

Rahmati, O., Pourghasemi, H. R., & Zeinivand, H. (2016). Flood susceptibility mapping using frequency ratio and weights-of-evidence models in the Golastan Province, Iran. *Geocarto International, 31*(1), 42-70.

Ramos, C., & Reis, E. (2002). Floods in southern Portugal: their physical and human causes, impacts and human response. *Mitigation and Adaptation Strategies for Global Change, 7*(3), 267-284.

Rangari, V. A., Umamahesh, N., & Bhatt, C. (2019). Assessment of inundation risk in urban floods using HEC RAS 2D. *Modeling Earth Systems and Environment, 5*(4), 1839-1851.

Renard, B., & Lang, M. (2007). Use of a Gaussian copula for multivariate extreme value analysis: Some case studies in hydrology. *Advances in water resources, 30*(4), 897-912.

Rozos, D., Bathrellos, G., & Skillodimou, H. (2011). Comparison of the implementation of rock engineering system and analytic hierarchy process methods, upon landslide susceptibility mapping, using GIS: a case study from the Eastern Achaia County of Peloponnesus, Greece. *Environmental Earth Sciences, 63*(1), 49-63.

Rumsby, B. T. (1991). *Flood frequency and magnitude estimates based on valley flood morphology and floodplain sedimentary sequences: the Tyne Basin, NE England.* Newcastle University,

Saaty, T. L. (1980). TheAnalyticHierarchyProcess. *McGrawhill, Juc. New York*.

Saaty, T. L. (1988). What is the analytic hierarchy process? In *Mathematical models for decision support* (pp. 109-121): Springer.

Sahni, P., DHAMEJA, A., & MEDURY, U. (2001). *Disaster mitigation: experiences and reflections*: PHI Learning Pvt. Ltd.

Samantaray, S., & Sahoo, A. (2020). Estimation of flood frequency using statistical method: Mahanadi River basin, India. *H2Open Journal, 3*(1), 189-207.

Sanyal, J., & Lu, X. X. (2006). GIS-based flood hazard mapping at different administrative scales: A case study in Gangetic West Bengal, India. *Singapore Journal of Tropical Geography, 27*(2), 207-220.

Sayama, T., Ozawa, G., Kawakami, T., Nabesaka, S., & Fukami, K. (2012). Rainfall–runoff–inundation analysis of the 2010 Pakistan flood in the Kabul River basin. *Hydrological Sciences Journal, 57*(2), 298-312.

Sharma, T. P. P., Zhang, J., Koju, U. A., Zhang, S., Bai, Y., & Suwal, M. K. (2019). Review of flood disaster studies in Nepal: A remote sensing perspective. *International Journal of Disaster Risk Reduction, 34*, 18-27.

Siddayao, G. P., Valdez, S. E., & Fernandez, P. L. (2014). Analytic hierarchy process (AHP) in spatial modeling for floodplain risk assessment. *International Journal of Machine Learning and Computing, 4*(5), 450.

Skinner, M. B. W., POrter, B. J. I., & Stephen III, C. *Environmental geology/Barbara W. Murck, Brian J. Skinner and Stephen C. Porter*. Retrieved from

Srinivas, K., Werner, M., & Wright, N. (2008). Comparing forecast skill of inundation models of differing complexity: the case of Upton upon Severn. In *Flood Risk Management: Research and Practice* (pp. 25-25): CRC Press.

Srivastava, O. S., Denis, D., Srivastava, S. K., Kumar, M., & Kumar, N. (2014). Morphometric analysis of a Semi Urban Watershed, trans Yamuna, draining at Allahabad using Cartosat (DEM) data and GIS. *Int J Eng Sci, 3*(11), 71-79.

Stedinger, J. R. (1993). Frequency analysis of extreme events. *in Handbook of Hydrology*.

Stedinger, J. R., & Griffis, V. W. (2008). Flood frequency analysis in the United States: Time to update. *13*(4), 199-204.

Stefanidis, S., & Stathis, D. (2013). Assessment of flood hazard based on natural and anthropogenic factors using analytic hierarchy process (AHP). *Natural hazards, 68*(2), 569-585.

Swain, K. C., Singha, C., & Nayak, L. (2020). Flood susceptibility mapping through the GIS-AHP technique using the cloud. *ISPRS International Journal of Geo-Information, 9*(12), 720.

Tang, W. H., & Yen, B. C. (1993). *Probabilistic inspection scheduling for dams.* Paper presented at the Reliability and Uncertainty Analyses in Hydraulic Design.

Tayefi, V., Lane, S., Hardy, R., & Yu, D. (2007). A comparison of one-and two-dimensional approaches to modelling flood inundation over complex upland

floodplains. *Hydrological Processes: An International Journal, 21*(23), 3190-3202.

Teng, J., Jakeman, A. J., Vaze, J., Croke, B. F., Dutta, D., & Kim, S. (2017). Flood inundation modelling: A review of methods, recent advances and uncertainty analysis. *Environmental modelling & software, 90*, 201-216.

Teng, W.-H., Hsu, M.-H., Wu, C.-H., & Chen, A. S. (2006). Impact of flood disasters on Taiwan in the last quarter century. *Natural hazards, 37*(1), 191-207.

Termeh, S. V. R., Kornejady, A., Pourghasemi, H. R., & Keesstra, S. (2018). Flood susceptibility mapping using novel ensembles of adaptive neuro fuzzy inference system and metaheuristic algorithms. *Science of the Total Environment, 615*, 438-451.

Tian, D., & Wang, L. (2022). BLP3-SP: A Bayesian Log-Pearson Type III Model with Spatial Priors for Reducing Uncertainty in Flood Frequency Analyses. *Water, 14*(6), 909.

Tranfield, D., Denyer, D., & Smart, P. (2003). Towards a Methodology for Developing Evidence-Informed Management Knowledge by Means of Systematic Review. *British Journal of Management, 14*(3), 207-222. doi:10.1111/1467-8551.00375

Tung, Y.-K. (2005). Flood defense systems design by risk-based approaches. *Water international, 30*(1), 50-57.

UNISDR, U. (2009). Terminology on disaster risk reduction. *Geneva, Switzerland.*

UNOCHA. (2020). Afghanistan ICCT Flood Contingency Plan (March - June 2020),UN OCHA Office for the Coordination of Humanitarian Affairs. Retrieved from https://reliefweb.int/report/afghanistan/afghanistan-icct-flood-contingency-plan-march-june-2020

UNOCHA. (2022). Afghanistan Flash Floods in August 2022, OCHA coordinates the global emergency response to save lives and protect people in humanitarian crises. Retrieved from https://reliefweb.int/report/afghanistan/afghanistan-snapshot-flash-floods-2022-31-august-2022

USWRC, W. R. C. H. C. (1975). *Guidelines for determining flood flow frequency*: US Water Resources Council, Hydrology Committee.

Vick, M. J. (2014). Steps towards an Afghanistan–Pakistan water-sharing agreement. *International Journal of Water Resources Development, 30*(2), 224-229.

Vrijling, J. K. (1993). *Development in probabilistic design of flood defenses in the Netherlands.* Paper presented at the Reliability and uncertainty analyses in hydraulic design.

Wang, Y., Fang, Z., Hong, H., & Peng, L. (2020). Flood susceptibility mapping using convolutional neural network frameworks. *Journal of Hydrology, 582*, 124482.

Webster, T. L. (2010). Flood risk mapping using LiDAR for Annapolis Royal, Nova Scotia, Canada. *Remote Sensing, 2*(9), 2060-2082.

Welsh, W. D., Vaze, J., Dutta, D., Rassam, D., Rahman, J. M., Jolly, I. D., . . . Hardy, M. J. (2013). An integrated modelling framework for regulated river systems. *Environmental modelling & software, 39*, 81-102.

WHO. World Health Organization (WHO). Retrieved from https://www.who.int/health-topics/floods#tab=tab_1

Wilson, J. P., & Gallant, J. C. (2000). *Terrain analysis: principles and applications*: John Wiley & Sons.

World-Bank. (2010). *Afghanistan - Scoping Strategic Options for Development of the Kabul River Basin : A Multisectoral Decision Support System Approach*.

Wu, H., Adler, R. F., Hong, Y., Tian, Y., & Policelli, F. (2012). Evaluation of global flood detection using satellite-based rainfall and a hydrologic model. *Journal of Hydrometeorology, 13*(4), 1268-1284.

Yanmaz, A. M. (2018). Applied water resources engineering.

Zhang, Q., Xu, C.-Y., Zhang, Z., Chen, Y. D., Liu, C.-l., & Lin, H. (2008). Spatial and temporal variability of precipitation maxima during 1960–2005 in the Yangtze River basin and possible association with large-scale circulation. *Journal of Hydrology, 353*(3-4), 215-227.

Zoleta-Nantes, D. B. (2002). Differential impacts of flood hazards among the street children, the urban poor and residents of wealthy neighborhoods in Metro Manila, Philippines. *Mitigation and Adaptation Strategies for Global Change, 7*(3), 239-266.